GEOTECHNICAL CHARACTERIZATION OF SOILS PRONE TO RAINFALL-
INDUCED LANDSLIDES IN RIZE (NORTHERN TURKEY)

A THESIS SUBMITTED TO
THE GRADUATE SCHOOL OF NATURAL AND APPLIED SCIENCES
OF
MIDDLE EAST TECHNICAL UNIVERSITY

BY

CELAL EMRE ÜYETÜRK

IN PARTIAL FULFILLMENT OF THE REQUIREMENTS
FOR
THE DEGREE OF MASTER OF SCIENCE
IN
CIVIL ENGINEERING

JULY 2019

Approval of the thesis:

GEOTECHNICAL CHARACTERIZATION OF SOILS PRONE TO RAINFALL-INDUCED LANDSLIDES IN RIZE (NORTHERN TURKEY)

submitted by **CELAL EMRE ÜYETÜRK** in partial fulfillment of the requirements for the degree of **Master of Science in Civil Engineering Department, Middle East Technical University** by,

Prof. Dr. Halil Kalıpçılar
Dean, Graduate School of **Natural and Applied Sciences**   _____

Prof. Dr. Ahmet Türer
Head of Department, **Civil Engineering**   _____

Assoc. Prof. Dr. Nejan Huvaj Sarıhan
Supervisor, **Civil Engineering, METU**   _____

Examining Committee Members:

Prof. Dr. Erdal Çokça
Civil Engineering Department, METU   _____

Assoc. Prof. Dr. Nejan Huvaj Sarıhan
Civil Engineering, METU   _____

Assoc. Prof. Dr. Hakan Ahmet Nefeslioğlu
Geological Engineering Department, Hacettepe University   _____

Assoc. Prof. Dr. Nabi Kartal Toker
Civil Engineering Department, METU   _____

Assoc. Prof. Dr. Mustafa Abdullah Sandıkkaya
Civil Engineering Department, Hacettepe University   _____

Date: 02.07.2019

I hereby declare that all information in this document has been obtained and presented in accordance with academic rules and ethical conduct. I also declare that, as required by these rules and conduct, I have fully cited and referenced all material and results that are not original to this work.

Name, Surname: Celal Emre Üyetürk

Signature:

ABSTRACT

GEOTECHNICAL CHARACTERIZATION OF SOILS PRONE TO RAINFALL-INDUCED LANDSLIDES IN RIZE (NORTHERN TURKEY)

Üyetürk, Celal Emre
Master of Science, Civil Engineering
Supervisor: Assoc. Prof. Dr. Nejan Huvaj Sarıhan

July 2019, 136 pages

Landslides are common type of natural hazards around the world. Every year, hundreds of landslides are induced by rainfall in Rize. These landslides are shallow failures, generally having a maximum depth of 5 m. Although many of these landslides are observed every year, there is limited data on characteristics of these soils in the literature. Characterizing these soils is of paramount importance for numerical modeling of the landslide mechanisms, for landslide susceptibility mapping and for establishing rainfall intensity-duration thresholds. This study aims to investigate the characteristics of soils in rainfall-induced landslides in Rize. Disturbed and undisturbed samples are taken from a total of 12 landslide sites to evaluate the physical and mechanical properties and the mineralogy. Experiments including grain size distribution, Atterberg limits, organic content by mass and pH determination, mineralogy studies via X-Ray diffraction and Scanning Electron Microscopy, direct shear tests, unconfined compression tests, soil-water retention studies, hydraulic conductivity tests are conducted. Also, in-situ unit weights are determined on undisturbed samples, and portable hand vane tests are conducted to evaluate the in-situ undrained shear strength. Results indicate that these materials are relatively loose, medium-stiff, mostly fine-grained soils (low and high plasticity silts and high

plasticity organic soils), and have relatively low pH. Direct shear tests on intact samples indicated that the average internal friction angle is in the range of 31.1-38.0 degrees in saturated condition; on reconstituted samples revealed the degree of saturation effects the shear strength and the volumetric response significantly.

Keywords: Rainfall-induced Landslide, Residual Soil, Volcanic Soil, Direct Shear Test, Drying

ÖZ

RİZE İLİNDE (KUZEY TÜRKİYE) YAĞMURLA TETİKLENEN HEYELAN SAHALARINDAKİ ZEMİNLERİN GEOTEKNİK KARAKTERİZASYONU

Üyetürk, Celal Emre
Yüksek Lisans, İnşaat Mühendisliği
Tez Danışmanı: Doç. Dr. Nejan Huvaj Sarıhan

Heyelanlar, tüm dünyada sıklıkla görülen doğal afetlerdendir. Rize ilinde her yıl yüzlerce yağmurla tetiklenen heyelan görülmektedir. Bu heyelanlar maksimum derinliği 5 m olan sığ heyelanlardır. Rize ilindeki yağmurla tetiklenen heyelanlar her yıl görülmekte olsa da, literatürde zeminler ile ilgili sınırlı veri mevcuttur. Zeminlerin karakterizasyonu, heyelan mekanizmasının sayısal modellenmesi, heyelan duraylılık haritaları ve yağış şiddet-süre eşik değerleri belirlenmesi açısından önem arz etmektedir. Bu çalışmada Rize ilindeki yağmurla tetiklenen heyelan bölgelerindeki zeminlerin karakterizasyonu amaçlanmaktadır. Zeminlerin fiziksel ve mekanik özelliklerini araştırmak için 12 heyelan bölgesinden örselenmiş ve örselenmemiş numuneler alınmıştır. Laboratuvar testleri olarak, dane boyu dağılımı, Atterberg limitleri ve zemin sınıflaması, organik madde miktarı ve pH değerleri, X-ışını difraksiyonu ve elektron mikroskobu ile zemin mineralojisi, örselenmemiş ve laboratuvarda hazırlanmış numuneler üzerinde direkt kesme deneyi, serbest basınç deneyi, su tutma eğrisi, zemin permabilite çalışmaları gerçekleştirilmiştir. Öte yandan, arazi birim hacim ağırlık ve kanatlı kesici deneyleri de yapılmıştır. Malzemelerin göreceli olarak gevşek, çoğunlukla ince daneli (düşük ve yüksek plastisiteli silt, yüksek plastisiteli organik zeminler) oldukları, düşük pH değerlerine sahip zeminler oldukları tespit edilmiştir. Direkt kesme deneyi örselenmemiş ve laboratuvarda

hazırlanmış numuneler üzerinde yapılmıştır. Örselenmemiş numuneler üzerinde gerçekleştirilen direkt kesme deneylerine göre zeminlerin efektif içsel sürtünme açıları 31.1-38.0 derece aralığında bulunmuştur. Laboratuvarda hazırlanmış örnekler üzerinde gerçekleştirilen direkt kesme deneylerinde ise zemin doygunluk derecesinin hem kesme mukavemetine hem de zeminin hacimsel davranışına önemli ölçüde etki ettiği görülmüştür.

Anahtar Kelimeler: Yağmurla Tetiklenen Heyelanlar, Rezidüel Zemin, Volkanik Zemin, Direkt Kesme Deneyi, Kurutma

To the people who lost their lives due to landslides…

ACKNOWLEDGEMENTS

TABLE OF CONTENTS

LIST OF TABLES

TABLES

LIST OF FIGURES

FIGURES

CHAPTER 1

INTRODUCTION

"Landslides are one of the most widespread and effective agents in sculpting the earth's surface" (Eckel, 1958), and they generally result in devastating consequences, such as economic loss and casualties. According to Schuster (1996), the annual economic losses resulting from landslides for United States, Japan, Italy and India exceed 10 billion US dollars. Although different causes exist for a landslide to occur, according to Sidle and Ochiai (2006), prolonged or intense rainfall incidents caused about half of the 40 most devastating landslide disasters around the world. Also, in most of the world's mountainous areas, landslides are triggered by rain infiltration (Iverson 2000).

Similar to other parts of the world, landslides also pose a significant threat to human lives and property in Turkey. Indeed, landslides are the second most destructive natural hazards after earthquakes in Turkey (Ildır 1995, Reis and Yomralıoğlu 2005). Although various factors are effective for a landslide to be triggered, the most important landslide triggering factor in northern Turkey (especially in Rize region) is rainfall. In fact, most of the landslides in Turkey were found to be related to rainfall (Okalp and Akgün 2016).

1.1. Problem Statement

Due to rainfall-triggered landslides in Rize many houses, roads and farmlands are significantly damaged every year, which in some cases result in casualties (Figure 1.1). Based on the records between 1973-2010, in Rize, annual casualties due to landslides range from 1 to 32 (Filiz et al. 2011). In particular, on 26 August 2010, heavy rainfall triggered landslides in Gündoğdu town (Figure 1.1) which resulted in 13 casualties, 174 destroyed houses and 96 houses requiring repairs (Yılmaz 2010).

Approximately 6.5 million US dollars were spent by the national government for the repair of infrastructure such as water pipelines, sewage systems, roads, etc. and 1276 farmers and their 30 million m² farmland (mainly tea plantation areas) were affected (Yılmaz 2010). Recorded daily rainfall was 166.2 mm on the day before the disaster and 52.5 mm on the day of the disaster (Filiz et al. 2011), hence within 2-days, more than the average August monthly rainfall (which is 195 mm according to Turkish State Meteorological Service (TSMS) was received.

(a)   (b)

Figure 1.1. (a) Rainfall triggered landslides in Rize city, Gündoğdu town 2010, (b) examples of rainfall triggered landslides in Rize city, Çayeli county, Yeşiltepe village in 2017 (photos from AFAD, 2018)

One of the mitigation methods used worldwide for rainfall-triggered landslides is to establish rainfall intensity-duration (I-D) threshold that can trigger a landslide. There are many studies in the world, as well as in Turkey, about the early-warning and prediction of these incidents. To establish thresholds for early prediction and warnings, previous records of slope failures are usually used. The application of these methods relies on the assumption that previous rainfalls which triggered a landslide before, will be likely to trigger another landslide in the future (Lu and Godt 2013). However, some of the limitations of these statistical rainfall thresholds are discussed in Ahmadi-adli et al. (2012). Moreover, the occurrence of landslides in response to rainfall involves transient infiltration of water into the unsaturated slope, in which soil hydraulic properties play an important role (Iverson 2000). Similarly, the effects of

unsaturated soil properties on the intensity-duration threshold for rainfall-triggered landslides are demonstrated (e.g, Ahmadi-adli et al. 2014, Kenanoglu et al. 2019).

Even though the city of Rize has been suffering from these catastrophic rainfall-induced landslides every year, the data on soil type and properties are yet rather limited. For future studies on numerical modeling of the mechanism, landslide stabilization works, spatial planning, landslide susceptibility mapping and rainfall intensity-duration thresholds, it is crucial to identify the soils related to these landslides. Thus, the lack of and the need for information about material properties in rainfall-triggered landslide sites in Rize is the primary motivation for this study.

1.2. Research Objectives

The main goal of this study is to investigate the properties of soils involved in rainfall-triggered landslides in Rize region. The investigation includes (i) characterizing the soil types, (ii) determination and evaluation of mechanical and physical properties of these soils. The results of this study are believed to be useful for future studies on rainfall-triggered landslides in Rize.

1.3. Structure of the Thesis

A brief overview of the literature is presented on landslide definition and classification, fundamentals of some of the basic unsaturated soil mechanics concepts, recent studies on landslides in Rize, regional geology and some properties of residual soils in chapter 2. In chapter 3, field and laboratory work is presented comprehensively. In chapter 4, the results of the test results are presented without any further comment or discussion. The results of the study are discussed and compared with the available literature in chapter 5. In chapter 6, the overall findings of the study are summarized, and some recommendations for the possible future research on this subject are given.

CHAPTER 2

LITERATURE REVIEW

2.1. Landslide definition and classification

According to Varnes (1958) and Cruden and Varnes (1996), landslides can be defined as "the movement of a mass of rock, debris or earth down a slope". Varnes (1978) classified the landslides mainly based on the types of movement and the type of material involved (Table *2.1*). Later, Cruden and Varnes (1996) suggested a naming sequence, such as activity, rate of movement, moisture content, material and type of movement for the description of landslides. The velocity classification of landslides suggested by Cruden and Vernes (1996) is shown in Figure 2.1.

Table 2.1. *Classification of landslides (Varnes, 1978)*

Type of movement		Type of Material		
		Bedrock	Engineering soils	
			Predominantly coarse-grained	Predominantly fine-grained
Fall		Rock fall	Debris fall	Earth fall
Topples		Rock topple	Debris topple	Earth topple
Slides	Rotational	Rock slump	Debris slump	Earth slump
	Translational	Rock block slide	Debris block slide	Earth block slide
		Rock slide	Debris slide	Earth slide
Lateral spreads		Rock spread	Debris spread	Earth spread
Flows		Rock flow (deep creep)	Debris flow	Earth flow
			(soil creep)	
Complex		Combination of two or more principal types of movement		

Extremely slow	Very slow	Slow	Moderate	Rapid	Very rapid	Extremely rapid

Velocity (mm/sec) 0.5×10^{-6} 50×10^{-6} 5×10^{-3} 0.5 50 5×10^{3}
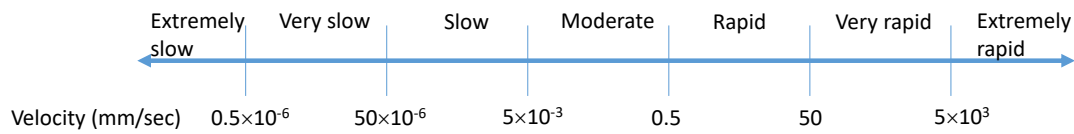
Figure 2.1. Velocity classification of landslides (Cruden and Varnes 1996)

2.2. Mechanism of rainfall-triggered landslides

Slope failure occurs when forces or stresses acting upon it exceeds the strength of the earth material, and heavy precipitation (due to rainfall or snow melting, etc.) is the most encountered cause for triggering a landslide (Lu and Godt 2013). Some of the rainfall-triggered landslides occur suddenly and they reach orders of kilometers runout distances at high travel speeds. Since the destructiveness of a landslide is proportional to its velocity (Lu and Godt 2013), rainfall-triggered landslides can be extremely hazardous. According to Lu and Godt (2013) precipitation-induced landslides can be explained using two models in the unsaturated zone. The two conceptual ways are: (1) using classical soil mechanics, (2) using unsaturated soil mechanics.

Classical soil mechanics explains precipitation-induced landslides by increasing pore pressures (Terzaghi 1950). On the other hand, unsaturated soil mechanics evaluate the change in the state of stress of soil due to infiltration and the resulting reduction in matric suction (Lu and Godt 2013), which contributes to shear strength as the degree of saturation of soil decreases (Lu and Likos 2004, Fredlund et al. 2012). A visual explanation of the triggering mechanism using unsaturated soil mechanics is given in Figure 2.2 (Ahmadi-adli 2014).

Focusing on the initiation of the failure, the unsaturated slopes are stable due to existing suction. However, as the rainfall starts and penetrates into the ground (infiltration), the unsaturated shear strength starts to decrease. Depending on the intensity and duration of the rainfall, the failure may take place or not.

6
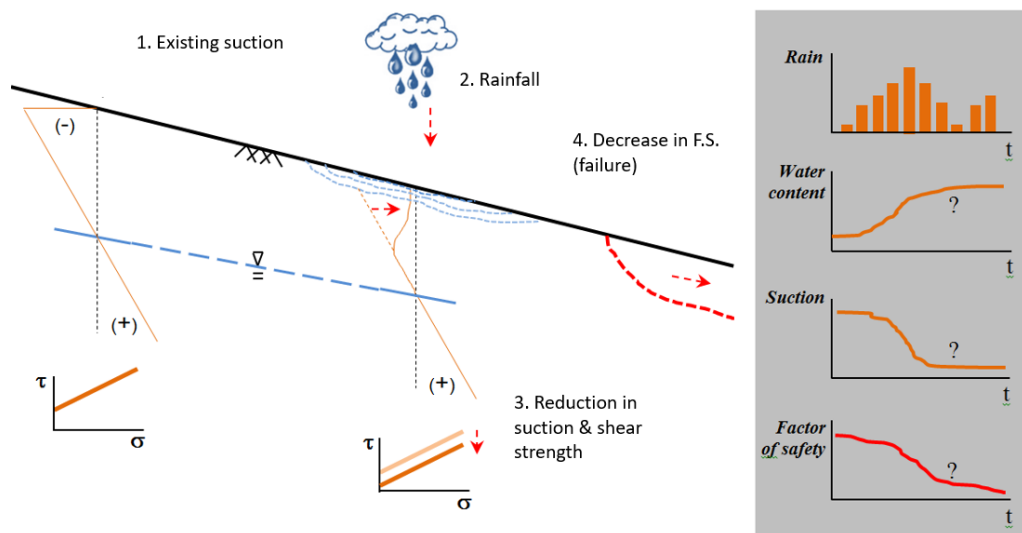
Figure 2.2. Schematic illustration of triggering of rainfall-induced landslides in unsaturated soils
(after Ahmadi-adli 2014)

2.3. Studies on landslides in Rize

Rainfall-triggered landslides in Rize are shallow landslides (failure depth about 3-5 m), and are classified as "rapid-very rapid" according to the velocity classification of Cruden and Varnes (1996) (Nefeslioğlu et al. 2011). Approximately 95% of the landslides in Rize occur on steep slopes and among the completely weathered rocks (Reis et al. 2008, Yalcin 2008). These materials are unsaturated residual soils decomposed from different volcanic rocks as described by Nefeslioglu et al. (2011). Nefeslioglu et al. (2011) noted that residual soils of basalts, andesitic lavas and pyroclasts are the lithologies most prone to shallow landslides in Rize. Landslides in Black Sea region are investigated since the early 1980s (Önalp, 1980, Önalp et al. 1987). There are a number of studies in the literature focusing on the landslides in Rize, such as landslide susceptibility mapping (Yalcin 2005, Akgün et al. 2008, Yalcin and Bulut 2007, Nefeslioglu et al. 2011, Dağ and Bulut 2012, Kaya et al. 2018) and land-use planning (Karsli et al. 2009, Reis et al. 2009); in terms of rainfall intensity-duration threshold and meteorological early warning (Reis et al. 2008, Baltaci 2010); and in terms of characteristics of soils (Tarhan 1991, Önalp 1991). Moreover, there are some studies in terms of agricultural aspects (Yuksek and Yuksek 2009).

Yalçın and Bulut (2007) conducted studies focusing on landslide susceptibility mapping in Ardeşen (Rize). They used Geographic Information System (GIS) and digital photogrammetric techniques and concluded that 28% of the region is under threat of landslides.

Akgün et al. (2008) studied landslides in Fındıklı (Rize) region. They used likelihood-frequency ratio and weighted linear combination models for their study. They produced susceptibility maps for Fındıklı region using two different models. They also noted that the main trigger of the landslides in the area is heavy rainfall.

Reis (2008) studied the land-use changes in Rize (covering about half of the city) by using remote sensing and GIS, and concluded that the main land-use change occurred between the period of 1976-2000. Reis (2008) noted that the forest area decreased by about 12100 ha, whereas tea cultivation areas increased about 13700 ha during this time period.

Reis et al. (2008) studied the precipitation and landslide relation in Rize. They noted that uncontrolled tea plantation has a major effect on the increase in the soil moisture since the surface run-off is restricted and infiltration into the ground increases.

Karsli et al. (2009) studied the effect of land-use changes on landslides in Ardeşen (Rize). They evaluated the landslides using a series of historical aerial photographs taken between 1973 to 2002. They noted that residents destroyed the forests for tea cultivation. They underlined that the landslide occurrence increased due to unplanned expansion of tea plantation and settlement areas. They also noted that the topography and the frequently occurring heavy rains are the main factors for the trigger of landslides in Ardeşen. They concluded that the slope, lithology, surface roughness, land cover type and proximity to roads have crucial effects on landslides occurrence. Moreover, they observed that 95% of the landslides occurred in highly or completely decomposed materials.

Nefeslioğlu et al. (2011) studied landslides in Çayeli (Rize) in terms of hazard mapping, and noted that frequency and the magnitudes of the events increased over

time. That is, the magnitude of the failures was about two to ten times greater after 1990 compared to before 1990. The mean slope gradient value on which the shallow landslides mostly occur is reported to be 29°. Also, no failure has been observed in the catchment above the slope gradient value of 50°.

2.4. Regional geology of the sampling sites

Regional geology is mostly governed by volcanic originated, young units, and due to the origin of the units and meteorological conditions, weathering occurs rapidly (Önalp 1980). According to Önalp (1980), the soils are originated from volcano-sedimentary rocks. Some of the soils were originated from the weathered lavas and tuffs, whereas some other residual soils were originated from weathering of rocks due to meteorological and vegetative effects. Nefeslioglu et al. (2011) noted that the Upper Cretaceous-aged basalts, andesitic lavas and pyroclasts are the lithologies most prone to shallow landslides in the catchment, and approximately 60% of the failures occurred in the residual soils of this volcanic succession.

Gedik et al. (1992), Tüysüz et al. (2008) and Alan et al. (2019) studied the geological formations of the related sites. However, here, the formations of the 12 landslide sites in this study are described briefly. Further information about other formations in Figure 2.3 can be found in Alan et al. (2019). The map of geologic formations in the region is shown in Figure 2.3, together with the location of 12 landslide sites in this study. Residual soils in Rize are weathering products of Tertiary alkaline volcanic, pyroclastic rocks and rhyolitic tuffs with basaltic-andesitic characteristics. The subtropical environment and humid climate of the region are known to promote intense chemical weathering of exposed and shallow subsurface volcanic units. According to Alan et al. (2019), *Caglayan formation (Kcl)* is composed of sandstone, marl and limestone, alternating with basaltic, andesitic lava and pyroclastics; *Cayirbag formation (Kcb)* mainly consists of rhyolite, dacite, pyroclastics, sandstones and limestones constituting the phases of acidic volcanism products; *Melyat formation (Tem)* is composed of andesitic and basaltic lavas, pyroclastic rocks and

sandstone and claystone; ***Pazar formation (Tmp)*** is composed of Early-Middle Miocene age sandstone, marl, conglomerate (mainly of volcanic origin) and claystone; ***Kackar granitoyid 2 (Tekg)*** is composed of granite, tonalite, diorite, gabbro and gabbro porphyry.
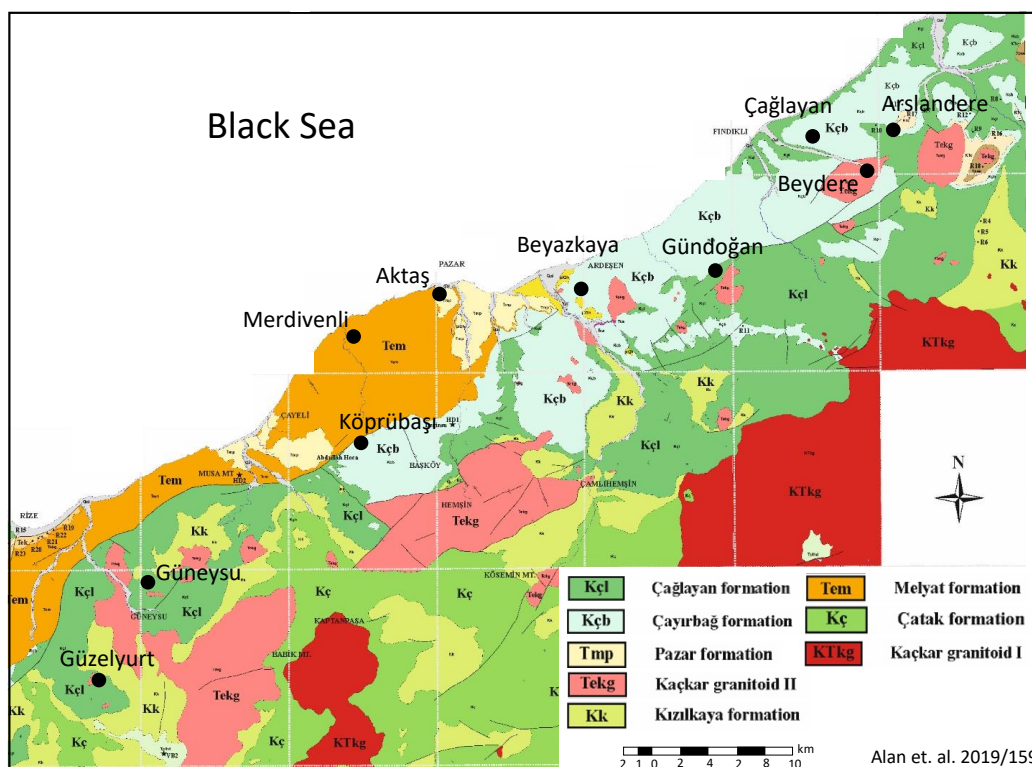
Figure 2.3. Location of the sampling sites on the geologic map of the study area in the city of Rize (adapted from Alan et al. (2019)

2.5. General properties of residual soils

The main concepts of "classical" soil mechanics are found to be inapplicable to the behavior of residual soils (Vaughan 1985). Residual soils are originated from the weathering (chemical or physical) of the underlying rock (Townsend 1985, Wesley 2010). Due to their process of formation, residual soils are less dense and weaker than soils formed from sedimentary rocks (Wesley 2010). Furthermore, residual soils tend to be more heterogeneous than sedimentary soils, and some soil mechanics concepts,

such as stress history, consolidation state (normal or over consolidation) do not pose any significance to residual soils (Wesley 2010). There are also some special clay minerals that exist only in residual soils, such as allophane and halloysite (Wesley 2010). In the literature, some researchers questioned the usage of some index tests and classification systems for residual soils (De Graft-Johnson and Bhatia 1969, Huvaj and Uyeturk 2018). They argued that the classification of these soils may be interpreted wrongly in the laboratory due to sample preparation techniques. Huvaj and Uyeturk (2018) discussed the effects of drying on Atterberg limits on residual soils of volcanic origin and concluded that drying changes the Atterberg limits (e.g. 30% decrease in liquid limit due to drying is reported) and may even change the soil classification. Similarly, Wesley (2010) suggested avoiding air or oven drying before testing if the soil is volcanic originated. Furthermore, according to Morin and Todor (1975) excessive mixing and drying changes the location of the soil on the plasticity chart.

Another important aspect about residual soils is the slope stability. Since the water table is below the slip surface in many slopes governed by residual soils, most of these slopes are stable due to suction (Wesley 2010). Furthermore, cohesion intercept due to suction and weak bonds between particles makes slopes remain stable at steeper angles (such as 45° or more), and therefore they are of significant importance for slope stability (Wesley 2010, Hürlimann et al. 2001).

Furthermore, the idealized soil profile and horizons for humid climates is shown in Figure 2.4. Although site specific thicknesses of different horizons are not available in Rize, the soil samples are believed to be taken from Horizon B, where completely weathered parent material exists.
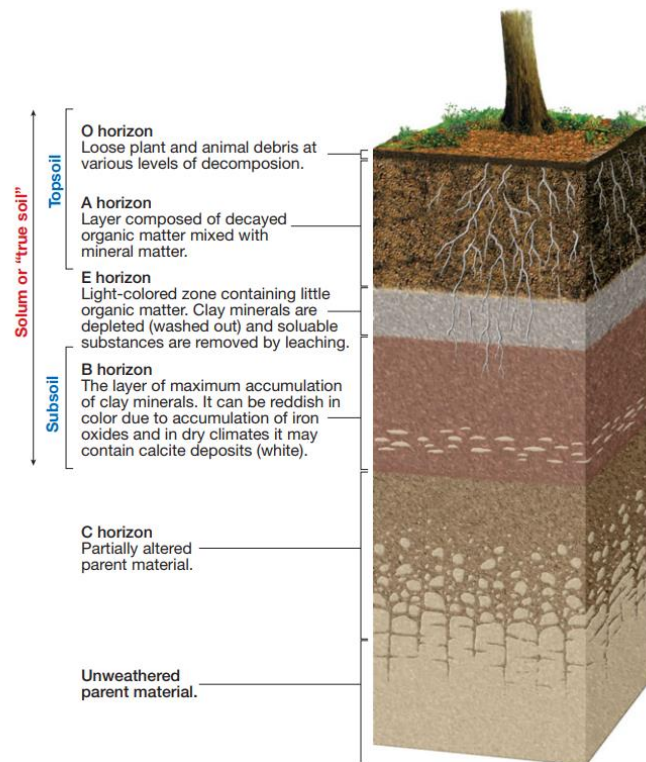
Figure 2.4. Idealized soil profile from humid climate (after Tarbuck et al. 2012)

2.6. Basic concepts of unsaturated soil mechanics

2.6.1. Soil suction

Total soil suction quantifies the thermodynamic potential of soil pore water relative to a reference potential of free water (Lu and Likos 2004). There are two contributors to the total soil suction: (1) osmotic suction, (2) matric suction. Osmotic effects in soils are caused by the dissolved solutes concentrations. Matric suction is the result of both capillarity effects (shape of the air-water interface) and short-range adsorption effects (electrical and van der Waals force fields around the soil-water interface) (Lu and Likos, 2004). Soil suction plays a crucial role in soil mechanics since it affects the shear strength, compressibility, swelling and permeability characteristics.

2.6.2. Soil water retention curve (SWRC)

In unsaturated soil mechanics, the soil-water retention curve (also known as soil- water characteristic curve) stands for a fundamental constitutive relationship (Lu and Likos, 2004), and it is the most important soil property to measure, which is used to interpret the key relationships of unsaturated soils properties (Fredlund et al. 2012). SWRC constructs the relationship between soil suction and soil water content. There are two main SWRCs exist based on suction application: (1) drying (desorption) SWRC, (2) wetting (adsorption) SWRC (Figure 2.5). In general, drying SWRCs can be obtained by a sequential suction increase, whereas wetting SWRCs can be obtained by a sequential suction decrease. More specifically, to obtain a drying curve, a saturated specimen is subjected to suction increments to drain the pore water. Up to a certain point (air-entry pressure), approximately constant water content values are observed with increasing suction values (Figure 2.5). Having reached this point, bulk water starts to drain from the pores in response to applied suction. The drainage of the bulk water continues until the residual water content point is reached. After the residual water content point, some residual water remains on the solid surface even if the suction is increased. Furthermore, once the residual suction is exceeded, vapor flow starts to dominate the moisture flow and liquid flow ceases (Frudlund et al. 2012).

In the wetting direction, the reverse of the physical phenomena observed in the drying direction occurs. The specimen having the residual water content starts to absorb water as the suction decreases. However, the last point of the wetting curve may differ from the start point of the drying curve due to entrapped air in the wetting process. Typical examples SWRCs for wetting and drying paths are given in Figure 2.5.
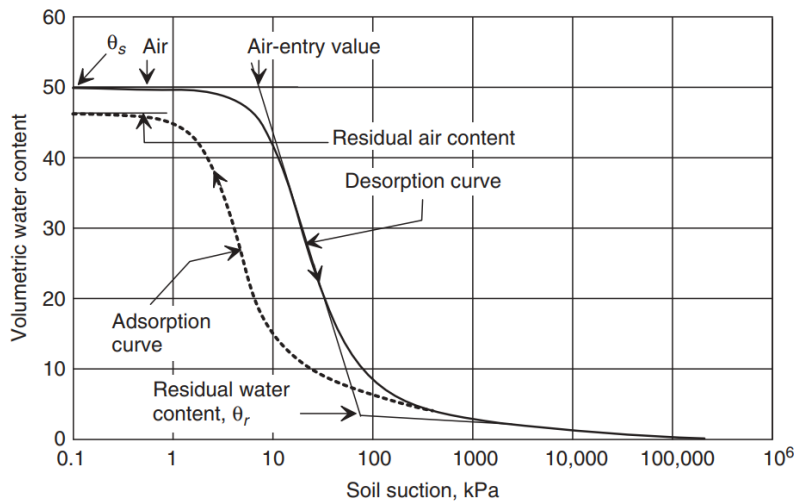
Figure 2.5. Typical SWRC in wetting and drying directions (after Fredlund et al. 2012)

As illustrated in Figure 2.5 the SWRCs for wetting and drying directions are hysteretic in nature. That is, no unique curve exists for representing for both wetting and drying direction.

2.6.2.1. Methods for generation of SWRC

There are two main methods for generating SWRCs: (1) direct laboratory experiments, (2) estimation techniques.

Various methods exist for laboratory determination of SWRC curves, and ASTM D6836 standardizes four methods for drying (desorption) path: (1) hanging column, (2) pressure plate extractor, (3) chilled mirror hydrometer, (4) centrifuge techniques. Although the results of the different methods are in good agreement, their applicability differs in terms of the suitable suction ranges. For example, hanging column is suitable for suction range of 0 to 80 kPa, whereas chilled mirror hydrometer is suitable for suction measurement greater than 1000 kPa.

Direct measurement of SWRCs is time-consuming, and requires trained personnel as well as special equipment. However, various estimation methods for SWRCs can be

found in the literature. Some of these estimation methods are based on the grain size distribution (Arya and Paris, 1981, Sattari and Toker 2016), and some others are based on regression models (Brooks and Corey, 1964).

2.6.3. Shear strength of unsaturated soils

In unsaturated soils, the state of stress is fundamentally different compared to saturated soils (Lu and Likos, 2004). While the saturated soils are two-phase systems (solid and liquid only), unsaturated soils are three-phase systems which are comprised of solid, liquid and gas. The behavior and response of unsaturated soils are significantly affected by the relative amounts of pore water and pore air. In saturated soils, the pore water pressure is compressive, whereas in unsaturated soils the pore water can withstand very high negative pore pressures resulting in creating a tensile force (Lu and Likos 2004). Thus, the effect of pore water is to reduce the effective stress for saturated soils, whereas, the end result of the pore water is to increase the effective stress through creating a tensile force and pulling the grains together for unsaturated soils (Lu and Likos, 2004).

The shear strength of saturated soils can be evaluated by using the Mohr-Coulomb failure criterion together with effective stress concept (Terzaghi, 1936):

$$\tau = c' + \sigma' \tan(\phi') \qquad (2.1)$$

Where:

τ = shear stress on the failure plane at failure

c' = effective cohesion

σ' = effective normal stress on the failure plane at failure

ϕ' = effective angle of internal friction

Bishop (1959), suggested an effective stress equation for unsaturated soils to account for the suction effects:

$$\sigma' = (\sigma - u_a) + \chi(u_a - u_w) \qquad (2.2)$$

Where:

σ = total stress

u_a = pore air pressure

u_w = pore water pressure

$(u_a - u_w)$ = matric suction

χ = Bishop's effective stress parameter depending on the degree of saturation (equal to 0 for saturated soils, 1 for dry soils)

The effective stress equation suggested by Bishop (1959) can be used to calculate the shear strength of unsaturated soils as:

$$\tau = c' + [(\sigma_n - u_a) + \chi(u_a - u_w)]tan\phi' \qquad (2.3)$$

Various approaches exist in the literature for the effective stress parameter χ. For example, according to Oberg and Sallfors (1995), for engineering purposes χ parameter can be taken equal to the degree of saturation. Similarly, Karube et al. (1996) used the effective degree of saturation concept and calculated the parameter as:

$$\chi = S_e = \frac{Sr - S_{res}}{1 - S_{res}} \qquad (2.4)$$

Where:

Sr = degree of saturation

S_e = effective degree of saturation

S_res = degree of saturation at the residual condition

Fredlund and Morgenstern (1977) introduced another shear strength formula for unsaturated soils:

$$\tau' = c' + (\sigma_n - u_a)tan\phi' + (u_a - u_w)tan\phi^b \qquad (2.5)$$

Where:

ϕ^b = angle indicating the rate of increase in shear strength with respect to a change in matric suction

Geometrical representation of Equation (2.5) is called the extended Mohr-Coulomb envelope (Fredlund et al. 2012), and is illustrated in Figure 2.6.
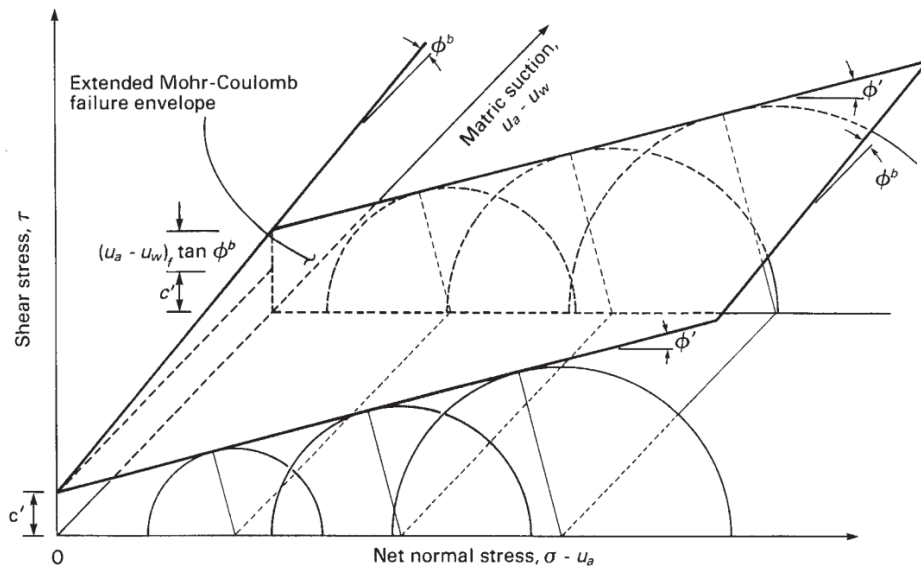
Figure 2.6. Extended Mohr-Coulomb failure envelope for unsaturated soils (adapted from Fredlund et al. 2012)

The parameters χ and $tan\phi^b$ are similar. Equating the shear strength equations proposed by Bishop et al. (1960) and Fredlund and Morgenstern (1977) one can obtain:

$$\chi = \frac{tan\phi^b}{tan\phi'} \qquad (2.6)$$

Lu and Likos (2006) presented the concept of suction stress characteristic curve (SSCC) for evaluating the effective stress in unsaturated soils, and proposed a suction stress equation similar to Terzaghi's effective stress:

$$\sigma' = (\sigma - u_a) - \sigma^s \qquad (2.7)$$

$$\sigma_s = -\frac{\theta - \theta_r}{\theta_s - \theta_r}(u_a - u_w) \qquad (2.8)$$

Where:

σ^s = suction stress

θ = volumetric water content

θ_r = residual volumetric water content

θ_s = saturated volumetric water content

CHAPTER 3

FIELD AND LABORATORY WORK

Investigation of the rainfall-induced landslides in this study is divided into two main parts: (i) field work and (ii) laboratory work. In the field work, disturbed and relatively undisturbed soil samples are collected for laboratory investigation and in-situ hand vane tests are conducted. In the laboratory work, physical and mechanical properties of the soils were determined.

3.1. Field work and sample collection

The aim of the field work is to obtain soil samples to conduct further laboratory experiments on natural soils, and to carry out hand vane tests. For this purpose, three trips were made in April 2017, July 2017 and August 2018 to Rize, where from around 40 soil samples were collected from 12 landslide sites in 10 villages. The names of the villages are indicated on digital elevation model in Figure 3.1. Photographs from some of the sampling sites are shown in

Figure 3.2. The main site selection criteria in the study was to obtain soil samples from rainfall-induced landslides areas. Thus, the sampling sites had the same failure mechanism.
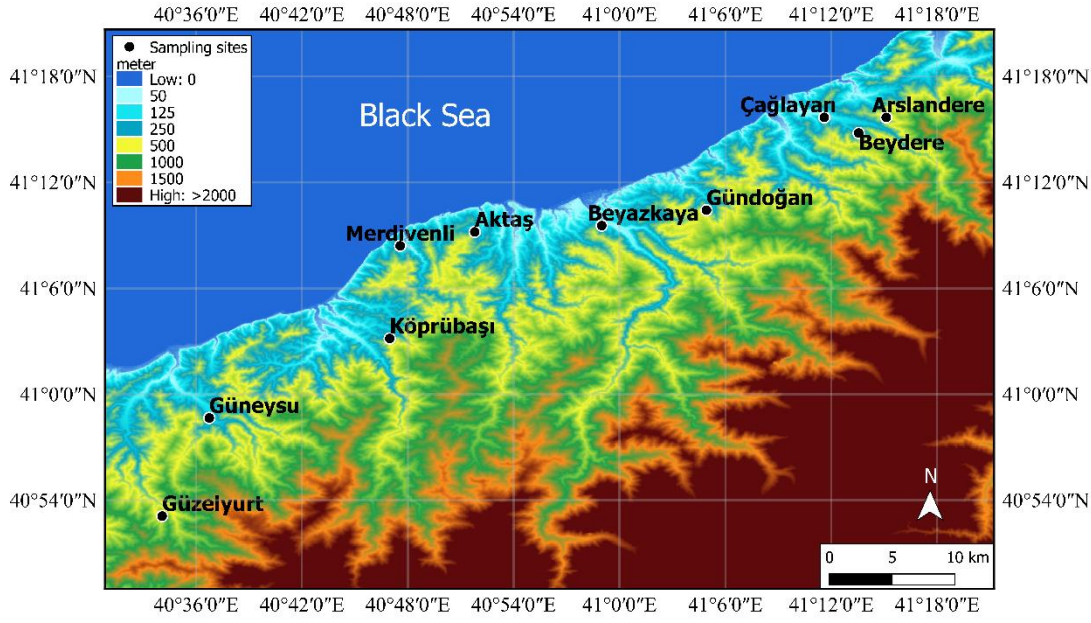
Figure 3.1. Location of the landslide sites on digital elevation model (data from Jarvis et al. 2008)

Sites in Rize are in Fındıklı county-Beydere village (site 1), Fındıklı county-Çağlayan/Arslandere village (site 2), Çayeli county-Köprübaşı village (site 3), Pazar county-Aktaş village (site 4), Fındıklı county-Çağlayan village (site 5), Pazar county-Merdivenli village (site 6), Ardeşen county-Gündoğan village (site 7), Ardeşen county-Beyazkaya village (site 8), Güneysu county (site 9), Güzelyurt county (site 10, 11, 12) (in Güzelyurt region samples were collected from three different landslide sites. Therefore, Güzelyurt region is regarded as site 10, 11 and 12).

Site #1

Site #2

Site #3

Site #4

Site #5

Site #6

Site #7

Site #8

Site #9   Site #10
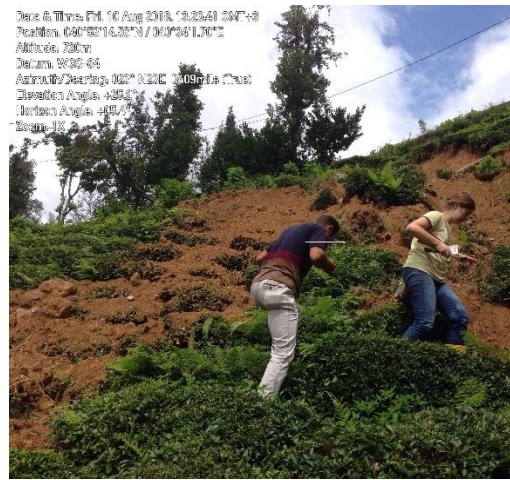
Site #11   Site #12

Figure 3.2. Landslide sites where samples are collected

Soil sampling was performed where the rainfall-triggered landslides took place. In other words, soil samples were taken from already failed slopes. One important feature of the sampling sites is that all of them are the areas where there is tea plantation. The contribution of plant roots to shear strength also exists in hillslopes (Lu and Godt 2013); however, the roots of the tea plants (about 50 cm root length) are well above the failure surface in Rize region. Disturbed (bag) samples were taken from the moved mass as well as from the unmoved side scarp and head scarp zones, whereas intact samples were only taken from the side and head scarps. The sampling depths ranged

between 0.2 m to 5 m with respect to the original ground surface before failure. These depths are considered to be representative of soils involved in landslides, since these landslides occur at a maximum depth of around 5 m. Intact samples were taken by manually inserting small (3.6 cm inner diameter and 10 cm height) and large (7.5 cm inner diameter and 20 cm height) steel tubes in the ground (Figure 3.3). During the tube insertion process, as the tube is slowly pushed in to the soil, the soil around the tube is removed for easy penetration of the sampling tube. It should be noted that, because of the tube insertion process, these samples are not perfectly undisturbed. That is, although the in-situ water contents of the soils were preserved, the in-situ void ratio may not be perfectly kept the same.

Disturbed samples were placed in plastic bags and intact samples were sealed with paraffin (wax) in order to preserve in-situ moisture contents. All samples were carefully transported to Middle East Technical University-Civil Engineering Department's Soil Mechanics Laboratory and kept in a humidity room until testing.

3.1.1. In-situ hand vane tests

In-situ undrained shear strength is measured via a portable hand vane device at the sampling sites (Figure 3.3) to obtain the peak and remolded undrained shear strength values at different parts of the investigated landslide, such as on the shear surface, on the head scarp and side scarps. The blade had the aspect ratio of 2 (height to diameter). At each test location, vane test is carried out two or three times at locations that are a few cm distances apart, to check the repeatability of the results and/or soil variability and average results are reported for that site. After the peak resistance is obtained, the blades are continuously rotated (3 full rotations) to achieve remolded strength. The test is also conducted by inserting the blade in the horizontal direction (at another location, a few cm's away), to determine the anisotropy, if any.

Figure 3.3. Field works at different landslide sites, (a) Intact sampling by small tube insertion at the side scarp of one of the landslides in site 10-1, (b) Field vane test at site 7

3.2. Laboratory testing of soils

Laboratory experiments on disturbed and intact samples were carried out to determine the index properties, characteristics and the mechanical properties of soils. The soil mechanics tests were conducted at Soil Mechanics Laboratory of the Department of Civil Engineering at Middle East Technical University in Ankara, Turkey. Disturbed samples were used for grain size distribution, Atterberg limits and soil classification, in-situ moisture content, specific gravity, organic matter content, pH measurement, compaction curves, soil water retention curves, saturated hydraulic conductivity measurements, direct shear tests by reconstituting samples, soil-water retention curves (on the main wetting path), X-Ray diffraction (XRD) and scanning electron microscopy (SEM) studies. Intact samples were used for in-situ unit weight calculations, direct shear and unconfined compression testing. All of the experiments were conducted according to related ASTM standard. Furthermore, the laboratory tests performed for each sample is presented in Figure 3.4.

Site name	Sample	Grain size distribution	Atterberg limits	In-situ moisture content	Organic content	pH	Specific gravity	Unconfined compression	Direct shear (Intact samples)	Direct shear (Reconstituted samples)	Harvard compaction	SWRC and HC
Beydere	1-1	X	X	X	X	X	X					
	1-2	X	X	X	X	X	X			X		
	1-3	X	X	X	X	X	X			X		
	1-4	X	X	X	X	X	X					
Caglayan	2-1	X	X	X	X	X	X					
	2-2	X	X	X	X	X	X					
	2-3	X	X	X		X	X					
	2-4		X	X	X					X		
Koprubasi	3-1	X	X	X	X	X	X					
	3-2	X	X	X	X	X	X					
	3-3	X	X	X	X	X	X					
	3-4	X	X	X	X	X	X					
	3-5	X		X						X		
	3-6	X	X	X	X	X	X			X		
Aktas	4-1	X	X	X	X	X	X					
	4-2	X	X	X	X	X	X					
	4-3			X	X	X	X					
	4-4	X	X	X	X	X	X					
	4-5		X	X	X	X	X	X	X			
Caglayan	5-1	X	X	X	X	X	X					
	5-2	X	X	X	X	X	X					
	5-3	X	X	X	X	X	X	X	X			
	5-4	X	X	X	X	X						
Merdivenli	6-1	X		X	X	X	X					
	6-2		X	X	X	X	X					
Gundogan	7-1	X	X	X	X							
	7-2	X	X	X								
	7-3	X	X	X								
	7-4	X	X	X								
	7-5		X	X	X				X	X		
	7-6		X	X	X				X	X		
Beyazkaya	8-1	X	X	X	X							
Guneysu	9-1	X	X	X	X		X					
Guzelyurt	10-1	X	X	X	X		X	X		X	X	X
Guzelyurt	10-2	X	X	X	X		X	X		X	X	X
Guzelyurt	11-1	X	X	X	X		X	X		X	X	X
Guzelyurt	12-1	X	X	X	X		X			X	X	X

Figure 3.4. Performed tests on samples

3.2.1. Grain size distribution

To classify the soils, first of all, sieve tests were conducted. For grain size distributions, two different methods were used: (1) pre-drying the soil at 60ºC oven, then sieving the fine portion by washing. After the fine portion is washed, it is used in the hydrometer test, and the remaining portion was sieved through different opening sieves (sieve stack), (2) without any pre-drying, sieving the soil through 0.425 mm sieve by washing. After sieving through 0.425 mm sieve, the passing portion was directly used for hydrometer test and the remaining portion is sieved through sieve stack. To accurately determine the fines content of the samples, sieve by washing

technique (ASTM D1140-17) was employed, because it was observed that some of the soil particles (or aggregates) disintegrated when they came in contact with water (Figure 3.6) in samples from various sites.

Method (2) was used for soils labeled as 9, 10, 11, 12, and method (1) was used for the remaining. Since method (1) is widely used in practice the procedure will not be explained much in detail. However, the procedure for method (2) will be briefly discussed.

3.2.1.1. Test procedure for method #2

In this method, firstly some moist samples were separated from the whole batch of sample, and distilled water is added to obtain a soil slurry (Figure 3.5a). After mixing the solution, it was left overnight for complete disintegration of the particles (Figure 3.5b). Then, using distilled water the mud is sieved through 0.425 mm sieve (Figure 3.6). The passing portion is kept, and extreme care was given for not to lose any soil particles since they would later be used in the hydrometer test (Figure 3.5b). However, this method may result in having too much soil slurry needed for the hydrometer test simply because as the soil plasticity increases, it becomes difficult to wash it through a small opening sieve. In fact, the sieving process for all of the samples resulted in too much soil slurry, and since the portion had fine particles it became difficult to get rid of the extra slurry (due to suspension of fine particles). Therefore, the slurry was divided into two identical portions in order not to obtain a non-homogenous soil slurry, special attention was given while splitting the soil slurry into portions for the hydrometer test. However, later it was decided to perform the hydrometer test for two different portions obtained in the splitting process to ensure that separation did not result in non-homogenous portions. Further details about the wet sieving process is given in Germaine and Germaine (2009).

Figure 3.5. (a) addition of distilled water, (b) soil slurry after mixing

Figure 3.6. Soil wet sieving through 0.425 mm sieve

3.2.2. Specific gravity

The specific gravity of the samples was determined based on ASTM D854-14. For specific gravity tests, two different methods were used: (1) pre-drying the soil at 60ºC oven, then sieving the soil through 2 mm sieve, (2) without and pre-drying, sieving the soil through 0.425 mm sieve in paste consistency before the testing.

Method (2) was used for soils labeled as 9, 10, 11, 12, and method (1) was used for the remaining.

3.2.3. Atterberg limits and soil classification

Atterberg limits tests were conducted according to ASTM D4318-17. While determining the liquid limit (LL), Casagrande cup method was preferred. In the test, after the specimen is placed into the cup, a groove is opened. By dropping the cup from a standardized height, energy is applied to the specimen. Thus, Casagrande cup method is a simulation of a miniature slope failure, and the energy necessary to fail a slope is measured in terms of water contents for a variety of water content ranges. (Germaine and Germaine 2009). Failure of the slope is reached when the groove is closed by a distance of 13 mm (continuously) at any point along the groove and the drop count necessary for the closure is proportional to the energy required for the slope failure.

For the Casagrande cup method, there are two different sub-methods: (i) multi-point method (ASTM D4318 Method A), (ii) one-point method (ASTM D4318 Method B).

In the multi-point method, the energy required for closing the 13 mm groove is determined at different water contents of the specimen. At least three data points (drop number against water content) is required. Having obtained the data points, the flow curve of the soil is generated, and the water content corresponding to 25 drops is the LL of the soil.

In the one-point method, the aim is not to generate the flow curve of the soil but rather obtaining one data point (drop number between 20 to 30) on the flow curve. In this method at least two trials are necessary to ensure the validity of the result. Then, the corresponding water contents are used to calculate the LL of the soil using the following equation:

$$LL = w \cdot \left(\frac{N}{25}\right)^{0.121} \tag{3.1}$$

Where:

LL = liquid limit (%)

w = water content (%)

N = number of drops of the Casagrande cup (between 20 and 30)

The plastic limits of the samples were determined by rolling the samples to 3.2 mm diameter by hand and taking water content at the time when the crumbling of the thread just starts at this diameter.

In this study, LL values were determined from wet to dry condition during the test (from low drop count to high drop count of the Casagrande cup) by allowing the soil samples to gradually dry at room temperature, frequently mixing them to achieve uniform drying. It was reported by Huang et al. (2009) that, a "wet to dry" procedure was believed to give a better representation of soil behavior. PL tests were conducted on a sample that was gradually dried at room temperature similar to LL test. It is important to note here that, after the hydration process in humidity room, no dry soil was added to wet soil to obtain drier condition, but rather, evaporation of the water was preferred to avoid any non-homogenous or non-hydrated part in the soil paste.

3.2.3.1. Specimen preparation for Atterberg limits tests

As mentioned earlier, the sampling was done in tea plantation areas. That is, in those areas biological activities such as decomposition of plant roots take place. Thus, the organic nature of the soils was also of concern for this research. According to the Unified Soil Classification System (USCS) (ASTM D2487), the organic nature of soils can be examined by comparing the LL values obtained from two different sample preparation procedures. Therefore, for soil classification, both of the methods described in ASTM D2487 were utilized so as to determine the LL_{Moist} and $LL_{110°C}$ of the samples.

To determine the LL_{Moist} value, sample preparation started from the in-situ water content, i.e. distilled water is added to soil in its natural moisture content state, as it came from the field, and the soil is sieved through No. 40 U.S. sieve (0.425 mm) in a wet/paste consistency (Figure 3.7b), whereas to determine $LL_{110°C}$, the soil sample is

first dried in an oven at 110ºC temperature, then it is pulverized to pass through No. 40 U.S. sieve and then distilled water is later added (Figure 3.7a). For both cases, the samples were left in humidity room for hydration according to ASTM standards. For the consistency of soil paste to be left for hydration at the humidity room, ASTM suggests mixing the soil with water at about 30 drop consistency. However, the author believes that using more water (resulting in lower drop count) is more reliable since by doing so, more water is provided for the soil particles to ensure that each particle gets hydrated as well as letting each particle to have access to water for obtaining a homogenous specimen. Thus, in this study, the author preferred consistency of about 5 to 10 for sample preparation. In fact, Germaine and Germaine (2009) also suggest 15 drop consistency for sample preparation. One drawback of using more water for sample preparation shows up while conducting the test. As stated before, since the evaporation of water at room temperature was preferred in this study, long time is needed to complete one test. Some samples used in Atterberg limits tests are shown in Figure 3.8.

Having determined the LLs with both preparation methods, the classification of the soils was done based on USCS. That is, according to USCS (ASTM D2487), soils are to classified as "organic" if $LL_{110ºC}/LL_{Moist}$ ratio is less than 0.75, where $LL_{110ºC}$ is the LL determined on samples dried at 110°C oven, and LL_{Moist} is the one determined on samples without any pre-drying.

(a)

(b)
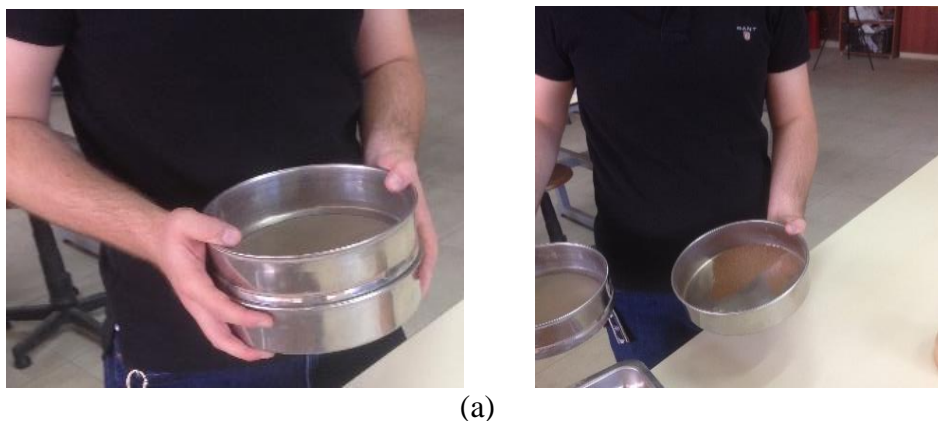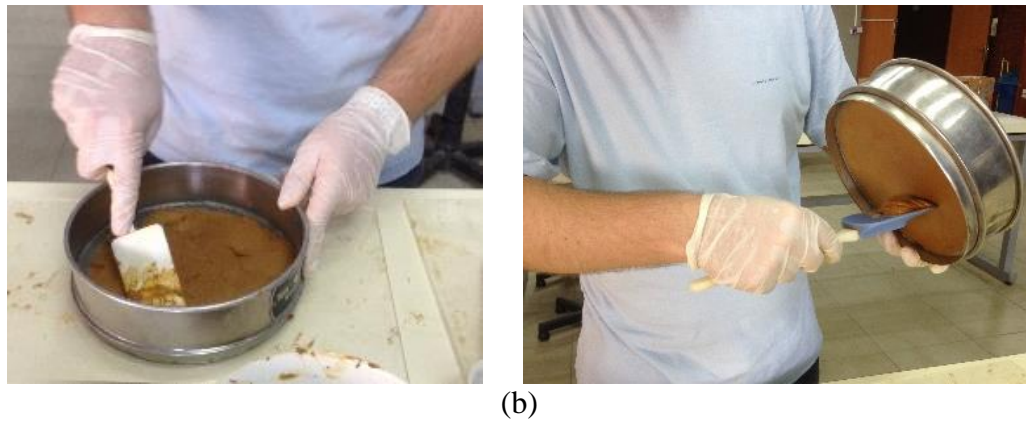
Figure 3.7. Sieving process for Atterberg limits tests (a) LL$_{110°C}$ samples, (b) LL$_{Moist}$ samples

Figure 3.8. Samples ready for Atterberg limits test

Furthermore, two more sample preparation methods were also performed to investigate drying effects on Atterberg limits. These preparation methods are the same as samples prepared for LL$_{110°C}$ tests, except the pre-drying temperatures were different: (i) at 60ºC, (ii) at 440ºC. These additional tests results were used for the investigation of drying effects only. Furthermore, the reason why 440ºC was selected is due to the fact that this temperature is used in organic content determination tests. Thus, after the organic contents of some of the samples was determined, the burned soils were used to determine the Atterberg limits.

3.2.4. Organic content determination

Soil classification regarding the organic nature of soils was done by using LLs determined from different sample preparation methods, described in the previous section. However, to quantify the organic matter contents, loss on ignition (LOI) method was also used. This method is also widely used in the literature for determination of organic contents of soils (Ball 1964, Skempton and Petley 1970, Huang et al. 2009, Huat et al. 2014, O'Kelly and Sivakumar 2014), and the method is standardized by ASTM D2974.

In the LOI method, firstly, the water content of the sample is determined, then the sample is burned at 440°C for a certain time. One important consideration in this test is the burning time at 440°C. In the related ASTM standard (ASTM D2974-14), the required time is not specifically described as constant time, but rather it is denoted as the samples must be kept in 440°C oven until dry mass is constant, and there is no further mass change. However, due to the high temperature it was observed that this approach may not be practical due to long times necessary for cooling and re-heating of the oven. In the literature, different time intervals for the burning of samples are suggested and used. Reddy (2015) gradually increased the temperature in the furnace to 440°C and left the samples in the furnace overnight. O'Kelly (2005) used 24 hours, O'Kelly and Sivakumar (2014) used 18 hours, Huang et al. (2009) used 16 hours and AASHTO T267 uses 5 hours.

In this study, determining the organic content of soils, firstly, 2 hours of burning time is used at 440°C furnace. Later, most of the samples are burned for 12 hours, and it is concluded that burning time can affect the results. In fact, 12 hours in 440°C furnace, gives slightly higher organic content percent, as compared to 2 hours of burning time. Later, for organic content determination, 12 hours was found to be sufficient. However, some of the samples could not be burned again for 12 hours, due to having a limited amount of soil. Therefore, it must be noted that for some of the samples

organic matter content may have been obtained slightly less, due to 2 hours of burning time. These samples are indicated while presenting the results.

In this study, the LOI tests were performed as follows: the moist soil samples (taken from sites) were first dried in 110°C oven to measure the water contents (which will be accounted later in the calculations) and dry mass is recorded. Then, the samples were again placed in the oven, and then the oven was brought to 440°C in 1 hour and samples were left in it for additional 12 hours (or 2 hours) and then the oven temperature was gradually decreased to about 100°C before removing the samples.

On the other hand, some researchers noted that in LOI test, heating temperature and heating duration can significantly affect the results, and the presence of select inorganic constitutes (such as hydrated alluminosilicates, carbonate minerals) can also lead to overestimated organic content especially at low organic content percentage (Christensen and Malmros, 1982, Howard and Hward, 1990, Huang et al. 2009). In fact, Huang et al. (2009) did not recommend LOI test to screen soils for the presence of small percentages (<10%) of organic matter.

3.2.5. pH of the samples

Measurement of soil pH values was done based on ASTM D4972. The measurements were performed by means of a potentiometer having an electrode system (Method A). To conduct the test, suspensions were prepared from soils that were passed through 2 mm sieve, and the pH values were measured.

3.2.6. Mineralogy of the samples

Mineralogy of the samples were investigated using both X-ray diffraction (XRD) and Scanning Electron Microphotographs (SEM).

For XRD analyses, the samples were ground with Retsch RS 200 tungsten carbide grinding equipment, and the bulk powder is analyzed at 2° 2θ/s step sizes and scanned from 2 to 65° 2θ CuKα. Using Inorganic Crystal Structure Database (ICSD) of

International Center for Diffraction Data by MDI Jade 7.0 software the bulk powder analyses were conducted and their abundances are calculated by "Easy Quant" patch of the software using their peak areas and reference intensity ratios. For clay fraction analysis, the powder is sieved through ASTM Sieve No. 230 (0.062 mm mesh size) and two slides were prepared by using the "smear mount method" of Moore and Reynolds (1997). After the completion of analysis of air-dried slide of the sample, the same slide is left in the 60°C ethylene glycol vapor bath for 8 hours and then analyzed. The other slide is heated up to 550°C for 2 hours. All the clay fraction analyses are performed at 1°2θ/s step sizes and scanned from 2 to 27°2θ CuKα.

SEM photographs of the samples were taken at Middle East Technical University's Metallurgical Engineering Department to visually observe the shape and fabric of the particles. SEM analysis was done only for one sample. Furthermore, for one sample, SEM observations after different drying temperatures were made. In fact, observations at different drying temperatures were made simply because to correlate them with Atterberg limits found at different drying temperatures.

3.2.7. Moisture content- dry density relationship

To obtain moisture content-dry density relationship different methods exists in the literature, some of them are as follows:

- Laboratory compaction characteristics using standard effort (ASTM D698)
- Laboratory compaction characteristics using modified effort (ASTM D1557)
- Moisture-density relations of soils using Harvard compaction apparatus (Wilson, 1970, ASTM STP479)

Although the first two of above-mentioned procedures are standardized by ASTM, the last one is not. The usage of Harvard compaction apparatus is regarded as special procedure by ASTM.

In this study, to obtain moisture content-dry density relationship, Harvard compaction apparatus (Wilson 1970) was preferred. The main reason for selecting this method is that this method requires very small amount of material when compared to the other two methods.

3.2.7.1. Specimen preparation

To conduct the experiments, samples in the in-situ moisture content were first dried at room temperature in order not to affect the soil samples irreversibly due to drying temperature. Having dried the soils at the room temperature, soils were pulverized and sieved through 2 mm sieve. For every data point on moisture content-dry density relationship plot, a certain amount of water is added to air-dried and pulverized soil. Then, soil pastes in sealed containers were left in humidity room for two days before the experiment. The compaction was performed in three layers with 25 load applications (Figure 3.9). However, it must be noted here that Harvard compaction method may not be suitable at high water contents. For example, bleeding of water took place for some samples, or at high water contents grooves due to compaction rod were observed (Figure 3.10). Thus, wet of optimum sides of the compaction curves for some samples could not be obtained.

(a) Soil placement   (b) Load application   (c) Compacted soil
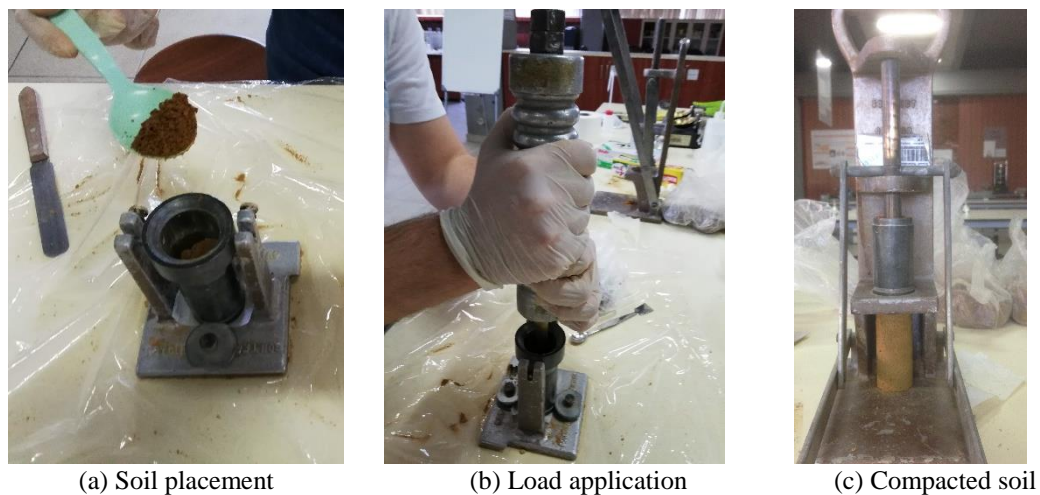
Figure 3.9. Harvard compaction test procedure

Figure 3.10. Encountered problems during Harvard compaction procedure

3.2.8. Unconfined compression tests

Unconfined compression tests were performed on intact samples, taken with small tubes. According to ASTM D2166, the height-to-diameter ratio of the specimens shall be between 2 and 2.5. Thus, specimens of around 35 mm diameter and 71 mm length were prepared using soils from small tubes (Figure 3.11). For the axial strain rate, 0.7 mm/min was selected. Moreover, the cylindrical area correction given in ASTM D2166 is employed:

$$A = \frac{A_0}{\left(1 - \frac{\epsilon_1}{100}\right)} \tag{3.2}$$

Where:

A is the average cross-sectional area during shearing

A_0 is the initial average cross-sectional area of the specimen

ϵ_1 is axial strain for the given load, expressed as a percentage

Figure 3.11. Specimen preparation for unconfined compression test from small tube samples

3.2.9. Direct shear tests

Direct shear (DS) test is the oldest method to quantify the shear strength of soils (Germaine and Germaine 2009). In this study, the shear strength characteristics of soils were investigated mainly by conducting DS tests. A total of 72 tests with intact specimens and 68 tests with reconstituted specimens were performed to investigate the mechanical properties of soils. Tests were conducted at consolidated-drained (CD) conditions according to ASTM D3080. The main reason for performing the direct shear tests under drained conditions is to evaluate the effective shear strength parameters. Furthermore, the drainage conditions for hillslopes lie between drained and undrained; thus, the effective stress with effective shear strength parameters should be used in slope stability analysis (Lu and Godt 2013). The requirement of the drained condition is that the shear rate must be selected such that no excess pore pressures is induced. To satisfy that requirement, the shear rates were selected based on t_{50}, or t_{90}, which are the times required for 50% and 90% average degree of consolidation, respectively. In conventional oedometer test, the top and bottom of the sample are pervious, that is, excess pore water pressure can only dissipate from top and bottom of the specimen. However, this is not the case in DS test. In DS test, in

addition to the top and bottom pervious boundaries, there is also a gap in the middle of the box (between the two halves of the shear box) which, in fact, changes the drainage length for the dissipation of excess pore pressure, and resulting in different consolidation times than the ones obtained from oedometer test. Thus, in this study, consolidation characteristics of soils were evaluated using DS test apparatus to mimic the excess pore pressure dissipation conditions during shearing.

The shear rates used in this study were determined as 0.016, 0.024, 0.037 mm/min following the requirements of ASTM D3080.

Another consideration in DS test is the soil to soil contact area. At the beginning of the experiment, the soil specimen is a continuum. As the shear distortion takes place, the lower part of the shear box moves relative to the upper part. As the displacement continues, the contact area of the two halves of the specimen decreases (Figure 3.12). To account for the decrease, an area correction may be applied while interpreting the results.
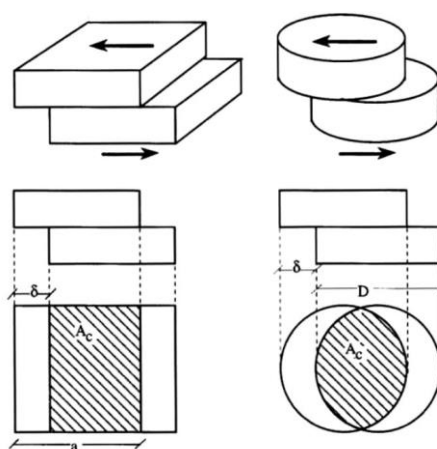
Figure 3.12. Change in contact area of the specimen (after Bardet, 1977)

However, it is noteworthy that the effect of the decrease in the contact area of the two halves is the same for normal and shear force. This means that if no cohesion exists in the specimen (the normal force is the only source of the shear resistance) the angle ϕ

will not be changed whether or not the area correction applied. When cohesion is expected, area correction should be done, which is also the case in this study.

Interpreting the results, the area correction was applied in this study as follows:

$$A_c = a(a - \delta) \qquad \text{for square box} \qquad (3.3)$$

$$A_c = \frac{D^2}{2}\left(\theta - \frac{\delta}{D}sin\theta\right) \qquad \text{for cylindrical box} \qquad (3.4)$$

where:

A_c is corrected area

$\theta = \cos^{-1}\left(\frac{\delta}{D}\right)$ in radians

δ is shear deformation

D is the diameter of the shear box

a is the side length of the square shear box

3.2.9.1. Specimen preparation

In this study, DS test were performed on intact and reconstituted samples in both saturated and unsaturated conditions (Figure 3.13).
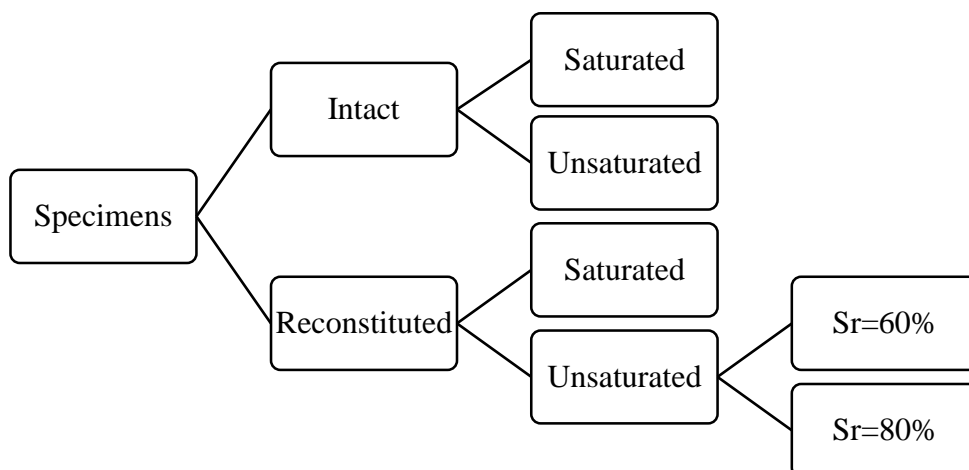
Figure 3.13. Specimens for direct shear test

Intact specimens

To prepare the intact specimens, first of all, soils in the sampling tubes were extruded into the cutting rings by means of a hydraulic piston (Figure 3.14a). The extruding rate was tried to be kept minimum in order not to disturb the soils in the sampling tubes during the extrusion process. The dimensions of the cutting rings used were 60-63 mm in diameter and 20 mm in height. Out of a 20-cm-long tube, typically 6 to 8 samples are extruded into rings, so that at least 3 different tests under different normal stresses in saturated and unsaturated conditions could be performed. A wire saw is used during the process (Figure 3.14b). Then, the rings with soil were wrapped with plastic film to conserve their moisture contents until testing.

| (a) | (b) | (c) |
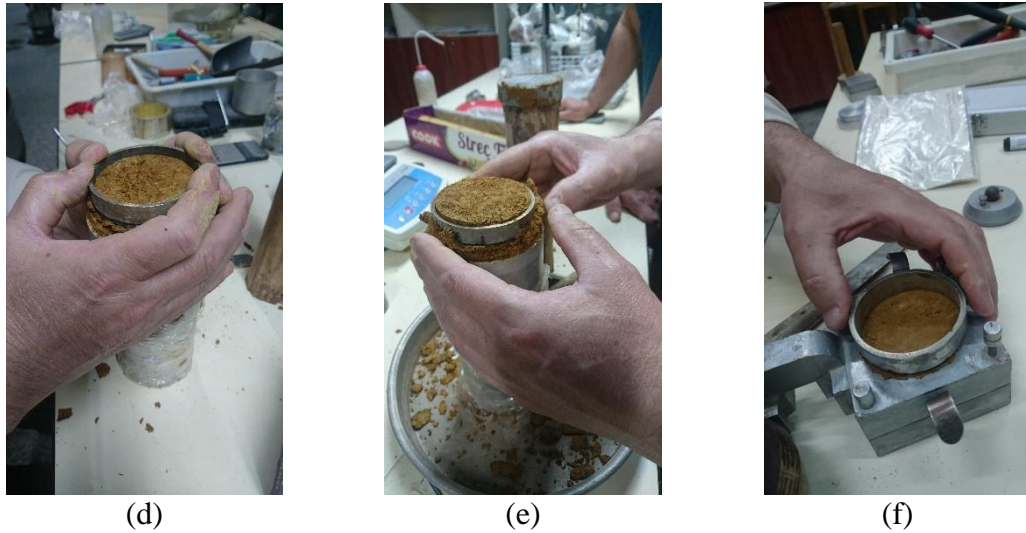
Figure 3.14. (a-b) Soil extrusion from sampling tube with hydraulic piston, (c) cutting ring separation with wire saw, (d-e) placement into rings, (f) specimen placement into the shear box

To start the testing procedure, cutting rings were placed on top of the shear box and soil in the rings were gently pushed into the shear box (Figure 3.14c). Then based on the testing condition the procedure given in section 3.2.9.2 were followed.

Reconstituted specimens

In order to study the shear strength characteristics of these soils at different degree of saturation conditions and at different densities, reconstituted samples are used. The aim when preparing reconstituted samples was to obtain a homogenous sample in terms of particle size distribution, water content distribution and to avoid possible impurities, such as plant roots. Reconstituted specimens were prepared from the samples taken from 3 different landslide sites in Güzelyurt village (sample #10-1,10-2, 11, 12).

To prepare the reconstituted samples, firstly, a homogenous batch of sample was needed. Thus, moist samples taken from sampling sites were first air-dried. Air-drying procedure was preferred so that samples could be prepared to the desired (controlled) water content and also because it is known that drying in oven at elevated temperatures causes irreversible changes in soils (Terzaghi et al. 1996, Huvaj and Uyeturk 2018).

Air-dried soils were then pulverized and sieved through 2 mm sieve, since maximum particle size of about 2 mm is required for the direct shear test. It may be noted here that the maximum particle size was selected based on the specimen dimensions to be used in direct shear testing. Having completed the sieving process, the necessary batch of samples were ready for specimen preparation.

Reconstituting a specimen requires various parameters, such as dry density (or void ratio) and preparation water content. In this study, in-situ dry densities of soils were preferred for reconstitution of samples, and preparation water contents were decided based on the test to be conducted (saturated test or unsaturated test).

Having decided the specimen dry density and preparation water content, the specimens can be prepared. Reconstituting a specimen for DS tests can be divided into two stages: (1) hydration stage, (2) compaction stage. In the hydration stage required amount of air-dried soil and distilled water are homogeneously mixed. After the mixing process, the soil-water mixture was wrapped with plastic film and the mixture was left in humid room overnight in order to obtain a sample with homogenous water content as well as to provide time for hydration of fine particles. In the compaction stage, the soil was placed in the shear box and it was compressed by means of a hydraulic press (or by hand, depending on the dry density) in one layer (Figure 3.15). Compacting the soil in one layer was deemed suitable since the height to diameter ratio of the container (shear box) is around 0.3.

One soil sample became like a soft paste when the required water was added for the saturated test. Thus, static compaction could not be performed for this soil and it was prepared differently. In this method, the shear box is filled with soil in paste consistency by using a spatula (Figure 3.15). Further details of this procedure is given in Huvaj-Sarihan (2009) and Maghsoudloo (2013). Special attention was given to ensure that no air bubbles were trapped in the specimen during preparation.

For every specimen, the preparation dry density was checked with water content measurements and amount of wet soil placed into the shear box. The preparation procedure is illustrated in Figure 3.15.

The target dry-density values for each sample are shown in Table *3.1*. For sample 12, tests with two different dry-densities were performed to investigate the density effects.

Table 3.1. *Target dry-density values for reconstituted direct shear tests*

Sample name	Target dry-density (g/cm³)
10-1	1.356
10-2	1.223
11	1.254
12	1.427
12	1.58

(a) soil placement for static compaction   (b) soil placement with spatula

<center>(c) soil compaction by hydraulic piston   (d) soil compaction by hand</center>
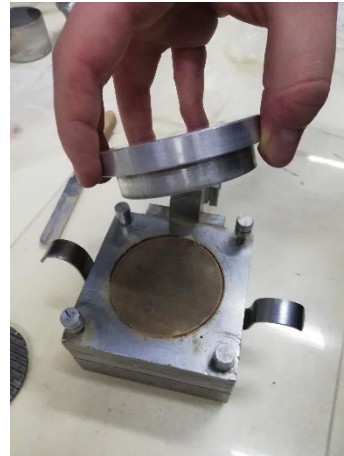
<center>*Figure 3.15.* Reconstituted specimen preparation for direct shear test</center>

Preliminary trials of reconstituting the specimens were started with preparing saturated specimens. At first, the water contents measured in-situ was used when preparing the saturated specimens (aiming the in-situ bulk density). However, after a couple of trials, it was observed that sample preparation aiming the in-situ bulk densities were problematic due to the fact that bleeding of water took place during the compaction phase. Then, to overcome this, water content corresponding to the degree of saturation (Sr) of 85% (when the soil is compacted and became ready for testing) was targeted. However, when the specimen was prepared at Sr of 85%, collapse of soil specimen was observed upon wetting while performing the saturated test. This collapse phenomenon was correlated with suction decrease in soil upon wetting (Huat et al. 2008). To avoid this problem, it was concluded that if the specimens to be used in saturated tests are prepared such that low suction exists in the soil (high degree of saturation), then collapse will not likely occur. Thus, specimens having Sr of about 95% was prepared for saturated tests.

On the other hand, for unsaturated tests, specimens having Sr of 60% and 80% were prepared by following the same specimen preparation method explained above.

3.2.9.2. Shearing stage

For saturated tests, a small seating load of about 14 kPa was applied to the specimen in the shear box and the vertical dial gage was placed. Then, distilled water was poured into the shear box to fill the water bath. After that, the remaining load, to obtain the aimed normal stress, was applied to the specimen, and the vertical dial gage is observed. The specimens were left overnight for saturation and consolidation. Finally, the shearing stage was started.

It is important to note that although submerging the specimen method was preferred, this method does not guarantee "fully saturated" conditions, and there is no control of saturation of the specimen. Thus, it may be argued that the correct term to be used here may either be "saturated" or "submerged". Nevertheless, for convenience, "saturated" term is used throughout this thesis instead of "submerged".

On the other hand, for tests at unsaturated state, the aim was to conduct the test at constant water content conditions. To avoid any confusion, it must be noted here that unsaturated tests were not suction-controlled or suction-measured tests but rather, the aim was to obtain constant water content conditions during the test. In order to obtain constant water content conditions, the tests were conducted while the shear box was covered with a moist towel to avoid evaporation during the 3 to 8 hours of shearing time. Also, similar to the saturated tests, the constant water content tests were started after compression (the consolidation term is avoided since the samples are not saturated) of the specimens were completed.

3.2.10. Saturated hydraulic conductivity

Saturated hydraulic conductivities of soils were determined by using ASTM D5084 standard. Saturated hydraulic conductivities were investigated for reconstituted samples tested with DS tests.

3.2.10.1. Specimen preparation

Hydraulic conductivity (HC) tests were performed on reconstituted samples. The samples having a height of 3 cm and a diameter of 3.6 cm was prepared. Dimensions were selected based on the minimum dimension requirement of 2.5-2.5 cm (height and diameter) as suggested by ASTM D5084. Moreover, small-sized specimens were preferred to avoid possible problems, such as saturation of specimen and having heterogenous parts in the specimen, and to use small amount of sample. The dry densities of specimens were selected as the same values as the DS tests performed on reconstituted samples.

Firstly, a procedure similar to reconstituted DS specimen was followed for HC specimen preparation. However, it was observed that the prepared specimens were non-homogenous. That is, the upper part of the specimen was denser than the lower part. In order to overcome non-homogeneities in the specimen, compacting the soil in 2 layers was tried as a solution. Compaction of the specimen in two layers was done by aiming the lower half of the specimen and the overall specimen have the target dry density. In this method, the lower 1.5 cm of the specimen was first compacted, then the remaining 1.5 cm of the specimen was compacted. However, there is one main concern with this method is that over compacting the lower part of the specimen. Thus, validation is necessary for this method to be considered as applicable. The validation of this method was done by dividing the sample into 1-cm thick 3 portions and calculating the bulk densities of each portion. By comparing the bulk densities of different segments along the specimen it was concluded that the used method was suitable. Furthermore, validation was done for each of the samples prepared. However, it is important to note here that, although the prepared specimen was considered to be homogenous, upon completion of the test two distinct layers were observed.

3.2.11. Soil-water retention curves

The wetting soil-water retention curves (SWRC) for the samples used for DS tests were obtained by using hanging column and pressure plate extractor methods.

3.2.11.1. Hanging column

Hanging column setup can be useful for suction ranges of 0 to 80 kPa (ASTM D6836). The hanging column apparatus at METU geotechnical laboratory is suitable for suction applications of 0 to 60 kPa. In this method, the setup has two reservoirs, and the suction is generated by using the relative elevation of these reservoirs (Figure 3.16a). Then, the suction is transmitted to the capillary tube and applied to the soil specimen by a saturated disc.

3.2.11.2. Pressure plate extractor

The pressure plate is the most used technique for matric suction control in the laboratory (Lu 2019). Pressure plate extractor is generally used for obtaining data points on SWRC at high suctions (0- 1500 kPa). The pressure plate extractor at METU geotechnical laboratory (Figure 3.16b) can provide suctions up to 700 kPa. Thus, above 700 kPa no data point could be obtained on SWRCs.

In both methods (hanging column and pressure plate extractor) the gravimetric water content corresponding to applied suction was determined. Volumetric water content is not calculated because of the volume change observed upon suction change.
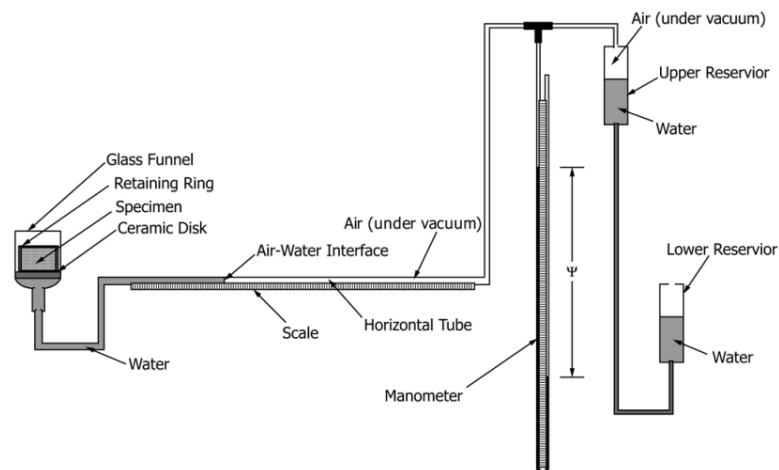
(a) Sketch of hanging column setup (adapted from ASTM D6836)

(b) Pressure plate apparatus (above the pressure plate soil specimens are shown)

Figure 3.16. Sketch of hanging column setup and pressure plate apparatus at METU

3.2.11.3. Specimen preparation

Specimens having 3.5 cm diameter and 1 cm height were prepared with the same initial dry densities as DS and HC tests. Also, the same initial degree of saturation with HC tests was targeted. For preparing the specimens, firstly, the required amount of water and soil were mixed, and the mixture was left in humidity room overnight. Then, the soil was compacted in one layer to the target bulk density (Figure 3.17). Having prepared the required number of specimens, the specimens were air-dried before testing (Figure 3.17).

(a) Equipment
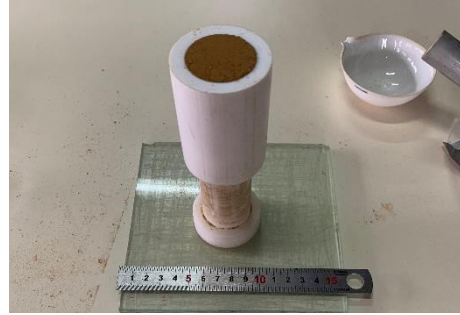
(b) Compacted soil

(c) Specimens ready for air-drying

Figure 3.17. Specimen preparation and prepared specimens for air-drying

CHAPTER 4

RESULTS OF THE STUDY

This chapter is mainly comprised of two main subsections. Firstly, the results of the index tests, then the results of shear strength tests are presented.

4.1. Index tests, soil classification and general characteristics

4.1.1. Specific gravity

The specific gravity values of the soils are in the range of 2.40 to 2.81, with 2.59 being the average value for 27 samples tested (*Table 4.1*). However, specific gravity values determined using method 2 (described in section 3.2.2) was found slightly greater than the average value of the ones determined using method 1. Here, the results are given as a minimum and maximum together with the average value.

4.1.2. Grain size distribution

Grain size distribution curves of a total of 31 samples are presented in *Figure 4.1* and *Table 4.1*). 27 out of 31 samples are fine-grained soils. The fines content (% < 0.074 mm) of all samples were between 29% and 89%, and clay-size fraction (%< 0.002 mm) in the whole sample, were between 1% to 39%. Also, the curves of the samples (described as method 2 in section 3.2.1.1) which are used in preparing reconstituted DS samples are presented separately (*Figure 4.2*).
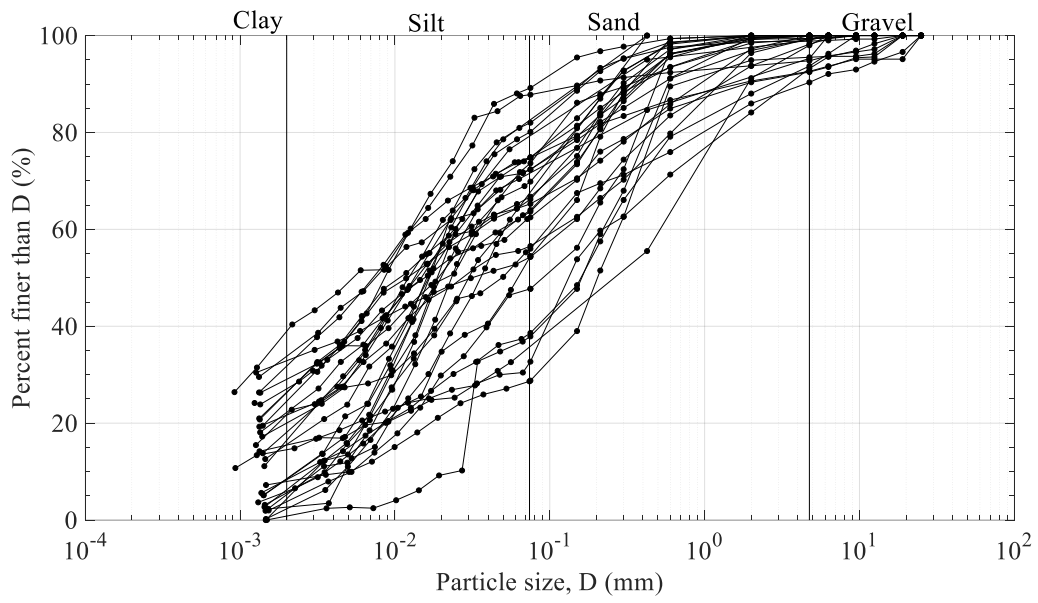
Figure 4.1. Grain size distributions of all samples
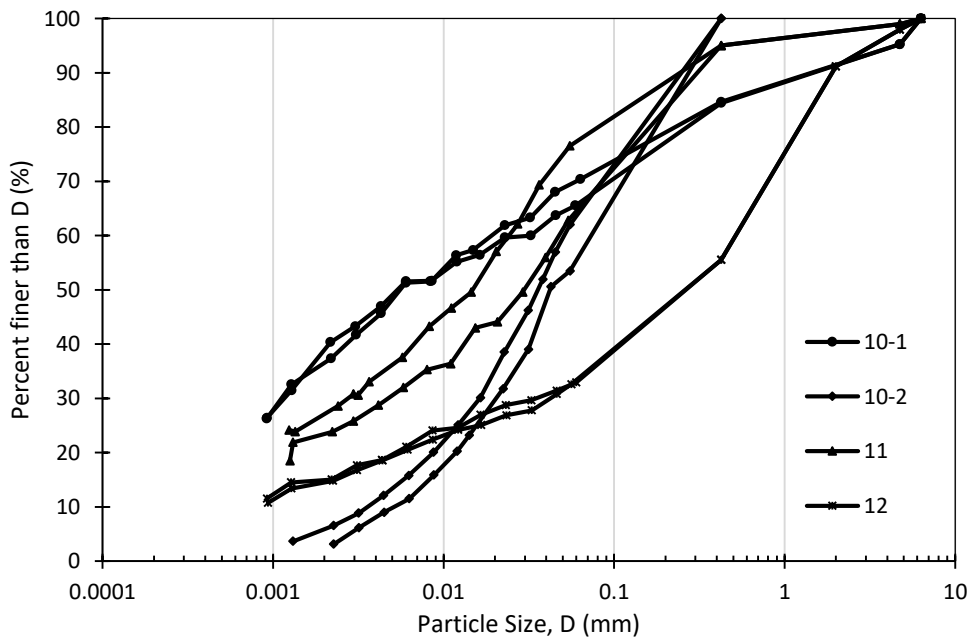
Figure 4.2. Grain size distributions of samples used as reconstituted samples for direct shear test (two tests were performed on each sample)

52

4.1.3. Atterberg limits

Atterberg limits tests indicate that about half of the soil samples are low plasticity silts (ML), whereas remaining are high plasticity silts (MH) and organic soils (OH) (*Figure 4.3*, Table *4.1*). Although, some soils were classified as organic given the group symbol OH, no soil was given as OL group symbol. To determine if the soils are organic or inorganic, the LL_{Ratio} ($LL_{110°C}$ / LL_{Moist}) values are evaluated for all the samples (Table *4.1*). Based on LL_{Ratio} being smaller than 0.75, 8 samples are classified as organic silt, OH (ASTM D4318-17). One important discussion here is that when the organic soils were given in group symbol of OL or OH, their silty or clayey nature cannot be represented. Similarly, Germaine and Germaine (2009) noted that naming the organic fine-grained soils according to ASTM standard, as OL or OH, does not fully reflect the "silty" and "clayey" nature of these soils; hence, they suggested using dual-symbols for organic soils. The author also supports Germaine and Germaine (2009), and thus, suggests naming the "OH" soils in Table *4.1*, with dual symbol preserving the silty nature of the soils, such as "MH-OH".

Furthermore, the activity (I_p / clay-size fraction) of 24 soil samples are calculated to be in the range of 0 to 1.48 with an average value of 0.53. The activity value can give information about the mineralogy of the particles (Mitchell 1993), for example, kaolinite, illite, halloysite and allophane minerals all have activity values in the range of 0.50-1.20.

Atterberg limit values obtained by different preparation methods (pre-drying at different temperatures) are presented in Table 4.2.
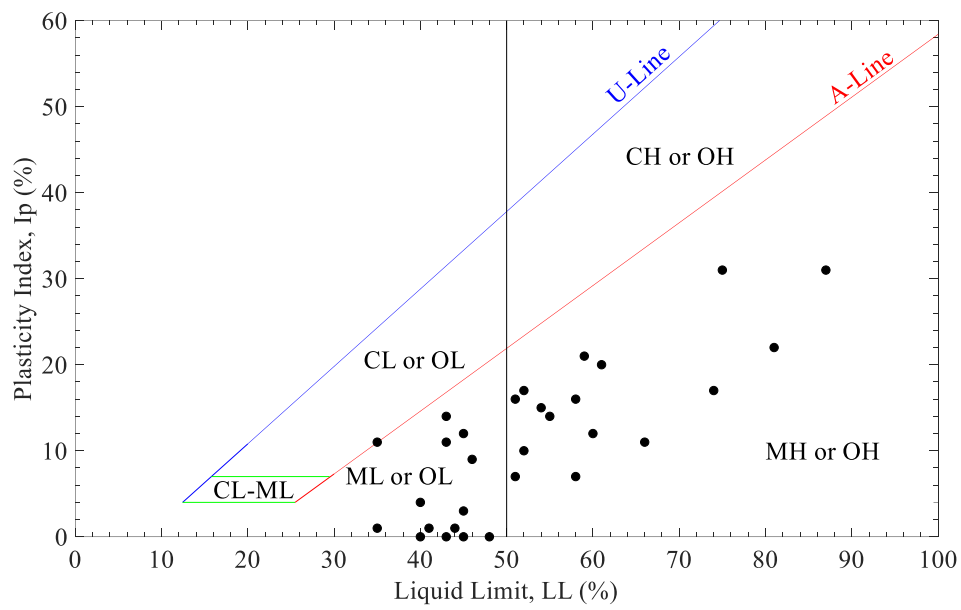
Figure 4.3. Atterberg limits of the samples on plasticity chart (based on LL_{Moist})

Table 4.1. *Index properties of soil samples*

Site Number-sample number	LL^d %	PL %	IP %	LL Ratio $\left(\frac{LL_{110°C}}{LL_{Moist}}\right)^a$	USCS	In-situ moisture content %	Organic content %	pH	Gs	% ≥ 4.75mm	% ≤ 74μm	% ≤ 2μm
1-1	45	33	12	0.82	ML	28	4.69	5.2	2.63	0	63.7	22.2
1-2	43	33	10	0.86	ML	31	4.52	5.0	2.65	0	66.2	26.4
1-3	35	24	11	0.94	ML	31	4.5	5.0	2.64	0.1	66.8	26.3
1-4	35	34	1	0.94	SM^b	32	5.01	3.7	2.68	6.3	38.6	8.3
2-1	58	42	16	0.74	OH	39	5.7	3.9	2.62	0.7	74.8	31.8
2-2	51	35	16	0.88	MH	34	4.39	3.5	2.65	0.6	56.6	21.7
2-3	75	44	31	0.71	OH	39	5.39	3.6	2.62	1.8	54.3	32.9
2-4	46	37	9	0.83	ML	32	4.3	-	-	-	-	-
3-1	81	59	22	0.68	OH	61	12.1	3.67	2.48	0	65.3	16.5
3-2	45	45	0	0.93	ML	63	5.59	4.8	2.53	0	69.9	2.3
3-3	66	55	11	0.76	MH	55	7.59	3.3	2.57	0	74.9	18.1
3-4	58	51	7	0.79	MH	55	6.38	3.4	2.58	0	74.8	6.3
3-5	-	-	-	-	-	-	-	-	-	0	80.1	8.5
3-6	48	48	0	0.96	ML	44	5.57	5.0	2.54	0	64	5.3
4-1	60	48	12	0.75	OH	51	7.03^c	4.4	2.42	0.6	71.6	15.6
4-2	40	36	4	0.98	ML	35	5.1^c	5.3	2.41	0	54.5	2.7
4-3	-	-	-	-	-	42	5.43^c	4.7	2.4	0	47.7	3.8
4-4	43	43	0	0.91	SM^b	39	5.01^c	4.8	2.43	0.2	37.9	0.8
4-5	-	-	-	-	-	44	4.57^c	4.8	2.45	-	-	-
5-1	52	35	17	0.77	SM^b	33	1.79^c	3.5	2.59	6.8	32.7	15.5
5-2	59	38	21	0.68	OH	42	2.41^c	3.6	2.59	0	89.2	33.8
5-3	47	31	16	-	-	32	2.67^c	5.6	2.56	9.7	56.0	20
5-4	42	31	11	-	-	29	2.33^c	3.5	-	0.7	73.6	29.1
6-1	-	-	-	-	-	38	3.83^c	5	2.46	4.5	28.8	8
6-2	87	56	31	0.66	OH	59	5.09^c	4.4	2.52	-	-	-
7-1	55	41	14	0.78	ML	41	7.54	-	-	5.2	87.8	24.5
7-2	41	40	1	0.8	ML	38	-	-	-	7.5	62.5	4.4
7-3	44	43	1	0.84	ML	43	-	-	-	1.2	82.0	8.4
7-4	42	41	1	-	-	37	-	-	-	7.4	72.4	5.6
7-5	61	41	20	0.82	MH	42	6.36	-	-	-	-	-
7-6	74	57	17	0.7	OH	-	11.6	-	-	-	-	-
8-1	45	42	3	-	ML	33	4.43	-	-	-	-	-
9-1	52	42	10	0.83	MH	49	3.37	-	2.79	0	82.5	21.7
10-1	43	29	14	0.81	ML	34	2.63	-	2.72	4.7	71.6	39
10-2	40	40	0	0.9	ML	44	2.75	-	2.81	0	67.5	5.9
11-1	51	44	7	0.78	MH	44	3.43	-	2.74	1	79.2	27.1
12-1	54	39	15	0.75	SM^b	31	2.06	-	2.77	2	35.7	14.5

[a] $LL_{110°C}$ is liquid limit of sample after oven-drying at 110℃, LL_{Moist} is liquid limit of samples tested by starting from natural moisture content

[b] Fine portions of these samples are classified as ML, ML, MH and OH respectively

[c] Organic content of these samples are determined by 2 hours of burning 440℃ furnace (others by 12 hours of burning).

[d] These values are LL_{Moist}

Table 4.2. *Atterberg limits obtained by different preparation methods*

Site number-sample number	Moist		110°C dried		60°C dried		440°C dried		$LL_{Moist} - LL_{110°C}$ (%)
	LL %	IP %	LL %	IP %	LL %	IP %	LL %	IP %	
1-1	45	12	37	6	39	11			8
1-2	43	10	37	11	40	13			6
1-3	35	11	33	9	33	9	-		2
1-4	35	1	33	0	35	0			2
2-1	58	16	43	10	48	12	40	0	15
2-2	51	16	45	14	46	11			6
2-3	75	31	53	14	62	22	-		22
2-4	46	9	38	0	40	1			8
3-1	81	22	55	6	58	8	49	0	26
3-2	45	0	42	0	43	0			3
3-3	66	11	50	5	54	7	-		16
3-4	58	7	46	1	49	5			12
3-6	48	0	46	0	48	2			2
4-1	60	12	45	3	48	3			15
4-2	40	4	39	0	40	0	-		1
4-4	43	0	39	0	-				4
5-1	52	17	40	10	-		-		12
5-2	59	21	40	8					19
6-2	87	31	57	11	-		-		30
7-1	55	14	43	7	42	3			12
7-2	41	1	33	0	-				8
7-3	44	1	37	0	36	0	-		7
7-5	61	20	50	11	-				11
7-6	74	17	52	0	-				22
8-1	45	3	39	0	40	0	-		6
9-1	52	10	43	0					9
10-1	43	14	35	9					8
10-2	40	0	36	0	-		-		4
11-1	51	7	40	0					11
12-1	54	15	40	9					14

4.1.4. Organic content

Organic matter content determination is done for a total of 35 samples (Table *4.1*). The calculations reveal that organic contents (percent mass change upon burning at 440ºC furnace) of these samples are in the range of 1.79% to 12.1% with an average value of 5.01%. It was discussed in section 3.2.4 that two different burning times were used for some samples. The comparison of the organic content values obtained by different burning times is shown in Figure 4.4.
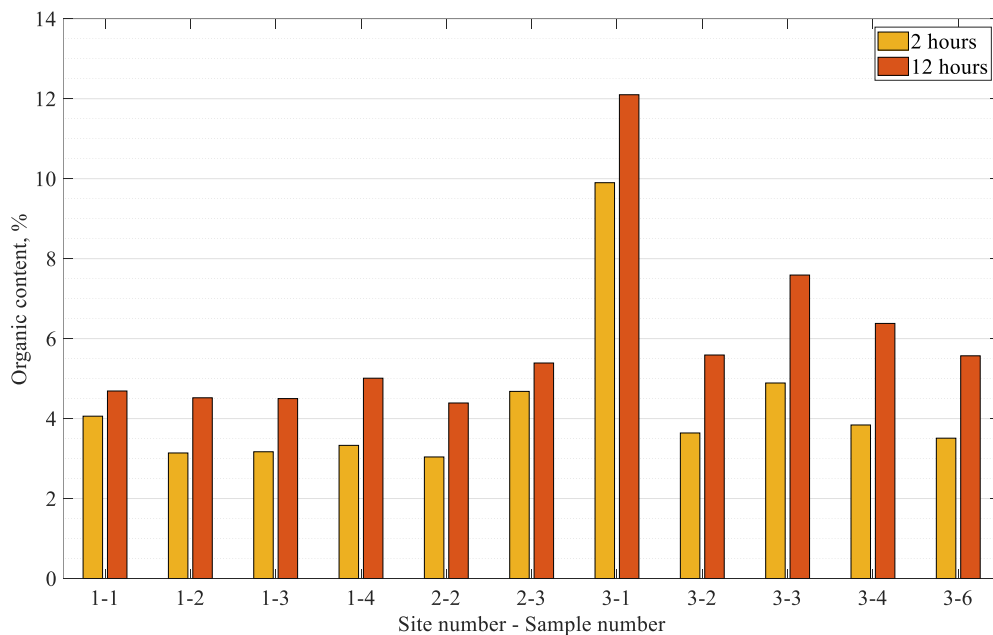
Figure 4.4. Organic matter content obtained by different burning periods

4.1.5. pH values

The average pH value of 23 samples is 4.3, with a minimum value of 3.3 and maximum value of 5.6 (Table *4.1*). For all samples, measured pH values indicate that all of the samples are acidic.

4.1.6. Moisture content- dry density relationship

Compaction curves of 5 soil samples are constructed (Figure 4.5). These 5 samples are typical soils in shallow landslides in Rize region. It must be noted here that "wet

of optimum" sides of some of the compaction curves could not be obtained, since wet side of the curve required water contents, which brought the samples into a very wet, mud-like consistency, and compaction could not be performed as it should be. Also, it may be noted that Harvard compaction method may not be suitable for some fine-grained soils at certain water contents due to the problems discussed in section 3.2.7.
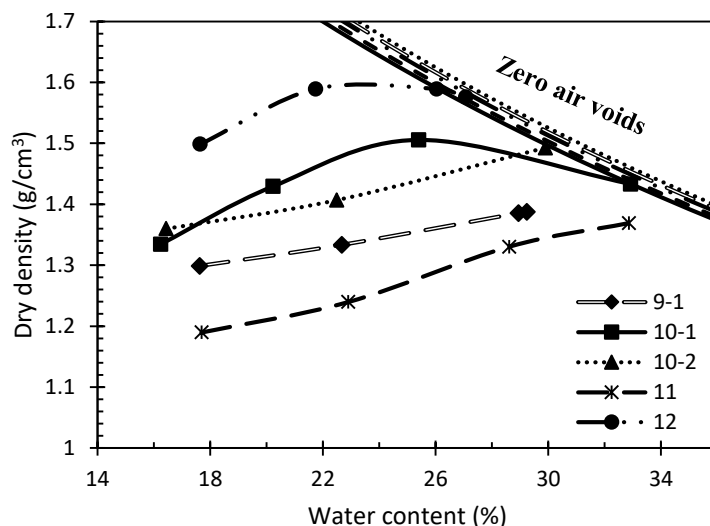
Figure 4.5. Moisture content- dry density relationships obtained by Harvard compaction apparatus

4.1.7. In-situ dry-density

In-situ bulk unit weights of soils from landslide sites are also measured via small and big sampling tubes. The results are presented in Figure 4.6 as dry unit weight values in a histogram. All of the samples used in this study have in-situ water contents in the range of 28 to 60 %, average in-situ bulk density value of 1.698 g/cm^3 (range between 1.52 to 1.92 g/cm^3). Void ratios of tube samples are in the range of 0.78 to 1.48 with an average value of 1.13.
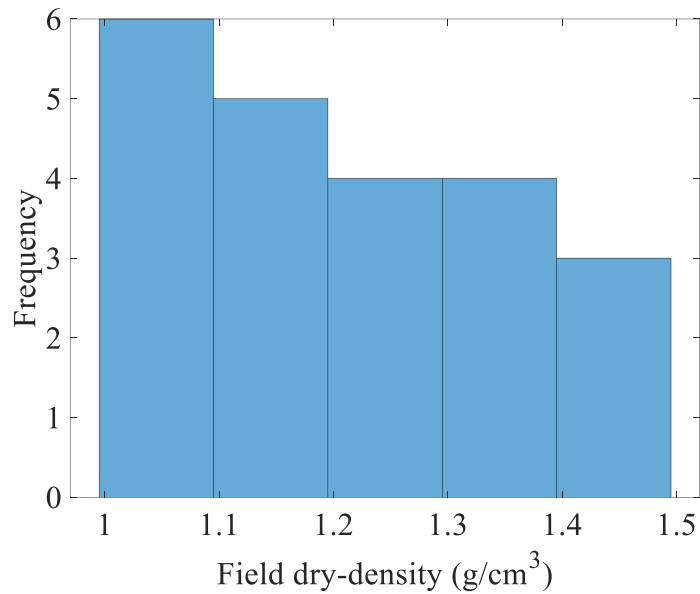
Figure 4.6. In-situ dry unit weight of soils

4.1.8. Soil mineralogy

Bulk XRD patterns of a total of 27 samples from sites 1 to 8 are analyzed. Percentage of "total clay + mica" are in the range of 21.7 to 89.9% with average value of 66%, whereas percent quartz is in the range of 0.8-64.6% with an average value of 19.2% (Table 4.3). Some of the other common minerals observed in bulk XRD patterns are feldspar, hematite and laumontite. XRD clay fraction analyses on 29 samples from sites 1 to 8 indicated that halloysite mineral existed in 23 out of 29 samples (none of the 4 samples from site 5 had halloysite). Other common minerals in 29 samples are illite, kaolinite, vermiculite, montmorillonite, gypsum and laumontite. Other rare minerals are magnetite, saponite, molybdenite, lizardite, nontronite, sepiolite, alunogen and brushite. Furthermore, semi-quantitative clay mineralogy analysis was also performed for some of the samples (Table *4.4*).

Table 4.3. Percentages of different minerals in bulk powder XRD analyses

Site	% Total clay + mica		% Quartz		% Other minerals		
	Ave.	Range	Ave.	Range	mineral	Ave.	Range
1 (4 samples)	64	62-70	30	26-34	k-feldspar	3	1-7
					hematite	2	1-3
2 (3 samples)	66	59-77	29	18-36	hematite	2	2-3
					pyrite	2	1-2
					magnetite	1	1-2
3 (5 samples)	86	82-89	3	1-9	plagioclase	4	1-9
					hematite	3	3-4
					lizardite	6	5-7
					laumontite	3	2-3
4 (4 samples)	87	84-90	1	1-2	feldspar	8	6-11
					magnetite	4	3-5
5 (4 samples)	48	34-68	50	32-65	hematite	1	1-1
6 (1 sample)	93	-	4	-	feldspar	2	-
					hematite	1	-
					zirconia	1	-
7 (5 samples)	40	22-68	20	6-32	feldspar	32	4-60
					magnetite	3	2-4
					laumontite	8	5-11
					anhydrite	7	-
					calcite	2	1-2
8 (1 sample)	43	-	14	-	feldspar	26	-
					hornblende	16	-

Table 4.4. *Semi-quantitative clay mineralogy analysis results (other minerals are not reported)*

Site number-sample number	Illite	Halloysite	Vermiculite	Montmorillonite	Kaolinite
			(%)		
4-1	49	26	12	6	6
4-2	27	5	30	18	-
4-3	33	12	20	25	-
4-4	28	9	29	22	-
5-1	59	-	16	9	12
5-2	4	-	41	-	47
5-4	9	-	20	21	39
6-1	6	-	42	30	11
6-2	11	27	21	11	-
7-3	5	21	30	-	32
7-4		28	20	-	34
8-1	3	10	58	6	9

4.2. Shear strength

4.2.1. In-situ hand vane test

When the vane is inserted in the vertical direction, peak undrained shear strength, $c_{u,peak}$ values range from 42 to 103 kPa, with an average value of 61 kPa indicating that the soils are in medium-stiff consistency. The remolded undrained shear strength, $c_{u,remolded}$ values are in the range of 4-17 kPa, giving sensitivity ($S_t = c_{u,peak}/c_{u,remolded}$) values in the range of 2.5 – 16.2, with an average value of 6.0 at these 8 sites. When the vane axis is horizontal direction, $c_{u,peak}$ values range from 27-88 kPa, with an average value of 50 kPa, and $c_{u,remolded}$ values range from 4-16 kPa, giving sensitivity values in the range of 3.6 – 14.7, with an average value of 6.0 at these 5 sites. High and low plasticity silts at the investigated sites are in "medium sensitive" to "extra sensitive" category, and with average sensitivity value of 6.0, they are in the range of "sensitive" classification according to Skempton and Northey (1952) sensitivity classification.

4.2.2. Unconfined compression test

The average undrained shear strength of intact samples obtained from unconfined compression tests is 36 kPa (range 10 to 52 kPa) as can be seen in Table *4.5*. Values of the axial strain at failure is in the range of 2.1 – 8.3%. Some of the samples exhibited a clear shear plane whereas some of them showed bulging behavior at failure (Figure 4.8)

Table 4.5. *Unconfined compression test results*

Sample name	Average water content (%)	Bulk density (g/cm³)	Void ratio	Strain at failure %	Cu (kPa)
5-3	34	1.86	0.918	5.6	34.9
5-3 (2)	31	1.92	0.812	5.9	51.6
4-4	43	1.59	1.391	3.1	9.8
4-4 (2)	40	1.72	1.141	2.1	15.5
7-5	45	1.73	1.233	8	26.2
7-6	53	1.57	1.576	4.2	39.6
7-6 (2)	53	1.62	1.519	5.2	46.2
10-1	30	1.72	1.063	6	51.2
10-1 (2)	30	1.6	1.227	-	-
10-2	50	1.73	1.478	8.3	43.2
11-1	37	1.83	1.061	8.3	43.2
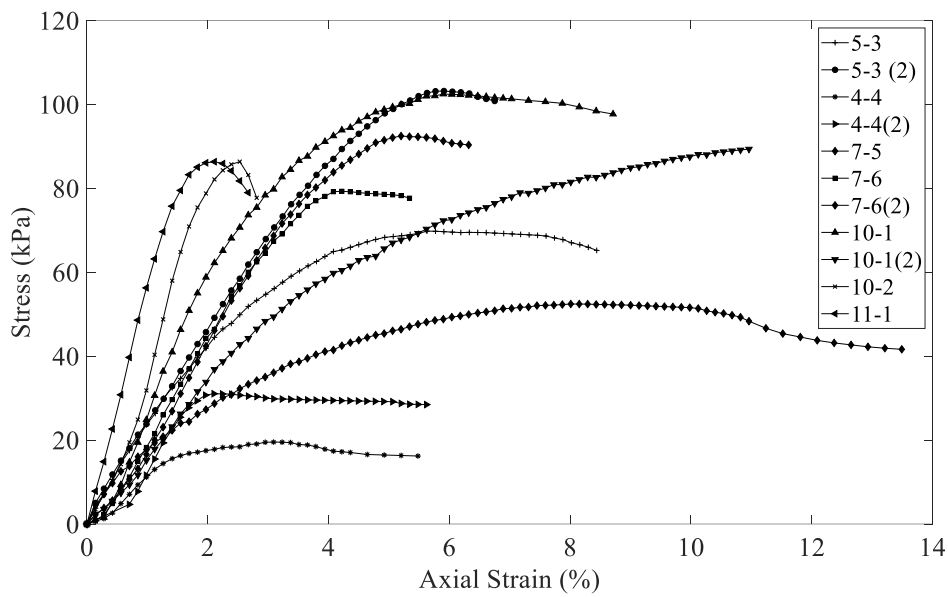
*Figure 4.7.*Unconfined compression test results
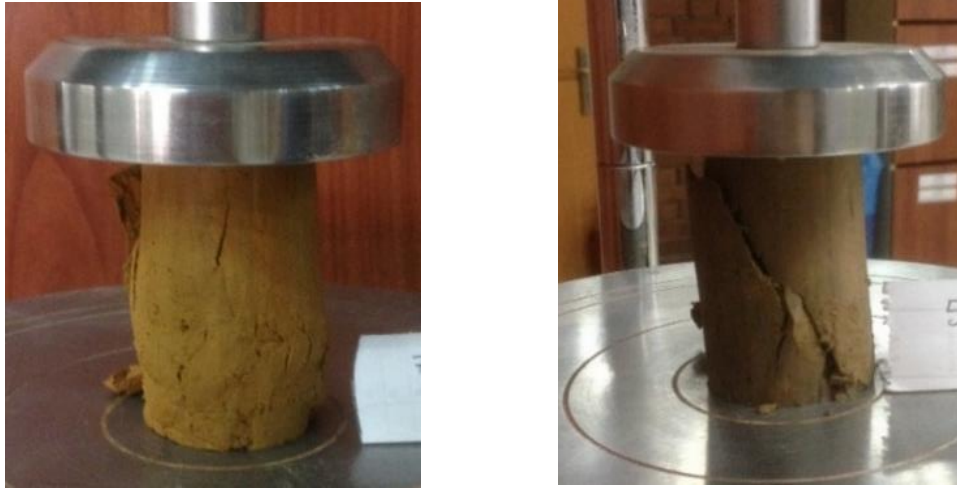
Figure 4.8. (a) bulging sample (b) sample having a distinct shear plane

4.2.3. Direct shear tests

In this section, the results on direct shear tests conducted on intact and reconstituted samples will be presented. However, before presenting the results it is important to discuss an important consideration about the test, which is the weight of the upper half of the shear box. According to ASTM D 3080, the weight of the top half shear box shall be less than 1 percent of the applied normal force during shear. In the tests in this study, the maximum normal stress is 65 kPa. Therefore, the weight of the upper shear box is more than 1% of the normal load. In low normal stress ranges, either a counter-balance system should be used where the upper box is floating, or weight of the upper box must be accounted in the normal stress calculations. According to Germaine and Germaine (2009) and Germaine (2019), an unknown normal force is applied to the specimen if the counterbalance is not used. Das (2002) states that all of the weight of the upper box must be added as normal force if a counterbalance is not used. However, in this study addition of 50% of the weight of the upper box is preferred in order to minimize the maximum error in normal stress due to the upper box.

The failure point is decided based on the shear stress-horizontal displacement plot such that if a peak shear resistance is observed throughout the test, this value is

considered as failure, on the other hand, if no clear peak shear resistance is present and the specimen exhibited strain-hardening behavior, the maximum shear stress value (generally the last data point) is considered as failure.

Also, some of the tests for both the intact samples and reconstituted samples are duplicated, and the results are found to be consistent. The repeated tests are shown with dashed red lines in related plots.

4.2.3.1. Intact samples

Direct shear test results for intact samples are shown in Appendix A, and failure envelopes are given in Figure 4.9. Also, in Figure 4.9 the average final water contents of unsaturated tests are given. In Table *4.6*, test results for saturated tests, average bulk density and initial water content of samples are summarized.

Table 4.6. *Direct shear test data for intact specimens*

Sample name	Average bulk density[a] (g/cm3)	Average initial water content (%)	c' (kPa)	ϕ' (°)
1-2	1.94 (1.88-2.00)	31	6.5	35.5
1-3	1.88 (1.73-1.99)	28	3.8	34.9
2-4[b]	1.72 (1.69-1.77)	34	-	-
3-5	1.57 (1.49-1.61)	55	6.1	35.2
3-6	1.67 (1.49-1.77)	37	7.6	31.1
4-4	1.69 (1.63-1.73)	42	3.4	50.3
5-1	1.81 (1.73-1.91)	33	6.0	36.0
7-5	1.74 (1.69-1.76)	44	3.4	38.0
7-6	1.58 (1.53-1.66)	60	4.5	35.7

[a] Range is reported in parenthesis
[b] Shear strength envelope could not be obtained due to having 2 data points
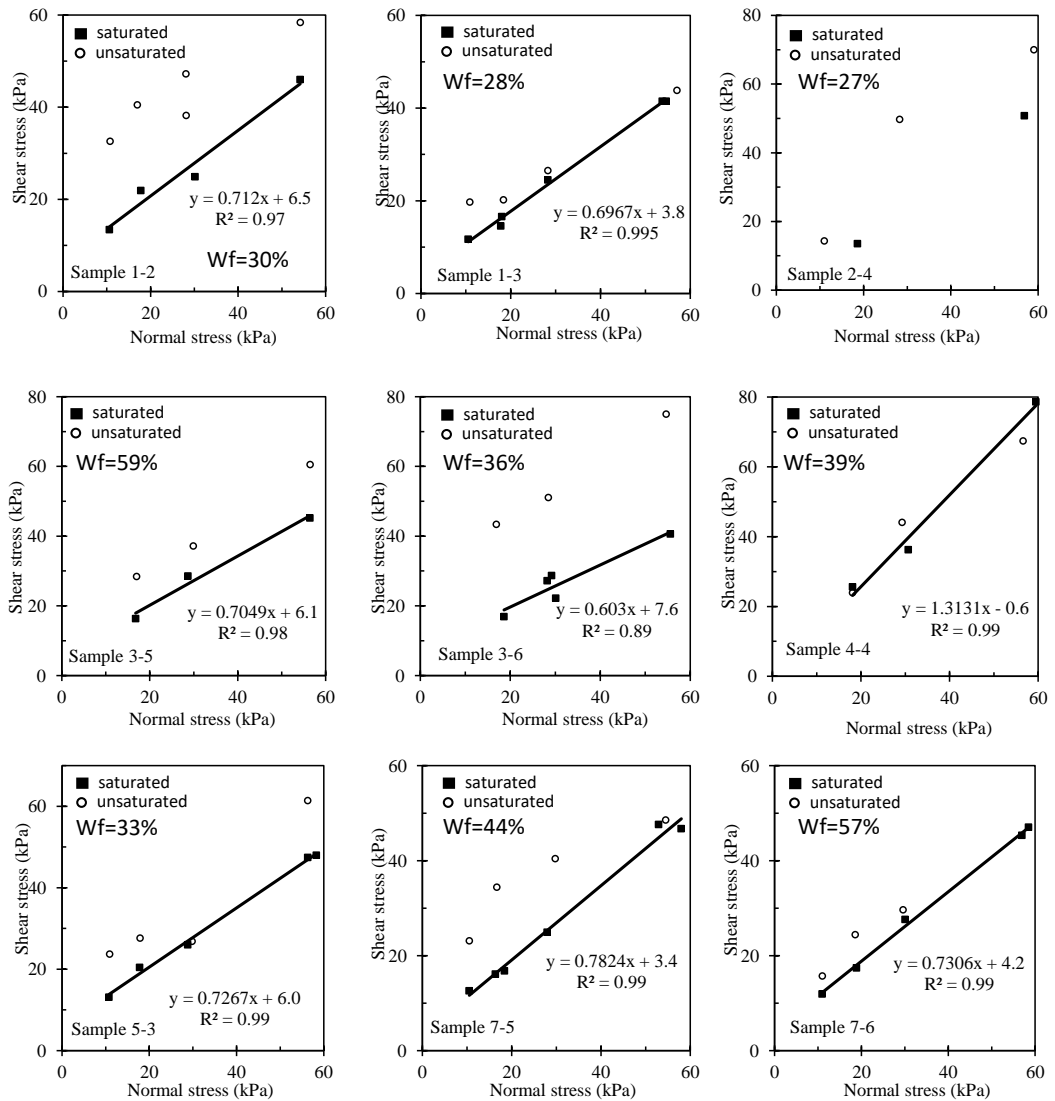
Figure 4.9. Failure envelopes for intact samples (the average final water contents for unsaturated tests, Wf, are given on the figures)

Shear stress-horizontal displacement plots show that some of the samples exhibit clear peak shear resistances and dilation behavior, whereas in some others, peak resistance is not observed and ultimate strength is reached within 8 mm shear displacement of the box together with a contractive behavior.

Shear strength envelopes of samples taken from individual sites are evaluated separately, the internal friction angles range from 31.1° to 50.3° in the saturated condition. When, all of the saturated test results are evaluated together, the c' and φ'

values are obtained with a very good fit as 4.4 kPa and 36.3°, respectively Figure 4.10. However, the results of the sample with the friction angle of 50.3° is excluded, since this value is considered as an outlier for the overall range. Furthermore, the results of some of the unsaturated tests (which were not submerged in water) results are found to be on (or very near to) the saturated envelope. Thus, these data points are considered as saturated data when fitting the best line.

Theoretically, the cohesion value for the fully saturated case should approach to zero, and as the degree of saturation is decreased, an increasing apparent cohesion is expected. In this study, a general trend of increasing shear resistance in the unsaturated samples is observed, however, individual friction angles are not reported for the unsaturated intact samples, since the tests were not suction-measured or suction-controlled and natural water content of the samples varied, even within each sample tube.

To check repeatability, some of the tests were duplicated, and it was observed that the duplicated results were in good agreement (Appendix A).
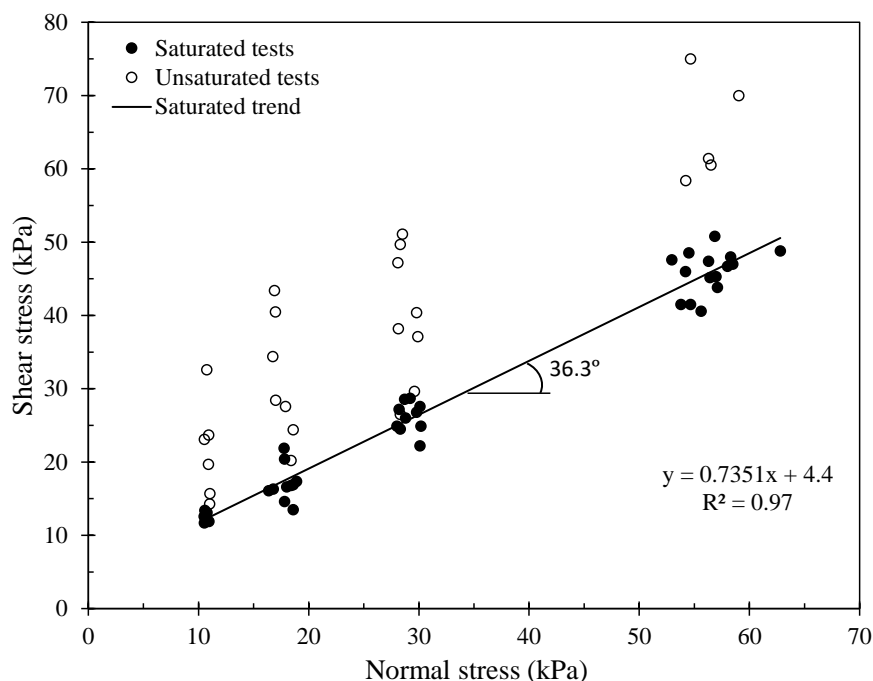
Figure 4.10. Overall direct shear test results for intact samples

66

4.2.3.2. Reconstituted samples

Soil samples 10-1, 10-2, 11, 12 were used for 68 direct shear tests on reconstituted samples. Although shear stress-horizontal displacement and vertical displacement-horizontal displacement graphs for intact samples are given in the appendix, these plots are given for reconstituted tests in this section (Figure 4.11, Figure 4.12, Figure 4.13), since they are to be later discussed in detail. In Figure 4.11, Figure 4.12, Figure 4.13, the negative displacement values indicate dilation (volume increase) and positive values indicate contraction (volume decrease). In the legends, saturated tests are denoted as "S-Y", and unsaturated tests are denoted as "UX-Y", where X indicates the preparation degree of saturation in percentage and Y indicates the initial applied normal stress.

The results and further details of reconstituted direct shear tests are presented in Appendix B.
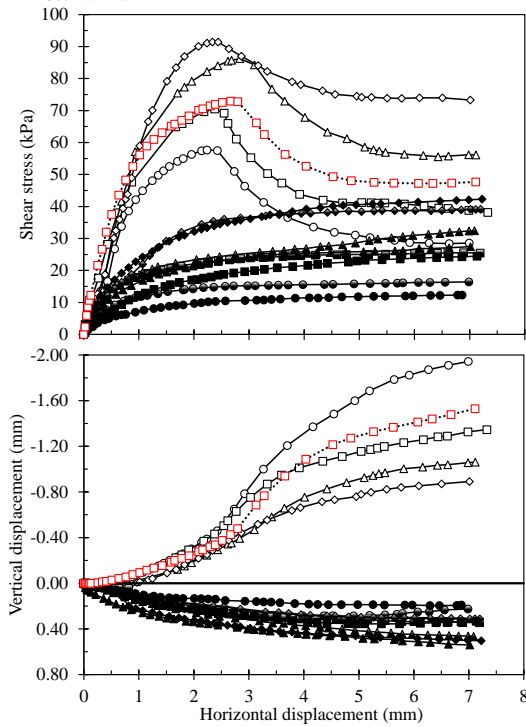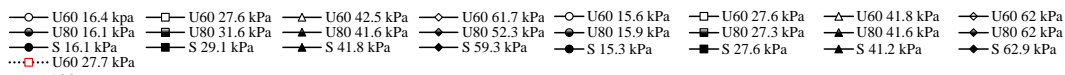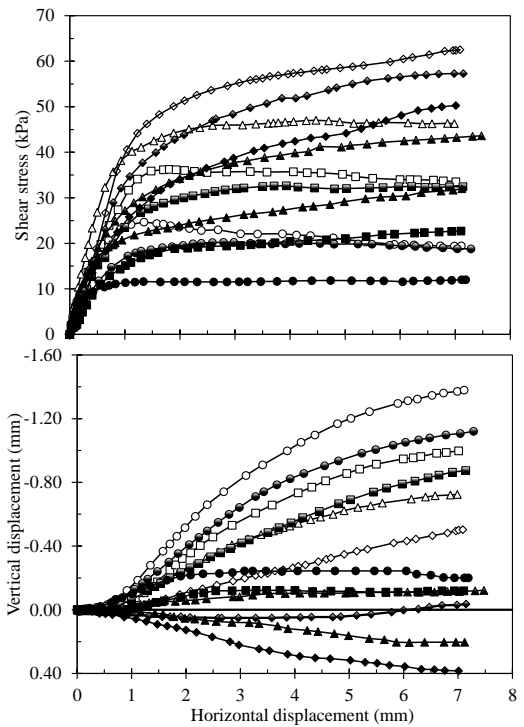
Figure 4.11. Direct shear results for (a) sample #10-1, (b) sample #10-2
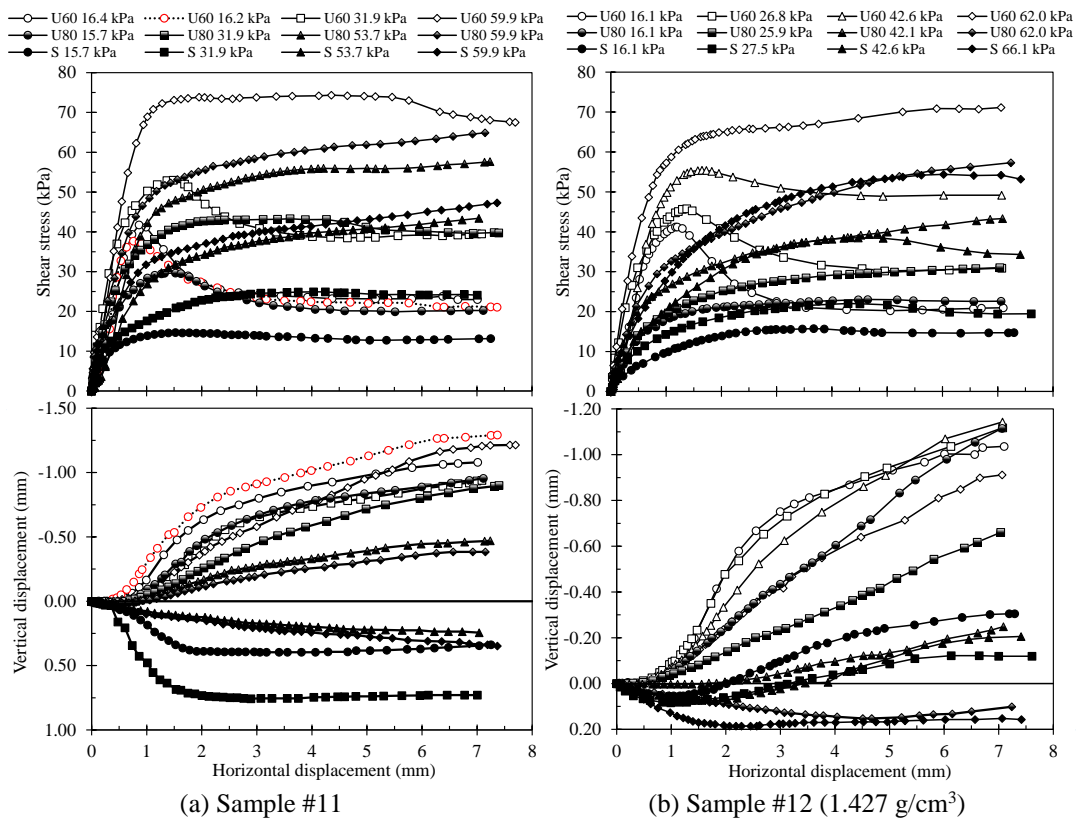
Figure 4.12. Direct shear results for (a) sample #11, (b) sample #12 (1.427 g/cm^3)
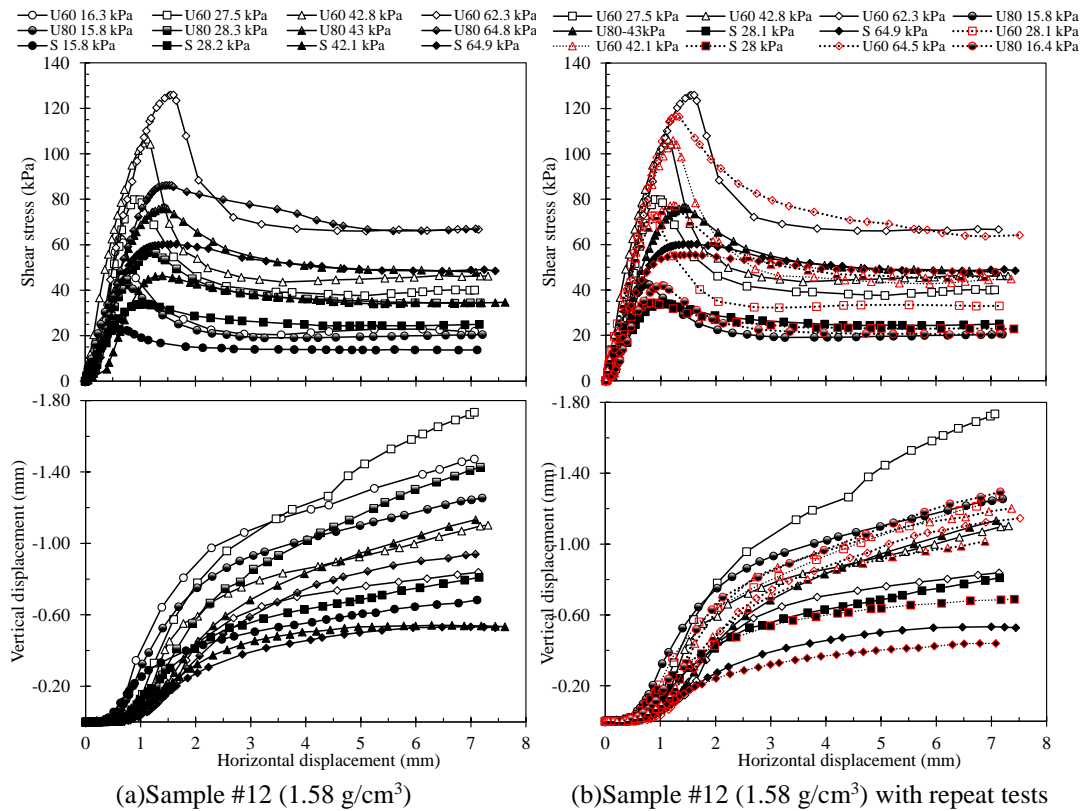
Figure 4.13. Direct shear results for sample (a) #12 (1.58 g/cm^3), (b) with repeat tests

Also, Mohr-Coulomb failure envelopes for each sample at different degree of saturation is shown in Figure 4.14, Figure 4.15, Figure 4.16.

For sample #12, both unsaturated and saturated tests were performed with 2 different dry-densities to evaluate the effects of dry-density (Figure 4.12 and Figure 4.13). The friction angles for different Sr cases for #12-1.58 g/cm^3 case are significantly different from each other, whereas friction angles in other samples were generally similar for the same sample, for different degrees of saturation. The friction angles for sample #12 are 34.4, 44.3 and 51.1degrees for saturated, Sr= 80% and Sr= 60%, respectively (Figure 4.16). Thus, some of the tests were duplicated. However, the duplicated test results are found to be in very well agreement (Figure 4.13b, Figure 4.16b).

70
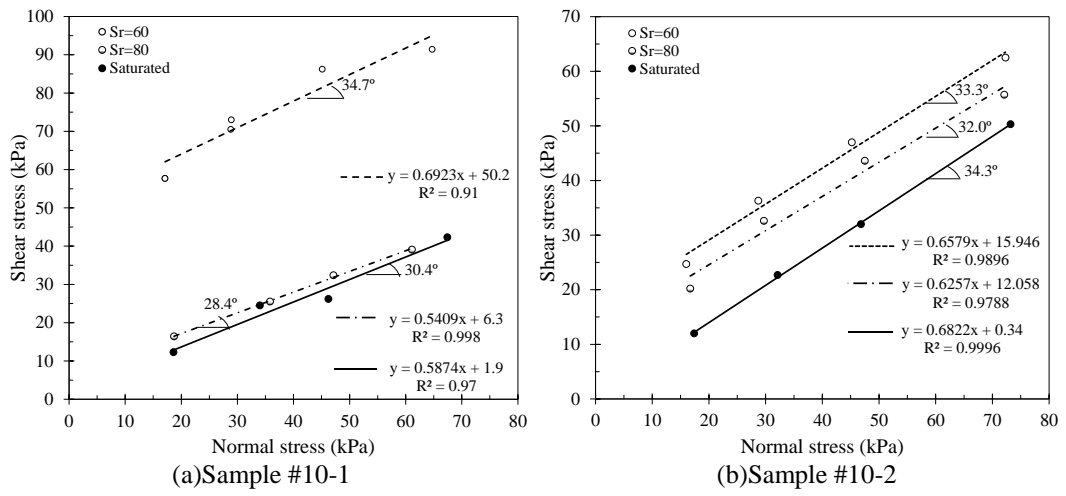
Figure 4.14. Mohr-Coulomb failure envelopes for sample (a) #10-1, (b) #10-2
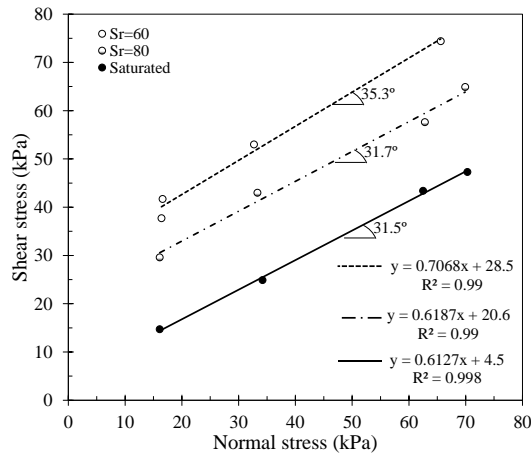
Figure 4.15. Mohr-Coulomb failure envelopes for sample #11

71
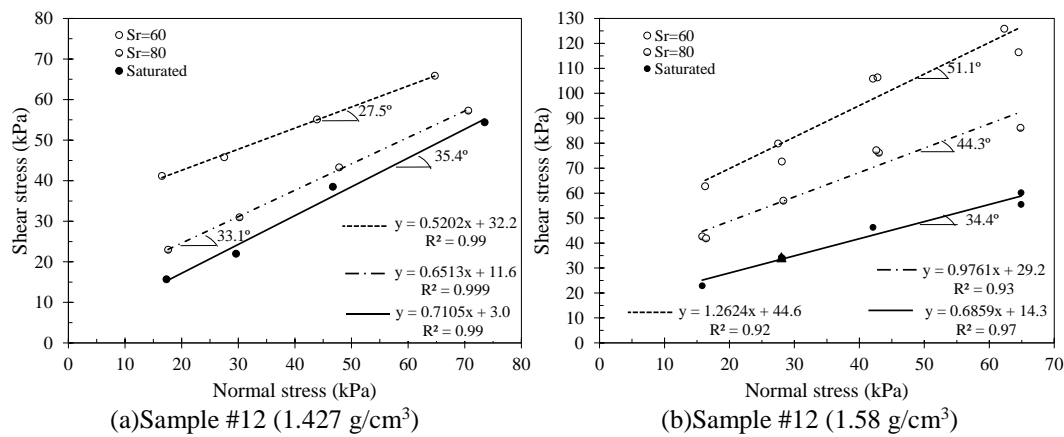
Figure 4.16. Mohr-Coulomb failure envelopes for sample (a) #12 (1.427 g/cm^3), (b) #12 (1.58 g/cm^3)

4.2.4. Saturated hydraulic conductivity

Saturated hydraulic conductivity test results were performed for 4 samples, which are used as reconstituted specimens for direct shear tests are shown in Table *4.7*. The results are found to lie within the range for low and high plasticity silts.

Table 4.7. *Saturated hydraulic conductivity test results*

Sample name	Hydraulic conductivity (m/s)
10-1	2.3×10^{-7}
10-2	1.1×10^{-6}
11	1.0×10^{-6}
12	1.5×10^{-7}

4.2.5. Soil-water retention curves

Soil-water retention curves on the main wetting path are shown in Figure 4.17 for 4 samples used as reconstituted samples in DS tests. Data is presented as scatter plot simply because these data is not used for further purpose (Figure 4.17).

72
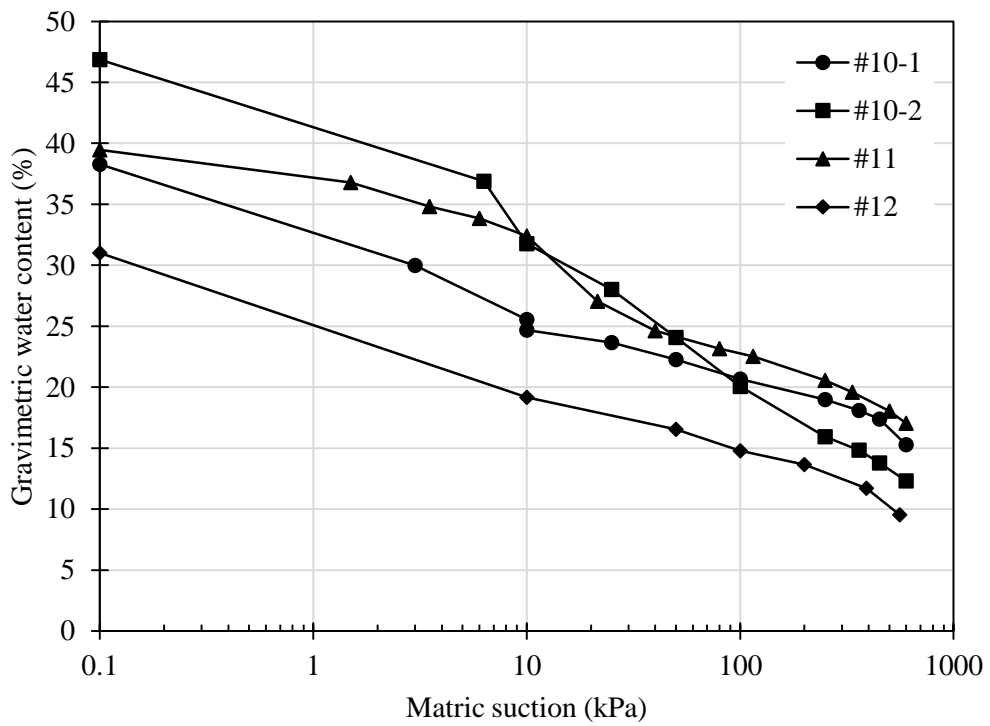
Figure 4.17. SWRCs of 4 reconstituted DS samples on the main wetting path

CHAPTER 5

DISCUSSION OF THE RESULTS

5.1. Effects of drying on Atterberg limits

In this section, the effects of drying on Atterberg limits on the investigated soils shall be discussed. The findings of this section are published by Huvaj and Uyeturk (2018) and Uyeturk and Huvaj (2019). Here, firstly, a brief literature background on the effects of drying will be given, then the data obtained in this study presented in Chapter 4 will be examined in comparison with the existing literature.

5.1.1. Literature background on the effects of drying on Atterberg limits

The influence of drying on Atterberg limits was noted as early as Casagrande (1932). Some data is available in the literature on the influence of drying on Atterberg limits, especially for weathered, residual, tropical/subtropical soils, containing certain minerals such as halloysite or allophane, and/or organic material (Eden 1960, Basma et al. 1994, Terzaghi et al. 1996, Jefferson and Rogers 1998, Malkawi et al. 1999, Kanıt et al. 2006, Özer 2008, Sunil and Krishnappa 2012, Ijaz et al. 2014). For example, a clay from New London, Connecticut, with organic matter of 2.6%, had liquid limit (LL) of 84% and plasticity index (Ip) of 34% when the sample is prepared starting from its natural moisture content; whereas after oven-drying, these values decreased to 51% and 9%, respectively (Casagrande, 1932). Hence, a difference of 33% in LL and 25% in Ip, and the ratio of $LL_{oven-dried}/LL_{Moist}$ of 0.61 was observed. Casagrande (1932) reported other soil samples having $LL_{oven-dried}/LL_{Moist}$ ratios of 0.71, 0.73, 0.85 having 2.5%, 2.0% and 0.0% organic content, respectively.

Terzaghi et al. (1996) stated that organic soils lose water irreversibly upon drying, due to oxidation. In the process, clay-sized particles will become cemented into larger

aggregates, thus increasing particle size and decreasing the liquid limit. The influence of organic matter percentage on Atterberg limits is reported by others as well (de la Rosa 1979, Zolfaghari et al. 2015, Sen at al. 2016, Al Rawi et al. 2017, Stanchi et al. 2015, Stanchi et al. 2017). Stanchi et al. (2015) reported that for sixty-two soil samples from northwest Italian Alps, as total organic carbon content (TOC %, in the range of 0-8%) increased, the liquid limit values, in the range of 20-100% (air-dried, ASTM D4318-17), increased.

Sen et al. (2016) studied the influence of organic matter percentage on engineering and index properties of soils by mixing dairy manure compost rich in organic content in various proportions (0% to 20% by mass) with a low plasticity clay. Liquid limit of the clay is reported to increase from 38% to 48% upon 20% organic matter addition. All liquid limit, plastic limit and plasticity index values are found to increase with the increase in organic content (Sen et al., 2016). Liquid limit increased beyond a threshold limit of 6% organic matter, whereas increase in plasticity index was beyond 2% of organic content (Sen et al. 2016).

Al Rawi et al. (2017) indicated a nonlinear relation between Atterberg limits and the organic content for Jordanian soils for a range of organic content between 2% to 20% by weight and liquid limits in the range of 40% to 62%. Al Rawi et al. (2017) stated that the rate of change of liquid limit with organic content depends on the liquid limit of original clays.

Terzaghi et al. (1996) reported particle size distribution and Atterberg limits data of Wesley (1973), for a residual soil sample from Indonesia. When tested, starting from its natural moisture condition, the soil has LL of 184% and Ip of 38%, and it is classified as fine-grained soil (with 95% fines content) as a high plasticity silt or organic silt, MH-OH according to Unified Soil Classification System (USCS, ASTM 2487-17). After air-drying, the fines content of this soil decreased to 19%, LL to 79% and Ip to 6%, and soil is classified as silty sand, SM. Furthermore, after oven-drying, the fines content became 15% and fines portion became "non-plastic" and soil is classified as silty sand, SM (Terzaghi et al. 1996). Terzaghi et al. (1996) explained this by noting that residual soils containing halloysite and allophane minerals lose

76

water irreversibly upon air-drying. This process causes aggregation of particles, thus increasing the grain size of the soil and decreasing the liquid limit. Similarly, Mitchell (1993) noted that, if the temperature is over 50°C or the relative humidity is lower than 50%, the hydrated halloysite loses its interlayer water irreversibly and this affects the results of grain size distribution and Atterberg limits, hence soil classification. Terzaghi et al. (1996) recommended, for soils suspected to contain halloysite or allophane, and for organic soils, to avoid drying the samples and to start the hydrometer and Atterberg limits tests from the natural water content of the samples. Jose et al. (1988, 1999) noted the effects of air/oven drying on the physical properties of Cochin marine clays from around Indian peninsula, which were characterized by high Atterberg limits and natural water contents. They concluded that oven drying reduces the liquid limit by more than 50%, which is attributed to aggregation of finer particles.

Sunil and Krishnappa (2012) studied the effect of drying on the index properties of lateritic soils from the west coast of India. Comparing air-dried and oven-dried (110±5°C) samples, they reported that $LL_{\text{oven-dried}}$/LL_{Moist} ratios of 11 samples were in the range of 0.76 to 0.97. Sunil and Krishnappa (2012) also note that activity (Ip / clay-size fraction) values of 1.25 to 2.34 in the air-dried condition, decreased by a factor of 0.65 to 0.97 in 11 samples.

Ijaz et al. (2014) study the effects of drying by using air-drying and oven-drying (at 110°C), on six samples from six different cities in Pakistan. The ratios of $LL_{\text{oven-dried}}$/LL_{Moist} were in the range of 0.88 to 0.97 for $LL_{air-dried}$ in the range of 30 to 61%. Some of these changes were explained by coagulation in microstructure of clayey soils (Jefferson and Rogers 1998); physical aggregation and flocculation of particles after drying (Basma et al. 1994, Terzaghi et al. 1996, Jose et al. 1999, Sunil and Krishnappa 2012); destruction of soil structure (Basma et al. 1994); nature of interparticle contacts and mineralogy (Jefferson and Rogers 1998); oxidation or loss of water of crystallization or other chemical changes (Terzaghi et al. 1996, O'Kelly 2005); organic substances acting as cementing/binding agents (Huang et al, 2009). The

observed changes in Atterberg limits were reported to be permanent, i.e. there is irreversible dehydration of clay structure (Mitchell 1993, Terzaghi et al. 1996, Sunil and Krishnappa 2012, Ijaz et al. 2014).

5.1.2. Discussion on the obtained data in this study

The Atterberg limits of all of the soil samples, in moist, 60°C dried and 110°C dried conditions, together with classification of the soils according to USCS, are presented Table *4.2*. The comparison of liquid limit, plastic limit and plasticity index values of all samples, prepared in moist and 110°C dried conditions are shown in Figure 5.1. All LL values at moist condition were higher than LL when samples were dried at 110°C (Figure 5.1a), and the difference was in the range of 1% to 30%, with an average difference of 12.5%. Plastic limit and plasticity index values were also higher in moist condition, as compared to 110°C dried condition. As an example, for one of the samples, LL of 91% when sample was prepared from moist condition became 62% after drying at 110°C, and its IP changed from 16% to 5% (Figure 5.2, Table *4.2*). After the data published by Huvaj and Uyeturk (2018), data for 5 soils were added to the plots given in Figure 5.1, and they are presented in a distinguishable way. This is due to the fact that additional data is very well in coherence with the data published before, and further validates the best line equation suggested by Huvaj and Uyeturk (2018). However, a new best line is also fitted to represent all of the data (Figure 5.1).

(a)

(b)

(c)
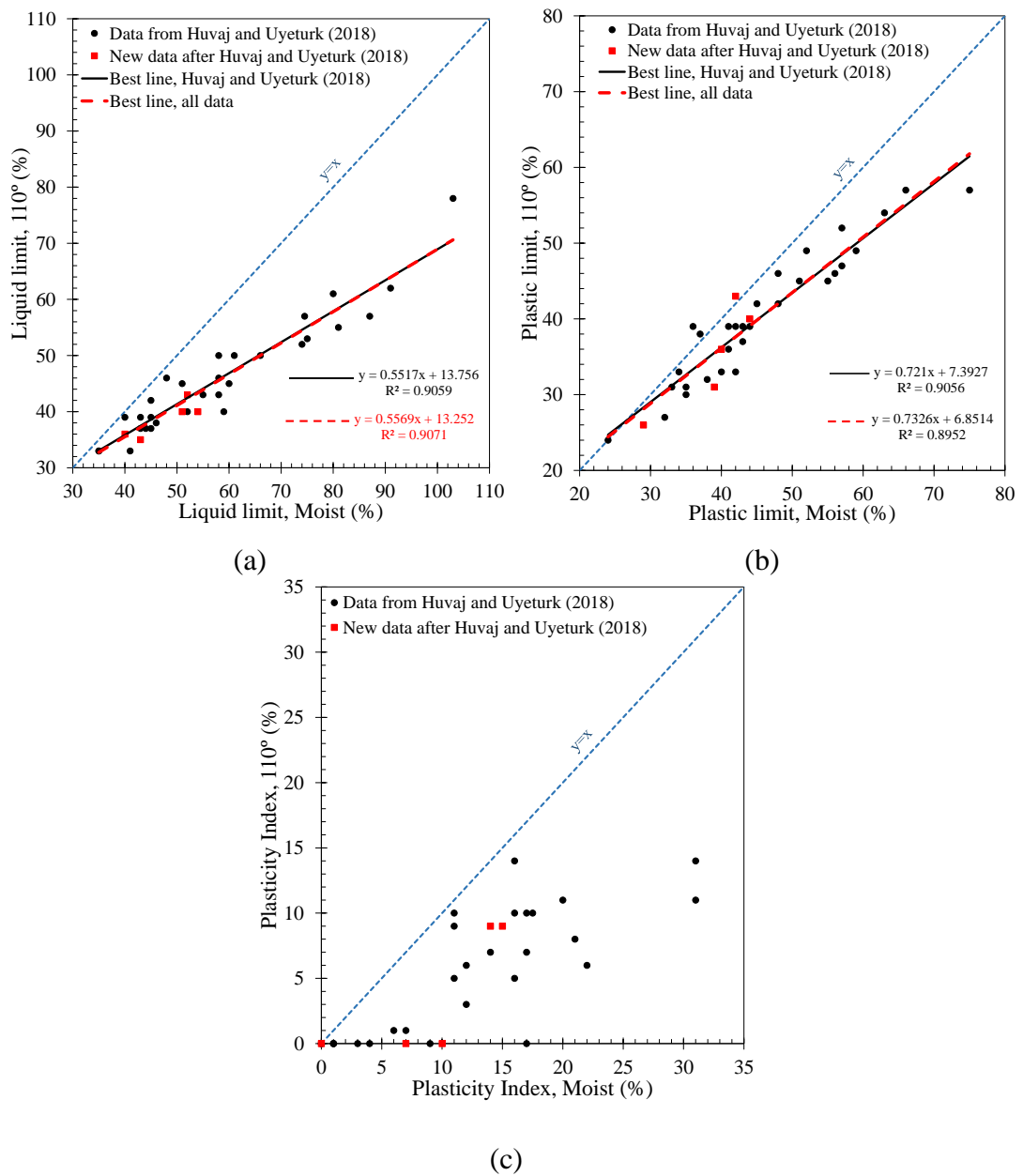
Figure 5.1. Comparison of liquid limits (a), plastic limits (b), plasticity indices (c) determined without any drying (Moist) and after drying at 110°C

79
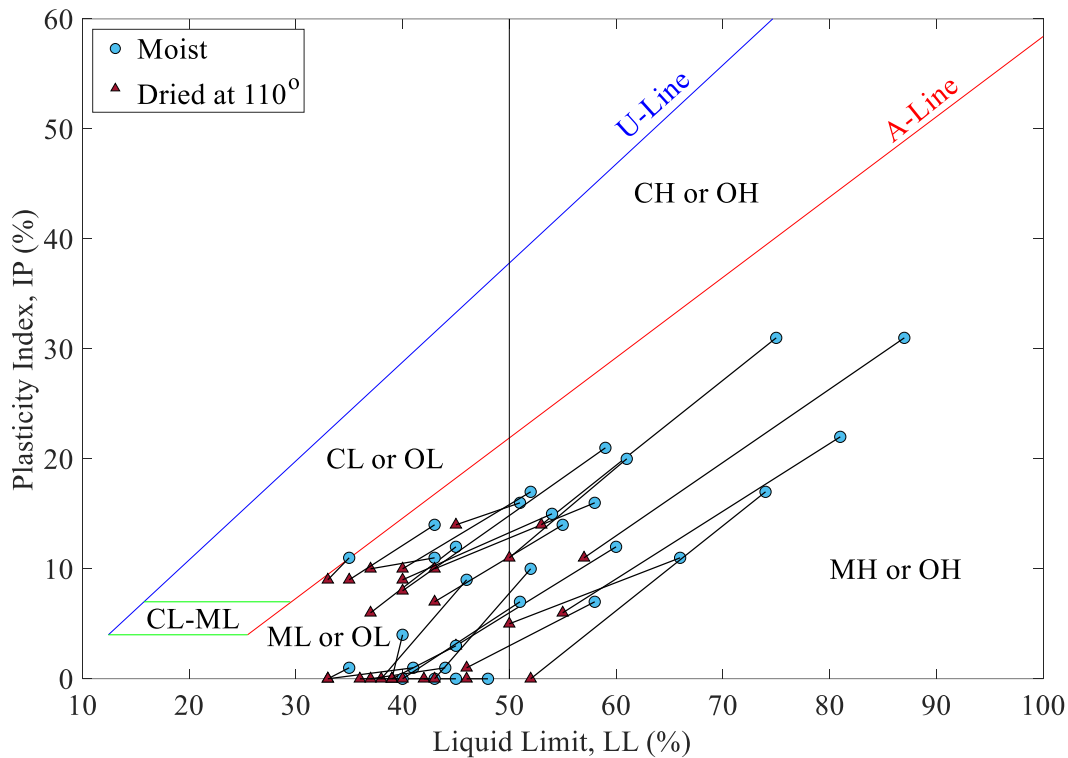
Figure 5.2. Changes in Atterberg limits of the samples from moist to 110°C dried tests

For all soils used in this study, the ratio of $LL_{110°C}/LL_{moist}$ was in the range of 0.66 to 0.98, and the LL_{moist} - $LL_{110°C}$ difference was in the range of 1% to 30% (Table *4.2*). All of the samples in this study were in the ML-OL or MH-OH zone in USCS plasticity chart (Figure 5.2). It was observed that oven drying at 110°C changed the Atterberg limits, and in some cases drying changes the soils classifications.

In order to further investigate the effects of different drying temperatures on Atterberg limits, tests were conducted on two samples from sites 2 and 3, by drying at 440°C. It should be noted that this temperature is not used in ASTM D2487-17, it was used in this study only to investigate the temperature effects. $LL_{110°C}/LL_{Moist}$ ratios of the samples were, 0.74 for the sample from site 2, and 0.68 for the sample from site 3. LL of samples, when they were prepared by drying at 440°C, is 40% and 49% for samples from site 2 and site 3, respectively (Figure 5.3). LL of samples when they were prepared by drying at other temperatures can be seen in Table *4.2*. Both samples have

80

IP of 0% when they were prepared by drying at 440°C (Figure 5.3). The significant effect of different drying temperatures on Atterberg limits and classification of samples is shown in Figure 5.3.
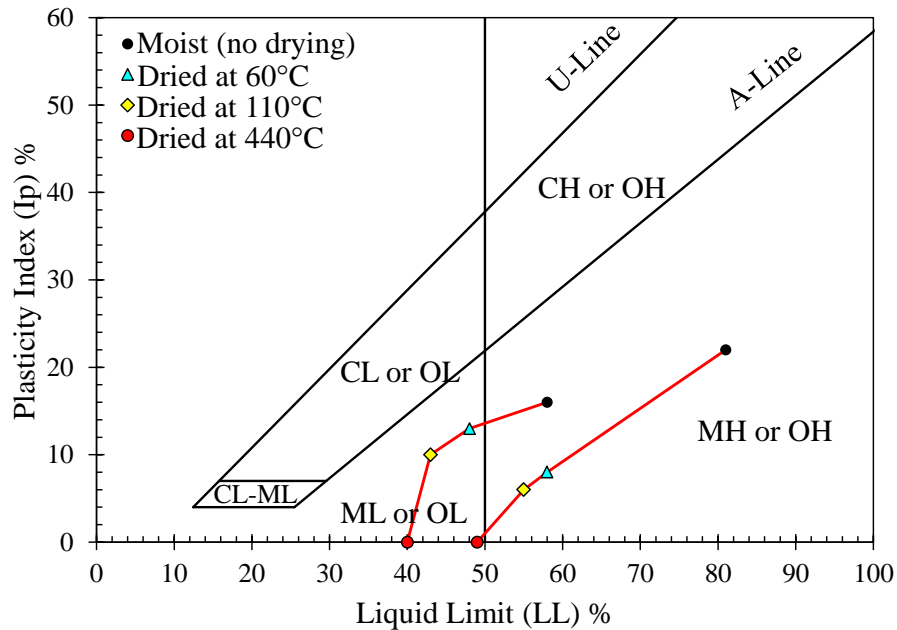
Figure 5.3. Changes in Atterberg limits of the samples: from moist to 60°C to 110°C and to 440°C dried sample preparation methods

Soil samples used in this study have organic contents in the range of 4.3% to 12.1% (Table *4.1*). According to different soil classification systems, soils having greater than 15% (or greater than 30%) organic matter would be classified as organic soil/peat (Huang et al. 2009, Canadian Soil Classification Working Group 1998, INDOT 2012, etc.). Soils with organic content of 1% to 7% are classified as soils "having traces of organic matter" and the ones having organic content between 7 to 13% are named as soils having "little organic matter" according to INDOT 2012 classification. German norm DIN 18196 uses threshold value 5% to call a fine-grained soil an "organic soil". In ISO 14688-2 (2004), the distinction is made between low organic content (organic content between 2 and 6%, by dry mass); medium organic content (organic content between 6 and 20%); and high organic content (organic content greater than 20%) soils. Huang et al. (2009) proposed a system for classifying organic soils which is based on the percentage of organic matter present: soils with organic content <3% are

81

termed "mineral soils"; if the organic content is >3% and <15%, soils are classified as "mineral soils with organics"; when the organic content exceeds 15% but is <30%, the term "organic soil" is employed. Therefore, all of the soils used in this study are classified as "mineral soils with organics" according to Huang et al. (2009).

In general, both liquid and plastic limits increase with organic content. This is because the water adsorption capacity of the organic matter usually exceeds the reduction caused by organic matter induced aggregation (Huang et al. 2009). As the organic content increases the ratio of $LL_{110°C}/LL_{moist}$ decreases (Huang et al. 2009). Figure 5.4 demonstrates the general relation between percentage of organic matter and $LL_{110°C}/LL_{moist}$ ratio. The horizontal line in Figure 5.4 indicates $LL_{110°C}/LL_{moist}$ ratio of 0.75, which is the boundary below which soils are classified as 'organic' according to USCS. Figure 5.4 also includes data from Huang et al. (2009). Data from the current study and from Huang et al. (2009) having LL_{Ratio} higher than 0.95 are not plotted in Figure 5.4, since the accuracy of LL can only be within ±2% (Olmstead and Johnston 1955), and that the $LL_{110°C}/LL_{moist}$ ratio greater than 0.95 cannot always be attributed to the percentage of organic content.
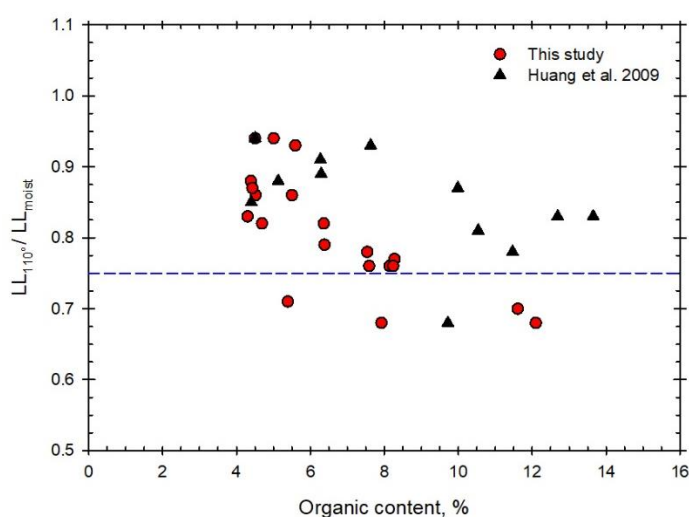
Figure 5.4. Relation between the ratio of $LL_{110°C}$ / LL_{moist} with organic content % (after Huvaj and Uyeturk 2018)

In Figure Figure 5.4, LL_{Ratio}/organic content versus organic content is plotted. In this plot, LL_{Ratio} is normalized by organic content %, therefore it can be considered as an indication of the change in LL_{Ratio} per organic content. In Figure 5.5, the results of this study and combined results of Huang et al. (2009) and this study were presented separately as power relations. When the data in Figure 5.4 is normalized as in Figure 5.5, a clear trend is observed. Huang et al. (2009) reported that the plastic limit ratio, $PL_{110°C}/PL_{Moist}$, shows similar sensitivity as the liquid limit ratio to the presence of organic matter.
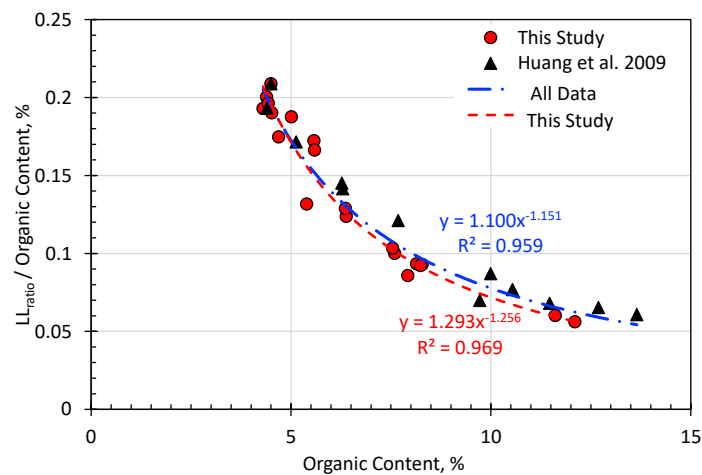
Figure 5.5. Relation between LL_{ratio}/organic content % versus organic content %

Huang et al. (2009) noted that the 25% reduction of liquid limit stated in the USCS system (i.e. $LL_{110°C}/LL_{moist}$ ratio less than 0.75) represents an organic content of about 15%. This means that soils classified as "inorganic", based on "$LL_{110°C}/LL_{Moist}$ ratio less than 0.75" criterion actually contain a significant amount of organic matter. This classification criterion fails to represent the influence of organic matter on soil behavior, and may not be adequate for evaluating the quality of soils for many construction purposes such as suitable fill materials etc.

Examples of SEM photos of a sample from site 3 is presented in Appendix C (Figure C.6) , where in air-dried and 110°C dried samples both had tubular halloysite minerals

(although not abundant), that were typically 2 to 10 micron in length, and that 110°C dried samples are relatively more aggregated even in smaller size scales.

Halloysite, allophane and nontronite are some of the common minerals in residual soils, particularly those derived from volcanic parent material and pyroclastic deposits (Terzaghi et al. 1996, Adamo et al. 2001). These minerals may result from the weathering of basalt and/or volcanic ash and scoria that are often deposited in association with lava flows. Halloysite is a member of the kaolin subgroup of clay minerals and it results from weathering, pedogenesis or hydrothermal alteration of ultramafic rocks, volcanic glass and pumices (Cravero et al. 2012). Halloysite is actually a well-known weathering product of pyroclastic materials (Dixon, 1989). Adamo et al. (2001) suggested that the process of formation of halloysite probably involves: (a) dispersion and deposition of erupted pyroclastic materials all over the volcanic area; (b) water erosion and accumulation in the valleys of the volcanic products; and (c) in-situ attack by water containing dissolved carbon dioxide. The intersheet water in the hydrated halloysite is removed irreversibly starting at 60°C to 75°C (Terzaghi et al. 1996). Tubular and spheroidal halloysite in pyroclastic deposits in the area of the Roccamonfina volcano, in Southern Italy was reported by Adamo et al. (2001). Other examples of halloysite deposits in pyroclastic rocks, rhyolitic tuffs and ignimbrites were also available in the southwest of the province of Rio Negro in Argentina (Cravero et al. 2012). Papke (1971) described large deposits of halloysite, formed by the hydrothermal alteration of volcanic rock (tuff), which occur in the Terraced Hills, Washoe County, Nevada. Cravero et al. (2012) stated that spheroidal halloysite (which is common in weathered ashes and pumices) was related to rocks with low porosity and tubular halloysite particles were related to rocks with open spaces.

Existence of halloysite mineral was reported in volcanic deposits in Northwestern Turkey together with alunite (Ece and Schroeder 2007), in Sile in northern İstanbul region (Ece et al. 2003), and in the south-southwest of Konya (Kadir and Karakas 2002), as well as in the city of Trabzon in northern Turkey (Arslan et al., 2006). Arslan et al. (2006) reported the widespread chemical weathering of Tertiary alkaline

volcanic rocks and formation of well-developed reddish-brown saprolite which was dominated by kaolinite, with minor quantities of halloysite, in pyroclastic deposits in Trabzon. Saprolite is a residual deposit, typical of humid and tropical to subtropical climates, and it is formed by extensive in-situ chemical weathering of rock. In nature, halloysite and kaolinite are the dominant alteration products in saprolite-type weathering products of pyroclastic and volcanic units (e.g. Nagasawa 1978, Murray 1988). The region where the soil samples were taken from was governed by the alteration products of the Tertiary alkaline pyroclastic rocks. The parent rocks of the reddish-brown saprolite were pyroclastic products (mainly breccias) of a Tertiary alkaline volcanic suite (Arslan 2003). The saprolite was dominated by kaolinite, with traces of halloysite and other minerals. These saprolite soils were also referred to as "lateritic soils" which were derived from chemical disintegration of the extrusive and pyroclastic rocks (Önalp and Balta 1987) and that they contained allophane as well (Balta 1987).

5.2. Examination of the power coefficient in one-point liquid limit test at various temperatures

In this section, the effects of drying on the power coefficient suggested by ASTM D4318-17 for the determination of one-point liquid limit is investigated. The main question for this discussion is to evaluate the usefulness of the suggested power coefficient for soils dried at different temperatures for sample preparation. Although limited data exist in this study to draw a very inclusive conclusion, it is, however, considered as a useful discussion for forming a baseline.

The findings of this section are published by Uyeturk and Huvaj (2018). Here, firstly, a brief literature background on the subject will be given, then the data obtained in this study presented in Chapter 4 will be examined.

5.2.1. Literature background

The standard Casagrande cup method for determining the liquid limit (LL) requires that, at least three trials be made, each at a different moisture content. In the conventional multi-point test, the aim is to obtain the water content of the soil sample that requires 25 blows for the closure of the opening (for a length of 13 mm), which is initially created by a groove tool as described by ASTM D4318-17. However, since obtaining 25 blows exactly is difficult, an interpolation with several data points are done to find the water content at 25 blows. Also, there is another way to determine the LL of a soil sample, which is called "one-point method" (US Waterways 1949, Olmstead and Johnston 1954, Eden 1955, Norman 1959, Mohen and Goel 1958, Roje – Bonacci 2004). This method requires obtaining blow count between 20 and 30 for the closure of the opening in Casagrande cup, by a 13 mm length and determining the water content of the soil sample at that consistency. Then, an equation is to be used to find the LL at 25 blow count. This method is also standardized by ASTM (ASTM D4318-17), as "method B", and by British Standards (BS1377). ASTM D4318-17 suggests an equation and a power coefficient to determine LL of a soil sample corresponding to 25 blow counts, from one data point:

$$LL = w \cdot \left(\frac{N}{25}\right)^{tan\beta} \tag{5.1}$$

The tanβ suggested by ASTM is 0.121, whereas 0.092 and 0.121 are used by British Standards BS1377 and German DIN18122 standards, respectively.

ASTM D4318-17 notes that one-point method may not be applicable for some soils, such as organic soils, and soils from the marine environment. Similarly, according to Eden (1955), the assumptions made in one-point method is not strictly correct for highly organic soils and Eden (1955) stated that "it should not be used on soils which contain an appreciable amount of organic matter".

The origin of the one-point method for determination of LL may have developed from

the U.S. Waterways Experiment Station (1949) study, which stated that "Dr. Arthur Casagrande suggested that flow lines determined by liquid limit tests, plotting both water content and number of blows to a logarithmic scale, might have a constant slope for soils of the same geologic origin". According to Norman (1959) and Mohan and Goel (1960), it is observed in the determination of LL tests that, slopes of the flow curves have nearly the same slope, and this led to an increased interest in one-point method to determine LL of soils.

Some of the benefits of one-point LL test were reported as, a substantial reduction in the time and cost of LL determinations, and reduced workload on technicians (U.S. Waterways Experiment Station 1949, Eden 1955, Önalp and Kılıç 1994). Önalp and Kılıç (1994) stated that for big projects with extensive site investigation and laboratory tests, a lot of LL tests are to be done, increasing the workload on technicians, which may increase the tendency of misinterpretation of the tests or mistakes in the long term.

According to Haigh and Vardanega (2014), one-point method is an applicable method to determine LL, and it is allowed in the codes around the world, and hence further examination is valuable. Although it is widely accepted and many codes worldwide allow the usage of the one-point method, a limited amount of research is done to investigate the one-point equation for different soils coming from various origins. Önalp and Arel (2013), Olmstead and Johnson (1955), Mohan and Goel (1959) recommended further studies to be conducted to investigate the power coefficient in one-point method for soils of different origins from different parts of the world. On the contrary, some researchers suggest that the geological origin of the soil need not be considered and that the variation in values of the power (tan β) for many different soils would be small (Eden 1955). The power coefficient obtained as a result of various researches are summarized in Table 1. Although the power coefficient seems to vary in a broad range (Table 5.1), the effect of it on LL is not that significant. Olmstead and Johnston (1955) suggested that, if the errors due to the one-point method fall

within the ± 2 percent range in LL, then one-point test should be an acceptable procedure.

Table 5.1. Power value in one-point LL equation from literature

Reference	Origin of Soil	Type of soils	Number of Soils	Average tanβ (range in parenthesis)
US Waterways (1949) -	Southern US (Alluvial Valley of the Mississippi River, the West and the East Gulf Coastal Plains)	medium to highly plastic inorganic clays, and a few silts and sandy clays	767	0.121*
Olmstead and Johnston (1954)	the US	-	759	0.135
Eden (1955)	Canadian	-	484	0.108 / 0.100
Mohan and Goel (1958)	India	Black cotton soils (montmorillonitic)	250	0.068
Norman (1959)	the UK/Overseas	-	455/49	0.092**
Jain and Patwardhan (1960), reported by Haigh & Vardanega (2014)	India	Gangetic alluvium	32	0.085
Kim (1973), reported by Haigh & Vardanega (2014)	Korea	Korean soils	1017	0.118
Önalp (1994)	Eastern Black Sea region, Turkey	Silts &clays	332	0.112
Vural (1998)	Adapazarı, Turkey	-	24	-
Roje – Bonacci (2004)	Dalmatian region, Croatia	CH clays	88	0.063 (range: 0.023 to 0.132)
Uysal (2004)	Adapazarı, Turkey	-	79	0.120
Önalp and Arel (2013)	Istanbul, Turkey	Marine clays	20	0.120
This study	Northern Turkey (Rize and Trabzon)	Weathered volcanic deposits	35	0.120

*also ASTM D4318-17, TS 1900-1
**also BS1377

By using 77 flow curves obtained from multi-point test, the power coefficient ($tan\beta$) in ASTM's suggested number is calculated for each test. The average $tan\beta$ values are calculated for three different sample preparation techniques and are presented in Table *5.2*. Table *5.2* shows clearly that, upon increase in drying temperature $tan\beta$ values are getting smaller. The frequency distribution of all $tan\beta$ values from all 77 tests is shown in Figure 6. The average value of $tan\beta$ from all 77 tests is 0.120 (with a standard deviation is 0.047). This power coefficient is in agreement with the ASTM 4318-17 suggested value of 0.121.

Table 5.2. *The average power coefficient, i.e.* $tan\beta$ *values in ASTM suggested equation, for different sample preparation techniques (after Uyeturk and Huvaj 2018)*

	Wet sample preparation	Dried at 60°	Dried at 110°	Average of all data
$tan\beta$	0.133	0.120	0.106	0.120
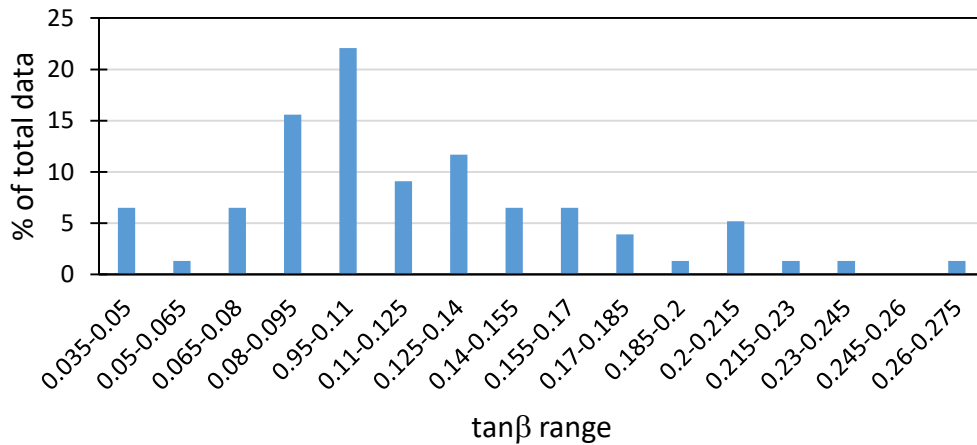
Figure 5.6. The frequency distribution of $tan\beta$ values in 77 LL tests (after Uyeturk and Huvaj 2018)

Having obtained the average $tan\beta$ values for wet, 60°C and 110°C oven dried sample preparation methods and the average $tan\beta$ value of all the samples, an analysis is made to compare the results of LL values calculated using these $tan\beta$ values and using ASTM D4318-17 suggested $tan\beta$ value. In the analyses, LL of all the samples are calculated by using (i) ASTM suggested $tan\beta$ value of 0.121, (ii) average

tanβ value of 0.120 which is the average obtained from all three different sample preparation techniques, (iii) average *tanβ* value determined only from the related sample preparation technique (Table *5.2*).

Table 5.3. *Liquid limit (%) values obtained by multi-point and one-point methods (adapted from Üyetürk and Huvaj 2018)*

Site number – sample number	Prepared from in-situ moisture content				Prepared by drying at 60°C oven				Prepared by drying at 110°C oven			
	Multi Point	One-Point			Multi Point	One-Point			Multi Point	One-Point		
		tanβ=0.121 (ASTM)	tanβ=0.120 (Ave. All Data)	tanβ=0.133 (Ave. Moist)		tanβ=0.121 (ASTM)	tanβ=0.120 (Ave. All Data)	tanβ=0.120 (Ave. 60°C)		tanβ=0.121 (ASTM)	tanβ=0.120 (Ave. All Data)	tanβ=0.106 (Ave. 110°C)
1-1	45	45	45	45	40	39	39	39	37	37	37	37
1-2	43	45	45	45	39	39	39	39	37	37	37	37
1-3	35	36	36	36	33	33	33	33	33	33	33	33
1-4	35	34	34	34	35	35	35	35	33	33	33	33
2-1	58	57	57	57	48	48	48	48	43	43	43	43
2-2	51	51	51	51	46	46	46	46	45	45	45	45
2-3	75	75	75	75	62	61	61	61	53	53	53	53
2-4	46	46	46	46	40	40	40	40	38	39	39	39
3-1	81	80	80	80	58	57	58	58	55	55	55	55
3-2	45	47	47	47	43	43	43	43	42	43	43	43
3-3	66	66	66	66	54	54	54	54	50	50	50	50
3-4	58	59	59	59	49	49	49	49	46	45	44	44
3-6	48	48	48	48	48	48	48	48	46	46	46	46
4-1	60	59	59	59	48	48	48	48	45	45	45	45
4-2	40	40	40	41	-	-	-	-	39	39	39	39
4-5	-	-	-	-	-	-	-	-	43	43	43	43
5-1	-	-	-	-	-	-	-	-	40	40	40	40
5-2	59	59	59	59	-	-	-	-	40	42	42	42
5-3	47	46	46	46	38	38	38	38	-	-	-	-
5-4	42	43	43	43	-	-	-	-	-	-	-	-
6-2	87	87	87	86	-	-	-	-	60	60	60	60
7-1	-	-	-	-	42	41	41	41	43	43	43	43
7-2	41	40	40	40	-	-	-	-	33	33	33	33
7-3	44	44	44	44	-	-	-	-	-	-	-	-
7-4	42	42	42	42	35	34	34	34	50	50	50	50
7-5	61	62	62	62	-	-	-	-	52	52	52	52
7-0.5-F	115	114	114	114	66	66	66	66	-	-	-	-
7-0.5-F2	88	88	88	88	-	-	-	-	-	-	-	-
7-0.5-F3	-	-	-	-	36	37	37	37	-	-	-	-
8-1	45	45	45	45	40	40	40	40	39	40	40	40
T-2	91	90	90	90	-	-	-	-	62	62	62	62
T-3	58	58	58	58	-	-	-	-	50	50	50	50
T-4	75	74	74	74	-	-	-	-	57	56	56	56
T-5	80	80	80	80	-	-	-	-	61	61	61	61

Figure 5.3 clearly shows that for the investigated soils, the LL values, when calculated by using different $tan\beta$ values differ from each other by 2% maximum. Furthermore, the comparison of LL obtained by multi-point method and that obtained by one-point method gives the same or very close LL value (*Table 5.3*, Figure 5.1). In Figure 5.1, the LL determined from multi-point method versus LL determined from one-point method (using average $tan\beta$ value of all samples) are compared graphically by plotting them with respect to the 45° line, and with upper and lower 2% difference boundaries. According to Eden (1960), different operators were found to give slightly different results when determining the LL of soils. Moreover, Olmstead and Johnston (1954) concluded that, based on many tests by experienced operators and/or different laboratories, the LL of a sample can be determined within ± 2% range. Hence, it can be concluded from Olmstead and Johnston (1954) that if one-point method provides the accuracy of ± 2% difference compared to multi-point test, the usage of one-point method is justified.
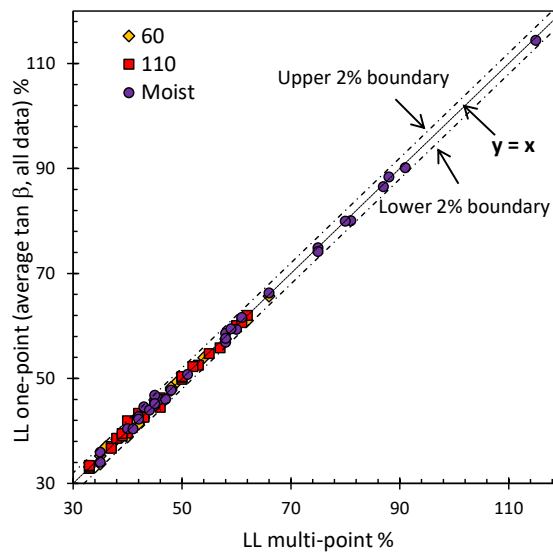
Figure 5.7. Comparison of LL obtained by multi-point method and one-point method

91

5.3. Evaluation of direct shear test results

5.3.1. Reconstituted samples

Direct shear tests are performed by using conventional equipment. That is, suction control or suction measurements are not possible. Thus, evaluating the results, matric suction could not be used as a stress state variable, rather specimen preparation degree of saturation (Sr) is used. However, Sr and matric suction can be used interchangeably for qualitative purposes. For example, increase in Sr implies decrease in matric suction when all else are constant.

Shear strength and degree of saturation relationship plots given for each sample are generated by calculating shear strength values corresponding to 20-40-60 kPa normal stresses from the corresponding failure envelope for the related degree of saturation, for easy comparison. Also, since degree of saturation of each reconstituted specimen is slightly above or below target Sr% (e.g. 60%), a round value is used (e.g. 60%) in the plots. Therefore, degree of saturation values of 60-80-100% are used. Furthermore, in order to generate the plots related to different Sr cases, average normal stress values are used. For example, in Figure 5.13 for 16 kPa case, the actual applied normal stresses for three different Sr cases are 16, 16.7 and 17.4 kPa. However, in this plot 16 kPa is written in the legend as a representative value for the stress range.

For a given sample, friction angles were found to be similar at different Sr cases (saturated, 80%, 60% degree of saturation) for most of the samples. Thus, the increase in shear strength at different Sr values is mainly due to the increase in cohesion component of the failure envelopes.

Dilatancy values are also reported and discussed for some of the samples, and are calculated by using the following equation:

$$tan\ \psi = -\frac{\Delta y}{\Delta h} \tag{5.2}$$

Where ψ is the dilatancy angle, Δy is the change in the vertical displacement and Δh is the change in the horizontal displacement with respect to the initial values of (0,0). In the plots "-" values indicate dilation (volume increase) and "+" values indicate contraction (volume decrease). Furthermore, interpreting the dilatancy values, first one or two data (at the beginning of the test) in the test results are ignored since they may be problematic.

5.3.1.1. Effect of preparation Sr and normal stress on friction angle, cohesion and stress-horizontal displacement behavior

For sample #10-1, a clear peak shear strength is observed for Sr=60% case (at about 2-3 mm of horizontal displacement), whereas no peak shear strength is observed for Sr=80% and saturated cases, reaching to an ultimate shear resistance at 7 mm horizontal displacement (Figure 4.11a). That is, specimens tested at lowest degree of saturation showed strain-softening behavior, while saturated and Sr=80% specimens showed strain-hardening behavior. Jotisankasa and Mairaing (2010) noted that samples having higher suction exhibited stronger bounds at particle contacts, which results in more brittle behavior.

For sample #10-2, generally, a clear peak is not observed, and the specimens exhibited strain-hardening behavior (Figure 4.11b).

The results for sample #11 are presented in Figure 4.12a, where strain-hardening behavior is observed for all the tests in saturated case. For Sr=80% case, peak shear strength is observed for the lowest normal stress case; however, as the normal stress increased, clear peak is not observed, but rather the behavior changed to strain-hardening response. Similarly, for Sr=60% case a very clear peak is observed followed by an abrupt decrease in shear resistance; however, as the normal stress increased, decrease in shear resistance gets flatter, and with the highest normal stress the maximum shear resistance is maintained by the soil skeleton until approximately 5.5 mm horizontal displacement.

Sample #12, (i) for lower dry-density case (1.427 g/cm^3), strain-hardening behavior is observed for saturated and Sr=80% cases (Figure 4.12b). A clear peak shear strength followed by an abrupt decrease in shear resistance is observed for the lowest normal stress of Sr=60% case; however, as the applied normal stress increased, the decrease gets flatter, and for the highest normal stress the shear response becomes strain-hardening rather than stress softening. (ii) For higher dry-density case (1.58 g/cm^3), all of the tests showed peak resistance; however, for unsaturated tests, abrupt decrease in shear resistance is observed, whereas for saturated cases the decrease in shear strength is gradual (Figure 4.13).

Friction angles are generally found to be similar for Sr=60%, 80% and saturated cases for an individual soil sample. For example, for sample #10-2 the friction angles are 34.3º, 32º and 33.3º for saturated, Sr=80% and Sr=60% cases, respectively (Figure 4.14b). However, for sample #12 with higher dry-density case friction angles are found to vary significantly for different Sr cases.

The cohesion intercepts found at different Sr cases are shown in Figure 5.8. The cohesion intercepts are decreased upon increase in Sr, and approached to zero except for sample #12 with high dry-density. For that case, although the cohesion decreased as the Sr increased, about 15 kPa of cohesion was still available. For sample #10-1, the cohesion value is not changing much from saturated case to Sr=80% case; however, for Sr=60% case, the cohesion value increased dramatically (Figure 5.8). One reason for this may be the specimen preparation method besides the suction increase due to Sr. That is, in Sr=60% case, the specimens were prepared by static compaction, which may result in change in the cohesion component.

Combining the friction angle and cohesion intercepts found at different Sr cases, shear strength increased with decreasing Sr (Figure 5.9).

Furthermore, the initial stiffness (that can be obtained from shear stress-horizontal displacement graphs) increased with increasing normal stress at a given Sr value, and initial stiffness increased upon decrease in Sr at a given normal stress, for all samples.

Increase in initial stiffness with matric suction increase (which implies decrease in Sr) is also noted by Gallage and Uchimura (2016).

Shear stress-horizontal displacement plots for sample 10-2, 11 and 12 are given in Figure 5.10. It is observed that at large displacements shear stress values of cases with different degrees of saturation cases at similar applied normal stresses approach to each other.

(a)Sample 10-1 (b)Sample 10-2

(c)Sample 11 (d)Sample 12
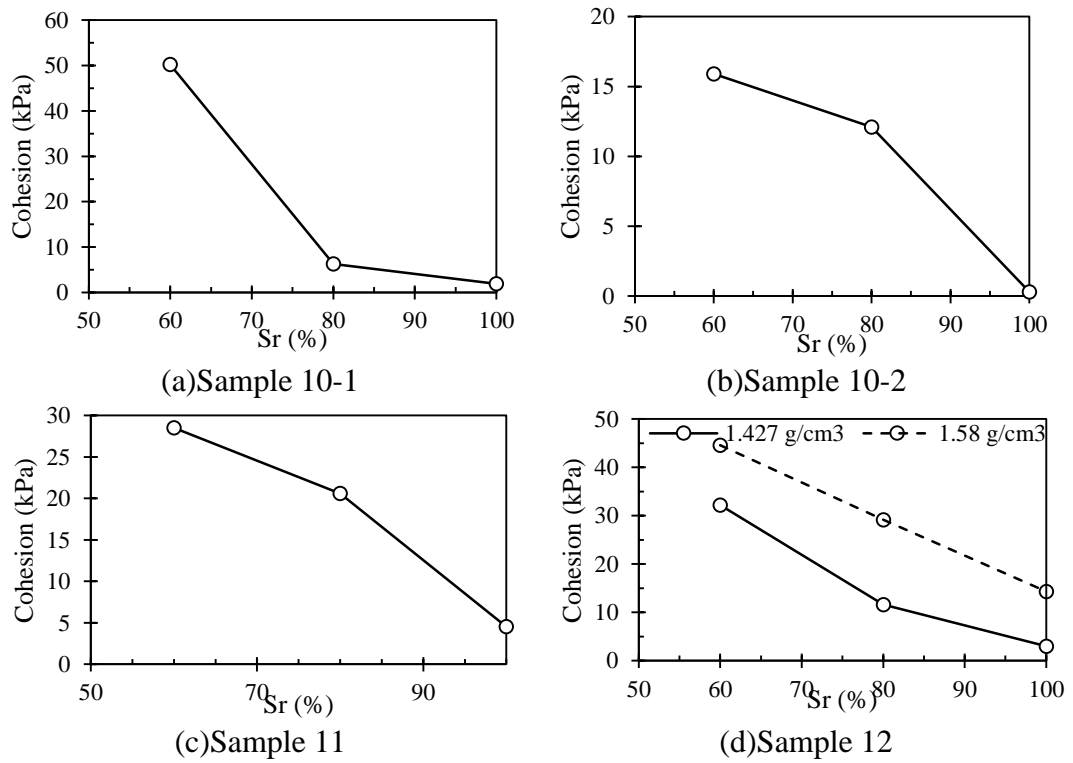
Figure 5.8. Cohesion and Sr relationships
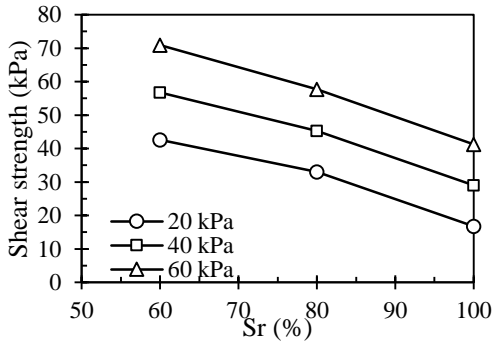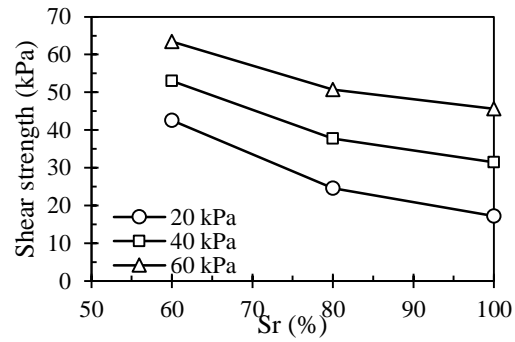
Figure 5.9. Shear strength and Sr relationship

Legend for left chart: —○— U60 16.1 kPa —□— U60 26.8 kPa —△— U60 42.6 kPa —◇— U60 62.0 kPa
—●— U80 16.1 kPa —■— U80 25.9 kPa —▲— U80 42.1 kPa —◆— U80 62.0 kPa

Legend for right chart: —○— U60 16.3 kPa —□— U60 27.5 kPa —△— U60 42.8 kPa —◇— U60 62.3 kPa
—●— U80 15.8 kPa —■— U80 28.3 kPa —▲— U80 43 kPa —◆— U80 64.8 kPa

(c)Sample 12 (1.427 g/cm³)   (d)Sample 12 (1.458 g/cm³)
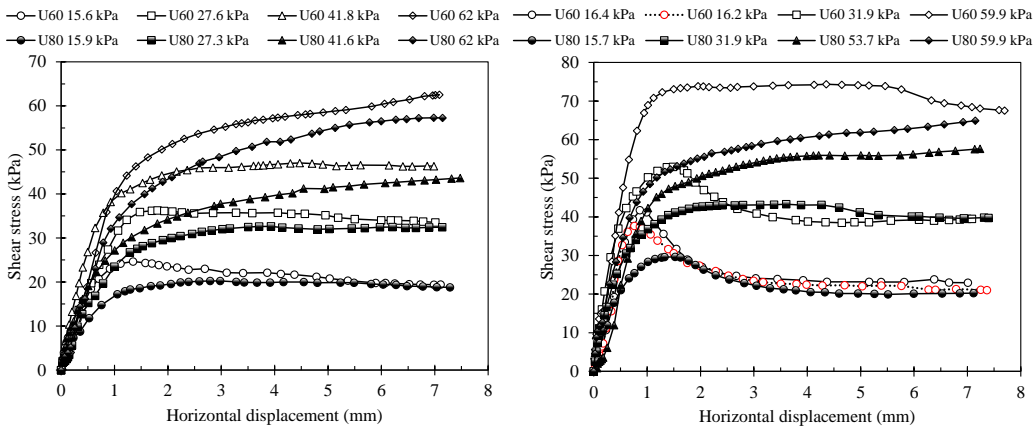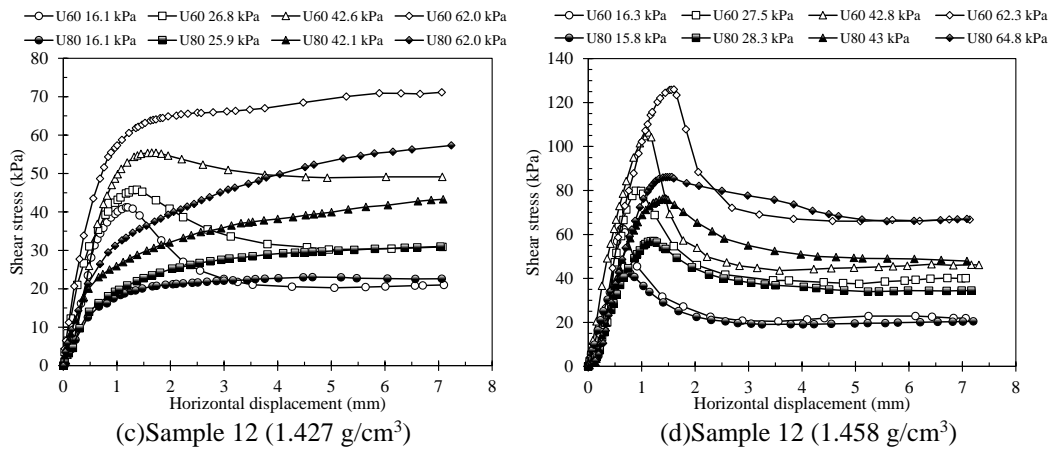
Figure 5.10. Shear stress-horizontal displacement plots for unsaturated tests

5.3.1.2. Effect of preparation Sr and normal stress on volumetric response during shearing

For sample #10-1, specimens having Sr=60% all exhibited dilatant (volume increase) behavior while saturated tests and Sr=80% tests contracted in volume in response to horizontal displacement. Furthermore, in general, contraction in volume is greater with increasing normal stress with test "S 41.8 kPa" being the exception (Figure 4.11a).

Clear volumetric response trend is observed in direct shear test results for sample #10-2 (Figure 4.11b). Specifically, contraction in volume is observed with increasing normal stress, and dilative response of the sample is greater upon decrease in Sr. That is, the most dilative response is observed for the sample having the lowest degree of saturation and at lowest normal stress. Also, most of the unsaturated tests exhibited volume increase, whereas most of the saturated tests showed volume decrease. Maximum dilatancy-normal stress and maximum dilatancy-degree of saturation relationships are shown in Figure 5.11 and Figure 5.13, respectively. It is observed that the normal stress and Sr significantly influence the dilatancy of soil. Maximum dilatancy increased with decreasing normal stress and Sr (Figure 5.11, Figure 5.13).

97
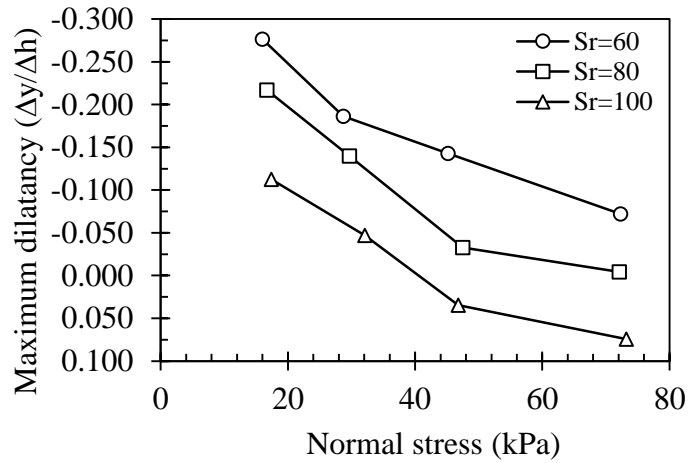
Figure 5.11. Maximum dilatancy and normal stress relationship for sample #10-2

Using the maximum dilatancy values shown in Figure 5.11, the maximum dilation angles are also calculated and shown in Figure 5.12.

Figure 5.12. Maximum dilation angle and normal stress relationship for sample #10-2

Figure 5.13. Maximum dilatancy and degree of saturation relationship for sample #10-2 (stresses are average values for all tests)

For sample 11, all of the unsaturated specimens showed dilative behavior, whereas all of the saturated tests showed contractive behavior (Figure 4.12). For unsaturated tests, dilation increased with decreasing Sr and applied normal stress. However, no trend with normal stress is observed for saturated tests in volume change behavior. The most dilative response is observed for the sample having the lowest degree of saturation and at lowest normal stress. However, unlike sample #10-2 the most contractive behavior is not observed for the saturated cases' largest normal stress, but observed for the second largest normal stress case.

Direct shear tests for sample #12 were performed for 2 different dry-densities: (i) 1.427 g/cm^3, (ii) 1.58 g/cm^3. The first one is the field dry-density, and the second one stands for a very dense state (Figure 4.12b, Figure 4.13).

For sample 12, for lower dry-density case, all of the unsaturated and saturated tests showed dilative behavior except the test with the greatest normal stress in saturated and Sr=80% cases. Volume contraction is observed for these specimens during shearing. It is observed that as the normal stress increased, maximum dilatancy increased for Sr=60% and 80% cases (Figure 5.14). However, for saturated case the maximum dilatancy decreased followed by and increase and again decrease. To

99

explain the zig-zag shape in Figure 5.14 it is necessary to note here that for the first 3 data points (low normal stress side) for saturated case, dilation behavior is observed after some contraction in the vertical displacement-horizontal displacement plot, whereas for the case with the highest normal stress, contraction is observed throughout the test. Combining these, the third data point is the transition point for volumetric response. Thus, it may be the reason for the deviation from the trend for the last 2 data points. Plotting the same data with different axis shows that, as Sr increased maximum dilatancy decreased (Figure 5.16). Using the maximum dilatancy values shown in Figure 5.14, the maximum dilation angles are also calculated and shown in Figure 5.15.
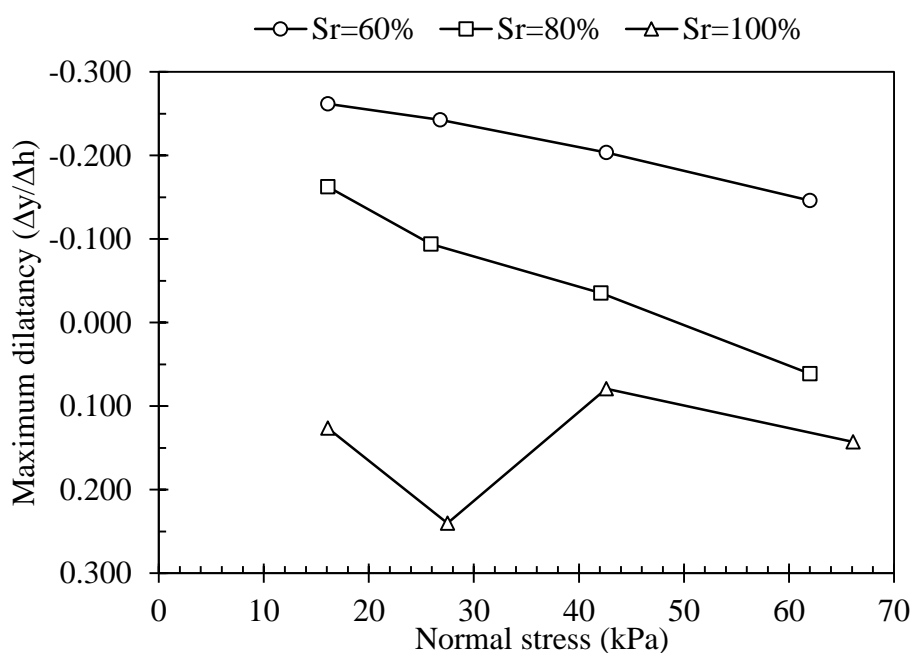
Figure 5.14. Maximum dilatancy and normal stress relationship for sample #12 (1.427 g/cm^3)
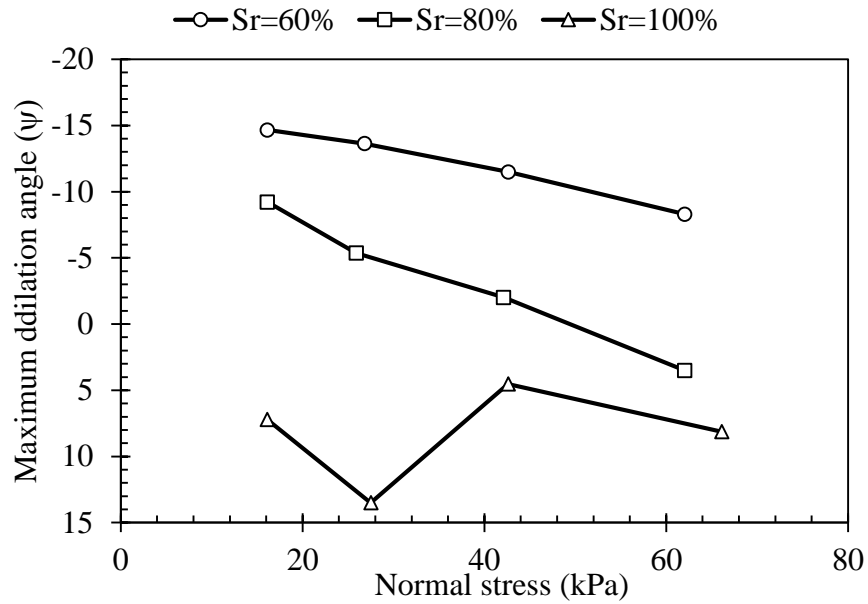
Figure 5.15. Maximum dilation angle and normal stress relationship for sample #12 (1.427 g/cm^3)
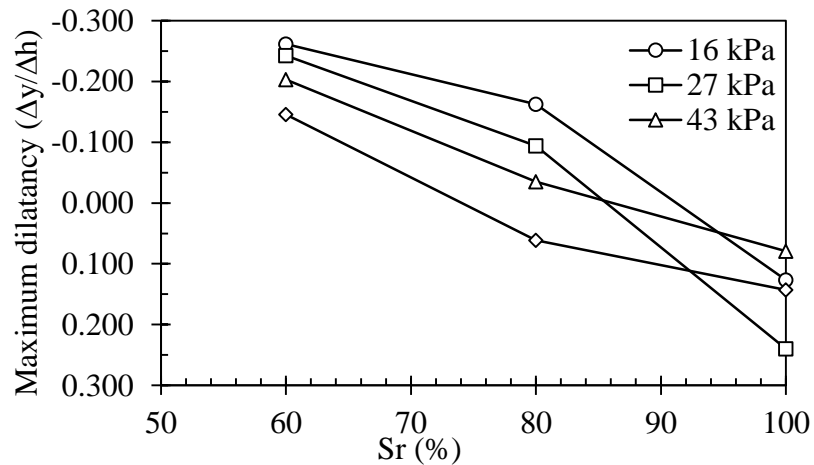
Figure 5.16. Maximum dilatancy and Sr relationship for sample #12 (1.427 g/cm^3)

For the specimens with having higher dry-density, dilative behavior is observed for all samples. Maximum dilatancy-normal stress and Sr relationships are shown in Figure 5.17 and Figure 5.19, respectively. The same conclusions can be drawn similar to the lower dry-density case. Also, using the maximum dilatancy values shown in Figure 5.17, the maximum dilation angles are also calculated and shown in Figure 5.18.

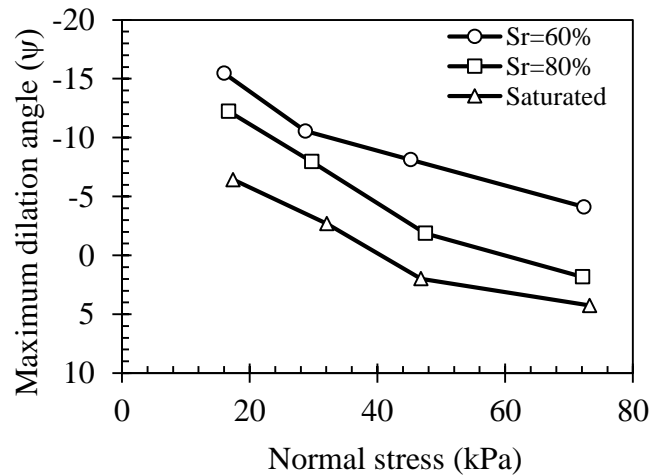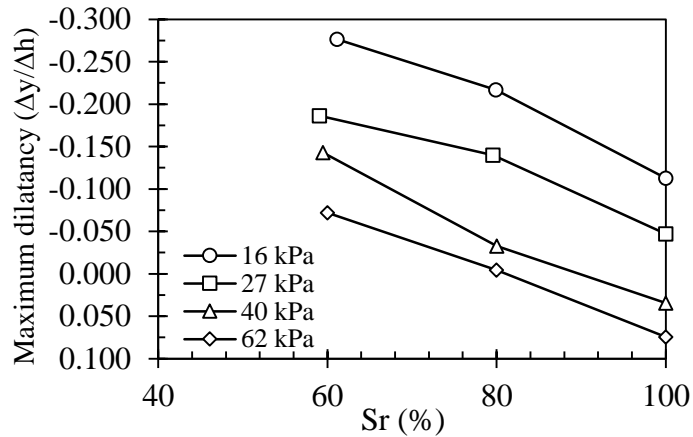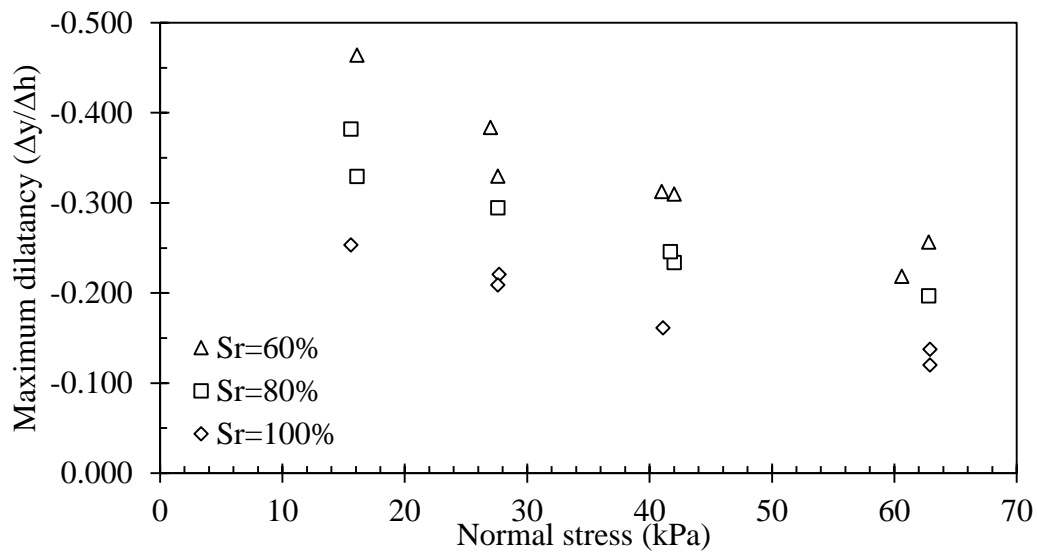*Figure 5.17.* Maximum dilatancy and normal stress relationship for sample #12 (1.58 g/cm^3)
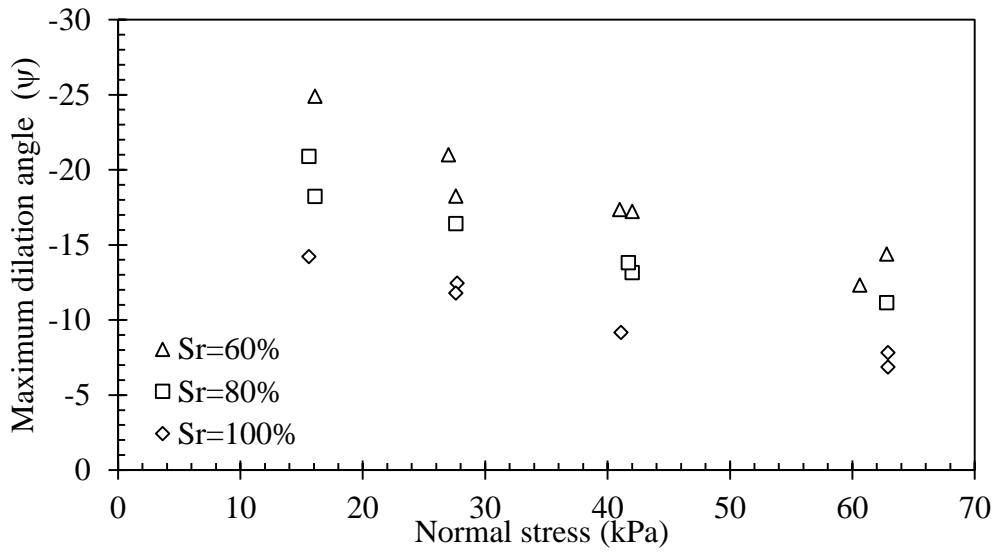
Figure 5.18. Maximum dilation angle and normal stress relationship for sample #12 (1.58 g/cm^3)
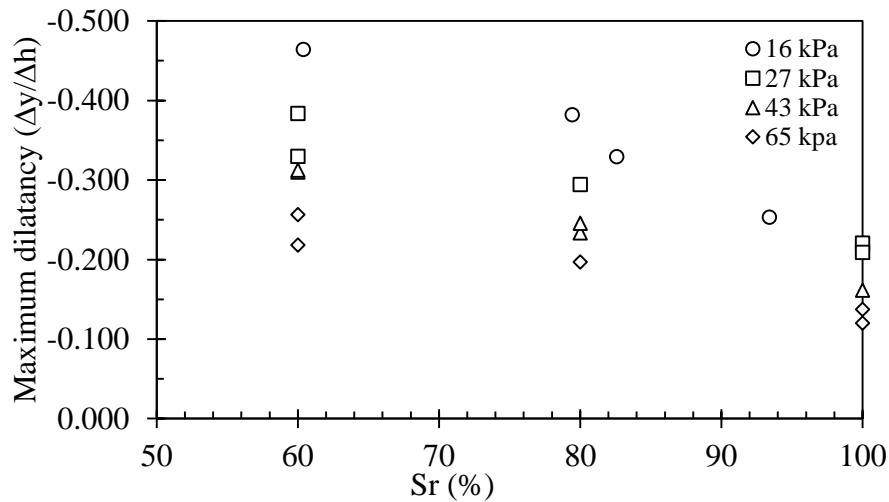
Figure 5.19. Maximum dilatancy and degree of saturation relationship for sample #12 (1.58 g/cm^3)

Similarly, the effects of suction in volumetric response of soils are noted in the literature (Ng and Zhou 2005, Thu et al. 2006, Hossain and Yin 2010). More dilative behavior of soils upon increase in suction is also noted (Hossain and Yin 2010, Thu et al. 2006), and the increase is found to be highly non-linear (Ng and Zhou 2005). Gallage and Uchimura (2016) stated that residual state is achieved at 5-6 mm horizontal displacement, and noted that at the residual state, discontinuities on pore-water paths may exist. Thus, atmospheric pressure exists in the shear plane, which results in disappearance of suction effects. Gallage and Uchimura (2016) concluded that the shear resistance increases with increasing normal stress, and volume change becomes more contractive.

5.3.1.3. Effect of preparation dry-density on friction angle, cohesion and stress-horizontal displacement behavior

The cohesion and internal friction angle values for sample #12 with 1.427 g/cm^3 dry-density case are 3.0 kPa and 35.4°, whereas corresponding values for 1.58 g/cm^3 case are 14.3 kPa and 34.4°. Dry-density and internal friction angle relationships for saturated case are shown in Figure 5.20. Internal friction angle for lower and higher

103

dry-density cases are found as 35.4° and 34.4°, respectively. Actually, it is expected that as the soil gets denser the internal friction angle increases. However, opposite behavior is observed for this sample. Thus, two additional tests were conducted for the denser case. Hence, the failure envelopes for lower and higher dry-density cases are generated using 4 and 6 data points, respectively. The internal friction angles are found to differ 1° from each other. Considering the direct shear test, 1° deviation can be regarded as being within the accuracy of the test. Therefore, it cannot be concluded that as the dry-density increased, the internal friction angle decreased. Nevertheless, it may be suitable to note that the increase in dry-density did not increased the internal friction angle for this sample.
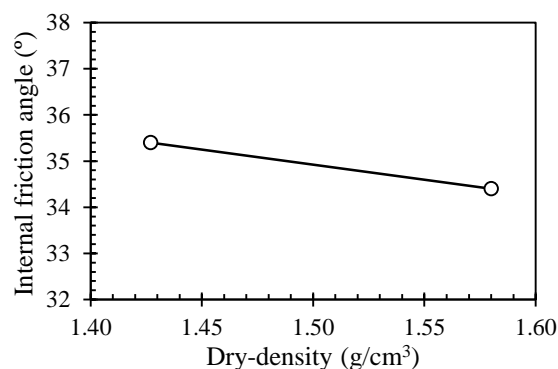
Figure 5.20. Dry-density and internal friction angle relationship for saturated case

However, it is observed that as the dry-density increased the cohesion value also increased (Figure 5.21). Combining the internal friction angle and cohesion results for 2 cases, the increase in shear strength is observed (Figure 5.22), which is mainly attributed to the increase in cohesion with dry-density rather than increase in internal friction angle.
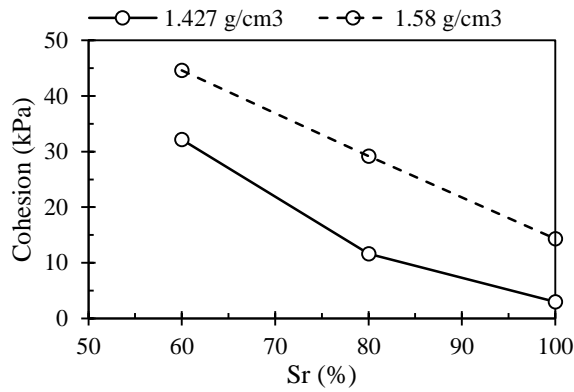
Figure 5.21. Dry-density and cohesion relationship for saturated case
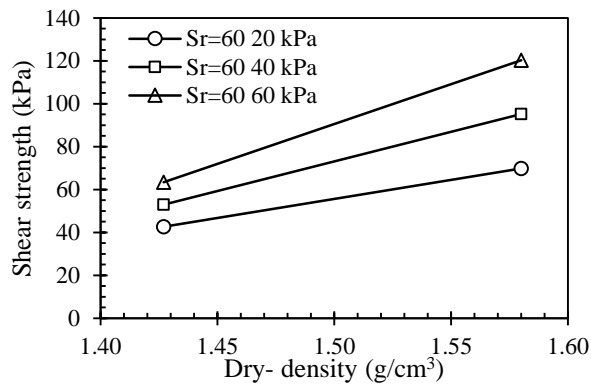
Figure 5.22. Dry-density shear strength relationship

Non-linearity of failure envelope for sample #12 having higher dry-density

Presenting the results, the failure envelopes are generated fitting a best-line; however, the failure envelopes at different Sr's for higher dry-density case showed a non-linear behavior (Figure 5.23). Since suction was not measured during the tests, no conclusion can be made about the non-linearity of the failure envelope for unsaturated case. Nevertheless, it is considered noteworthy to mention since non-linearity is observed for no other test data in this study.
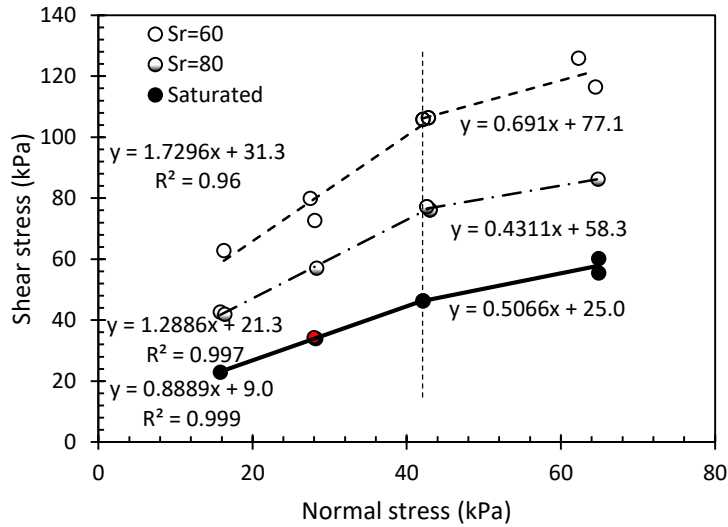
Figure 5.23. Non-linear behavior of higher dry-density case for sample #12 (1.58 g/cm^3)

5.4. Overall comparison of the findings with the literature

Landslides in residual soils derived from volcanic rocks are common around the world, e.g. in Hong Kong (Irfan 1998), Hawaii (Zhu and Anderson 1998), Canary Islands (Hürlimann et al. 2001), Singapore (Rahardjo et al. 2004), El Salvador (Bommer et al. 2013), New Zealand (Jacquet 1990).

Residual soils are heterogeneous in nature and they are commonly reported to contain special clay minerals, such as allophane and halloysite (Jacquet 1990, Terzaghi et al 1996, Hürlimann et al. 2001, Rahardjo et al. 2004, Wesley 1990, 2010, Huvaj and Üyetürk 2018).

Residual soils are reported to have low in-situ dry-density, and when compacted, low Standard Proctor dry-density and high optimum water content, as well as a high shear strength (e.g. tropical residual soils in Kenya reported by Dixon and Robertson 1970, residual soils in Canary Islands by Hürlimann et al. 2001 and by De Vallejo et. al 2008, in West Indies by Rouse et al. 1986, in Ecuador and Columbia by O'Rourke and Crespo 1988), in other regions by Townsend 1985, Wesley 2010, Moon 2016).

Relatively high void ratio is another distinct feature of residual soils. For example, high void ratio, high porosity and significant volumetric collapse upon saturation have been reported for non-plastic silts of volcanic origin in Campania region in Italy, by Picarelli et al. (2015).

De Vallejo et al. (2008) studied the engineering geological characteristics of residual volcanic soils in Tenerife, Canary Islands and reported that Proctor compaction dry-density values are typically low (12-15 kN/m^3 and optimum water contents of 18-43%) and mentioned that dry densities below 10 kN/m^3 may be found in other volcanic regions of the world. Low Proctor unit weights are attributed to the porous micro-cluster structure of these soils (Townsend 1985). Typical values of Standard Proctor densities of 1.1 to 1.68 kg/m^3 and high optimum water contents (up to 65%) are reported by Townsend (1985) for residual soils from Panama, Venezuela, Brazil, Indonesia, Nigeria, Kenya, and Columbia.

Factors for the observed high shear strength, before remolding, is considered to be related to non-platy halloysite mineral, common in residual soils (Wesley 2010) and also, to cohesion (Wesley 2010). O'Rouke and Crespo (1988) studied the geotechnical properties of cemented volcanic soils known as Canhagua in Ecuador and Columbia, and they stated that the soil has high porosity (40 to 50%) and low dry unit weight (11 to 14 kN/m^3). Rouse et al. (1986) studied the volcanic soils in Dominica, West Indies, and they observed highly porous soil structure and high field water contents (42 to 180%), which results in low dry unit weights (5.47 to 10.01 kN/m^3).

Significant volumetric collapse (significant decrease in void ratio) and static liquefaction upon saturation and during shearing (remolding) have been reported for residual soils (Lambe and Whitman 1969, Lumb 1975, Townsend 1985, Hürlimann et al. 2001, Rao and Revanasiddappa 2002, Picarelli et al. 2015, Moon 2016). This is thought to be related to existing interparticle bonding in residual soils, and significant loss of strength and changes in mechanical behavior upon irreversible breaking this bonding (both electrostatic and physical), hence significant sensitivity (ratio of peak

to remolded shear strength) have been reported for residual soils (De Vallejo et al. 1981, Townsend 1985, Jacquet 1990, Rahardjo et al. 1997, Hürlimann et al. 2001, Bommer and Rodriguez 2002, Rao and Revanasiddappa 2002). In fact, Jacquet (1990) studied the sensitivity of volcanic ash soils in New Zealand, and determined sensitivity values of 5 to 55. The effect of bonding is examined by Hürlimann et al. (2001) based on direct shear tests on undisturbed and remolded residual soils.

It is difficult to assess the strength parameters of residual soils from the literature due to the variability in test methods, degree of compaction, degree of saturation, and actual soil characteristics. In the case of lateritic soils, shear strength parameters that are higher than those suggested by plasticity indices, with effective friction angles between 20-30 degrees for lateritic clays and between 30 and 40 degrees for lateritic gravels, and cohesion of 0-60 kPa are common (Townsend 1985).

Focusing on the Rize region, reported porosity values for other landslides in Rize are in the range of 42%-64% (Yalcin 2005) and 55%-60% (Yuksek et al. 2003). Reported void ratio values for other landslides in Rize are in the range of 0.731 to 1.807 (Yalcin 2005). The porosity of soft natural clays usually ranges between 30% and 60% (it can even exceed 90%), whereas natural sand deposits are found with porosities varying from about 25% to 50% (Terzaghi et al. 1996). Therefore, the porosity values of the studied soils were in agreement with the similar soils reported in the literature.

It is stated in the literature that continuous wash-out due to precipitation and due to heavily and unconscious usage of ammonium sulfate fertilizer, soils became highly acidic in Rize region and this changed the properties of the soils in this region (Karsli et al. 2009, Özyazıcı et al. 2013, Özkutlu et al. 2015). According to Karsli et al. (2009), usage of ammonium sulfate resulted in increasing the number of the landslides in the vicinity. Thus, uncontrolled tea plantation seems to have a negative effect from slope stability point of view. The acidic nature of these soils underlying tea plantation is verified by measurments in this study (section 4.1.5).

Furthermore, weathering results in variation of pH of soil and groundwater over a period of time (Gratchev and Sassa 2009). Due to the sensitiveness to the local environment, pH changes can result in change in strength of fine-grained soils environment in terms of undrained cyclic behavior and the magnitude of this change depends on the mineralogy of clay fraction (Gratchev and Sassa 2009). Gratchev and Sassa (2009) showed that the pH was more influential on a more plastic soil, e.g. a kaolin-sand mixture became slightly more resistant to liquefaction in an acidic environment, while the illite-sand mixture became more susceptible to liquefaction, and the bentonite-sand mixture was observed to be the most sensitive to changes in pH.

CHAPTER 6

CONCLUSIONS AND RECOMMENDATION FOR FUTURE STUDIES

6.1. Conclusions

This section summarizes the findings of this study, regarding the properties of soil samples retrieved from 12 rainfall-induced landslides in residual soils of Rize in northern Turtkey.

6.1.1. Atterberg limits and soil classifications

1. The results of the Atterberg limits tests clearly indicates that the method of sample preparation has a significant influence on the LL and PL values of soils. Drying significantly changes the Atterberg limits of volcanic originated residual soils, hence the classification of such soils may change depending on the sample preparation technique.

2. Both liquid limit (LL) and plasticity index (IP) values of the soils decrease gradually as the sample preparation method change from moist preparation to preparation by drying at 60°C to 110°C and to 440°C.

3. Soils containing organic matter and /or soils formed by weathering of volcanic rocks should not be oven-dried, when soil mechanics index tests are to be conducted, simply because it was observed that their Atterberg limits significantly changed due to drying.

4. There seems to be a relationship between organic content and the ratio of $LL_{110°C} / LL_{Moist}$, which require more data and further examination.

5. The existing soil classification methods for soils, in this study having 4.3% to 12.1% organic matter, or $LL_{110°C}/LL_{Moist}$ ratio equal to or slightly greater than 0.75, may fail to represent the influence of organic matter on soil behavior.

6. To differentiate soils having the same group symbol, but having different characteristics, there must be a different naming convention to represent the characteristics of organic soils.

7. As the organic content of the sample increases, the LL_{Moist} also seem to increase.

8. Burning time can affect the determination of the organic matter content of the soil. As the burning time is increased from 2 hours to 12 hours, the organic matter increased by about 0.63%-2.70%.

9. ASTM D4318-17 suggested power coefficient ($tan\beta$) value of 0.121 can be used. This power value is demonstrated to give good results for ML-OL and MH-OH type residual soils used in this study. The results of this research support the conclusion given by the US Waterways (1949) and Eden (1955) that the average slope value appears to be independent of soil type and geologic origin.

10. Differences between the LL values obtained by one-point method and multi-point methods are insignificant (i.e. less than or equal to 2%), therefore one-point method can be considered as an alternative to multi-point test considering the benefits it provides.

6.1.2. Soil characteristics

1. The soils, taken from the shear surfaces, main and side scarps, and within the landslide mass are similar materials, i.e. there is not a different material above and below the shear surface.

2. The soils are mainly fine-grained soils (i.e. low plasticity and high plasticity silty materials having organic contents and organic soils, ML, MH, OH).

3. They contain halloysite mineral and organic matter up to 12% by dry mass.

4. Organic soil classification based on USCS (ASTM D2487) may result in erroneous classification of the volcanic residual soil, since the change in liquid limit may result from both the organic matter and mineralogical composition of the soils.

5. All of the tested soils are found to be acidic (pH < 7), and further research is encouraged to understand the effects of chemical fertilizers and the decreasing pH values on soil properties in residual soils.

6. The soils have high porosity, high void ratio and low dry-density. The soils are of medium-stiff consistency and they are classified as medium to extra sensitive category, based on the ratio of peak and remolded undrained shear strength.

7. The data presented in this study highlights some features of these soils, and contributes to the international literature. The results could be useful for future studies on numerical modeling of the mechanism of these landslides, landslide mitigation measures and land-use planning, landslide susceptibility mapping and rainfall intensity-duration thresholds, which is known to depend on the unsaturated hydro-mechanical properties of the soils. The data obtained in this study could be used as a proxy for unsaturated hydro-mechanical properties of these soils in preliminary assessments.

6.1.3. Shear strength characteristics

1. Degree of saturation or water content and normal stress dramatically influences the strength characteristics of residual soils for reconstituted tests.

2. For reconstituted samples, internal friction angles are in the range of 30.4° to 35.4°, and they are found to be similar at different Sr. Reconstituted samples exhibit a good frictional resistance, although having low dry-densities.

3. For almost all of the intact samples, internal friction angles are in the range of 31.1° to 38.0° with an average of 36.3°.

4. Cohesion intercept of Mohr-Coulomb failure envelope increases with decreasing degree of saturation.

5. Strain-hardening and strain-softening response of the soil changes with change in degree of saturation and normal stress.

6. Dilation (volume increase) and compression (volume decrease) in response to horizontal displacement changes are affected by degree of saturation and

normal stress: for unsaturated tests dilation (or less contraction) occurred during shearing, whereas contraction (or less dilation) is observed for saturated tests.

7. For some of the samples, maximum dilatancy decreased with increasing degree of saturation and applied normal stress.

8. Shear stress-horizontal displacement plots approach each other (i.e. gives similar shear resistance) for unsaturated tests conducted at different degree of saturations, at large horizontal displacements, under similar normal stresses.

9. For one sample, prepared at 2 different dry-density, increase in dry-density did not increase the internal friction angle, whereas increased the cohesion intercept. Combining these, the increase in the dry-density increased the shear strength.

6.2. Recommendation for further research

Conducting this research, the following are considered as possible future subjects to be studied:

- Unsaturated soil properties, such as SWRCs and hydraulic conductivity functions can be generated for different soil samples from Rize for modelling of the rainfall-induced landslides in Rize.

- Suction controlled or suction measured tests can be conducted on soils to accurately investigate the unsaturated shear strength of the soils.

- Numerical modelling of these landslides.

REFERENCES

Adamo, P., Violante, P., Wilson, M. J. (2001). Tubular and spheroidal halloysite in pyroclastic deposits in the area of the Roccamonfina volcano (Southern Italy). Geoderma, 99(3-4), 295-316.

AFAD, Turkish Disaster and Emergency Management Directorate (2018). https://heysemp2018.afad.gov.tr/tr/26149/Heyelan-Albumu/?mbaopn=1

Ahmadi-adli M, Huvaj N, Toker, N.K. (2012). Rainfall triggered landslides in unsaturated soils: A numerical sensitivity analysis. In 10th International Congress on Advances in Civil Engineering (pp. 17-19).

Ahmadi-adli, M. (2014). Shallow Landslides Triggered by Rainfall in Unsaturated Soils. Doctor of philosophy dissertation in civil engineering, Middle East Technical University.

Ahmadi-adli, M., Huvaj, N., Toker, N.K. (2012). Rainfall triggered landslides in unsaturated soils: a numerical sensitivity analysis. In Proceedings of 10th International Congress on Advances in Civil Engineering, Middle East Technical University, Ankara, Turkey (pp. 17-19).

Ahmadi-adli, M., Huvaj, N., Toker, N.K. (2014). Effects of air entry value on rainfall induced slope instability. Geo-Congress 2014. Atlanta: American Society of Civil Engineers.

Akgün, A., Dag, S., Bulut, F. (2008). "Landslide susceptibility mapping for a landslide-prone area (Findikli, NE of Turkey) by likelihood-frequency ratio and weighted linear combination models." Environ Geol 54:1127–1143. doi: 10.1007/s00254-007-0882-8

Al Rawi, O., Assaf, M.N., Rawashdeh, T. (2017). Effect of organic content on the engineering properties of Jordanian clayey soils, IJCIET, 8, 1018-1026

Alan, İ, Balcı, V, Keskin, H, Altun, İ, Böke, N, Demirbağ H, Arman S, Elibol H, Soyakil M, Kop A, Hanilçi N. (2019). Tectonostratigraphic characteristics of the area between Çayeli (Rize) and İspir (Erzurum). Maden Tetkik ve Arama Dergisi, (158), 1-57.

AASHTO T267-86 (2008). Standard method of test for determination of organic content in soils by loss of ignition.

Arslan, M., Kadir, S., Abdioğlu, E., Kolayli, H. (2006). Origin and formation of kaolin minerals in saprolite of tertiary alkaline volcanic rocks, Eastern Pontides, NE Turkey.

Arya, L. M., Paris, J. F. (1981). A physicoempirical model to predict the soil moisture characteristic from particle-size distribution and bulk density data 1. Soil Science Society of America Journal, 45(6), 1023-1030.

ASTM (2008), Standard Test Methods for Determination of the Soil Water Chararcteristic Curve for Desorption Using a Hanging Column, Pressure Extractor, Chilled Mirror Hygrometer, and/or Centrifuge, D6836 ASTM International

ASTM (2011). Standard test method for direct shear test of soils under consolidated drained conditions. D3080-11. ASTM International.

ASTM (2012). Standard Test Methods for Laboratory Compaction Characteristics of Soil Using Modified Effort (56,000 ft-lbf/ft3 (2,700 kN-m/m3))

ASTM (2014). Standard test methods for moisture, ash, and organic matter of peat and other organic soils. D2974-14. ASTM International.

ASTM (2014). Standard test methods for specific gravity of soil solids by water pycnometer. D854-14. ASTM International

ASTM (2015). Standard test methods for laboratory compaction characteristics of soil using standard effort (12,400 ft-lbf/ft3 (600 kN-m/m3)). D698-12. ASTM International

ASTM (2016). Standard test method for unconfined compressive strength of cohesive soil. D2166-16. ASTM International

ASTM (2016). Standard test method for measurement of hydraulic conductivity of saturated porous materials using a flexible-wall permeameter. D5084-16 ASTM International.

ASTM (2017). Standard practice for classification of soils for engineering purposes (unified soil classification system). D2487-17. ASTM International.

ASTM (2017). Standard test method for particle-size distribution (gradation) of fine-grained soils using the sedimentation (hydrometer) analysis ASTM D7928-17. ASTM International.

ASTM (2017). Standard test methods for liquid limit, plastic limit, and plasticity index of soils. ASTM D4318–17. ASTM International.

ASTM (2017). Standard test methods for particle-size distribution (gradation) of soils using sieve analysis ASTM D6913-17. ASTM International.

ASTM (2018). Standard Test Methods for pH of Soils. ASTM D4972-18. ASTM International.

ASTM STP 479-EB (1970). Special procedures for testing soil and rock for engineering purposes.

Atterberg, A., (1911). Uber die physikalische bodenuntei suchung and uber die plastizitat der tone int. mitt far bodenkunde, Berlin, 1.

Ball, D.F. (1964). Loss-on-ignition as an estimate of organic matter and organic carbon in non-calcareous soils. European Journal of Soil Science, 15(1), 84-92.

Balta, İ. (1987). Doğu Karadeniz toprakları. Proceedings of the 2nd National Soil Mechanics and Foundation Engineering Conference, İstanbul, 377-391. (in Turkish)

Baltacı, H. (2010) Doğu Karadeniz Bölgesi (Rize, Tabzon, Giresun) heyelan-yağış ilişkisinin incelenmesi ve mininmum eşik değerlerinin belirenmesi. M.S. Thesis. Istanbul Technical University, Istanbul (in Turkish)

Bardet, J.P. (1997). Experimental Soil Mechanics, Prentice-Hall, Inc., Upper Saddle River, New Jersey

Basma, A. A., Al-Homoud, A. S., Al-Tabari, E. Y. (1994). Effects of methods of drying on the engineering behavior of clays. Applied Clay Science, 9(3), 151-164.

Bishop, A. W. (1959). The principle of effective stress, Teknisk Ukeblad I Samarbeide Med Teknikk, Oslo, Norway, 106(39), 859–863.

Bommer, J. J., Rodríguez, C. E. (2002). Earthquake-induced landslides in Central America. Engineering Geology, 63(3-4), 189-220.

Brooks, R., Corey, T. (1964). Hydraulic properties of porous media. Hydrology Papers, Colorado State University, 24, 37.

Canadian Agricultural Services Coordinating Committee, Soil Classification Working Group., (1998). The Canadian system of soil classification. NRC Research press.

Casagrande, A., (1932). Research on the Atterberg limits of soils, Public Roads, v.13, pp.121-136

Christensen, B. T., Malmros, P. Å. (1982). Loss-on-ignition and carbon content in a beech forest soil profile. Ecography, 5(4), 376-380.

Cruden, D. M., Varnes, D. J. (1996). Landslides: investigation and mitigation. Chapter 3-Landslide types and processes. Transportation research board special report, (247).

Dağ, S, Bulut, F (2012) Coğrafi bilgi sistemleri tabanlı heyelan duyarlılık haritalarının hazırlanmasına bir örnek: Çayeli (Rize, KD Türkiye). Jeoloji Mühendisliği Dergisi, 36(1), 35-62 (in Turkish)

De Graft-Johnson, J.W.S., Bhatia, H.S. (1969). General report—engineering characteristics. Proc. Specialty Session on Engineering Properties of Lateritic Soils, 7th Int. Conf. on Soil Mechanics and Foundation Engineering, Mexico, 1969, Vol. 2, 13–43.

de La Rosa, D. (1979). Relation of several pedological characteristics to engineering qualities of soil. European Journal of Soil Science, 30(4), 793-799.

de Vallejo, L. G., Salas, J. J., Jimenez, S. L. (1981). Engineering geology of the tropical volcanic soils of La Laguna, Tenerife. Engineering geology, 17(1-2), 1-17.

de Vallejo, L. I. G., Hijazo, T., Ferrer, M. (2008). Engineering geological properties of the volcanic rocks and soils of the Canary Islands. Soils and Rocks, 31, 3-13.

DIN 18196, (1998). Bodenklassifikation für bautechnische Zwecke, 409–412.

Dixon, H.H., Robertson, R.H.S. (1970). Some engineering experiences in tropical soils. Quarterly Journal of Engineering Geology and Hydrogeology, 3(3), 137-150.

Dixon, J.B. (1989). Kaolin and serpentine group minerals. Minerals in soil environments, (mineralsinsoile), 467-525.

Ece, O. I., Nakagawa, Z. E., Schroeder, P. (2003). Alteration of volcanic rocks and genesis of kaolin deposits in the Sile region, northern Istanbul, Turkey. I: Clay mineralogy. Clays and Clay Minerals, 51(6), 675-688.

Ece, O. I., Schroeder, P. A., (2007). Clay mineralogy and chemistry of halloysite and alunite deposits in the Turplu area, Balikesir, Turkey. Clays and Clay Minerals, 55(1), 18-35.

Eckel, E.B. (1958). Introduction. En E.B. Eckel, Landslides and Engineering Practice. Washington D.C.: National Academy of Sciences, National Council.

Eden, W. J. (1955). Trial of One-Point Liquid Limit Method, Proceedings of Ninth Canadian Soil Mechanics Conference, Ottawa, December 15th to 16th 1955 (National Research Council for Canada), Appendix A. Eden, W. 1960. Use of a one-point liquid limit procedure. In Papers on Soils 1959 Meetings. ASTM International.

Eden, W. (1960). Use of a one-point liquid limit procedure. In Papers on Soils 1959 Meetings. ASTM International.

Filiz, M, Avcı, H, Usta, P. (2011). Heyelanların Yerleşim Alanlarına Etkilerinin İncelenmesi (Rize-Gündoğdu Örneği), e-Journal of New World Sciences Academy - Engineering Sciences, v. 6(4), p. 1200-1211 (in Turkish)

Fredlund, D. G., and Morgenstern, N.R. (1977). Stress state variables for unsaturated soils. Journal of Geotechnical and Geoenvironmental Engineering, 103(ASCE 12919).

Fredlund, D.G., Rahardjo, H., and Fredlund, M.D. (2012). Unsaturated soil mechanics in engineering practice. New York: John Wiley and Sons Inc

Gallage, C., and Uchimura, T. (2015). Direct shear testing on unsaturated silty soils to investigate the effects of drying and wetting on shear strength parameters at low suction. Journal of Geotechnical and Geoenvironmental Engineering, 142(3), 04015081.

Gedik, A., Ercan, T., Korkmaz, S., Karataş, S. (1992). Rize-Fındıklı Çamlıhemşin arasında (Doğu Karadeniz) yer alan magmatik kayaçların petrolojisi ve Doğu Pontidlerdeki bölgesel yayılımları. Geological Bulletin of Turkey, 35, 15-38.

Germaine, J. T (2019). Personal commincation.

Germaine, J. T., and Germaine, A. V. (2009). Geotechnical laboratory measurements for engineers. John Wiley & Sons.

Gratchev IB, Sassa K (2009) Cyclic Behavior of Fine-Grained Soils at Different pH Values. J Geotech Geoenvironmental Eng 135:271–279. doi: 10.1061/(ASCE)0733-9410(1992)118:1(51)

Haigh, S. K., Vardanega, P. J., (2014). Fundamental Basis of Single-point Liquid Limit Measurement Approaches, Applied Clay Science, Vol. 102, pp. 8-14

Hossain, M. A. Yin, J. H. (2010). Shear strength and dilative characteristics of an unsaturated compacted completely decomposed granite soil. Canadian Geotechnical Journal, 47(10), 1112-1126.

Howard, P. J. A., Howard, D. M., (1990). Use of organic-carbon and loss-on-ignition to estimate soil organic-matter in different soil types and horizons. Biology and Fertility of Soils, 9(4), 306-310.

Huang, P., Patel, M., Santagata, M.C., Bobet, A. (2009). Classification of organic soils. Publication FHWA/IN/JTRP-2008/02. Joint Transportation Research Program, Indiana Department of Transportation and Purdue University, West Lafayette, Indiana.

Huat, B. B., Aziz, A. A., Ali, F. H., Azmi, N.A. (2008). Effect of wetting on collapsibility and shear strength of tropical residual soils. Electronic Journal of Geotechnical Engineering, 13, 1-44.

Huat, B. B., Prasad, A., Asadi, A., Kazemian, S., (2014). Geotechnics of Organic Soils and Peat. CRC Press.

Hürlimann, M., Ledesma, A., & Martı, J. (2001). Characterisation of a volcanic residual soil and its implications for large landslide phenomena: application to Tenerife, Canary Islands. Engineering Geology, 59(1-2), 115-132.

Huvaj, N. and Uyeturk, E., (2018). Effects of drying on Atterberg limits of pyroclastic soils of Northern Turkey. Appl Clay Sci 162:46–56. doi: 10.1016/j.clay.2018.05.020

Huvaj-Sarihan, N. (2009). Movement of reactivated landslides (Doctoral dissertation, University of Illinois at Urbana-Champaign).

Ijaz, A., Ali, S. A., Room, S., Rana, M. A., Aleem, M., (2014). Effects of soil and air drying methods on soil plasticity of different cities of Pakistan. International Journal of Engineering Research and Applications, 4(12), 49-53.

Ildır, B. (1995). Türkiye'de heyelanların dağılımı ve afetler yasası ile ilgili uygulamalar. Proceedings of the 2nd national landslide symposium, Turkey, Sakarya University, pp 1-9

INDOT, (2012). Indiana Department of Transportation Geotechnical Manual, Office of Geotechnical Services INDOT, www.in.gov/indot/files/GTS_2010GTSManual_2012.pdf (retrieved on January 28, 2018)

Irfan T Y (1998) Structurally controlled landslides in saprolitic soils in Hong Kong, Geotechnical and Geological Engineering, 16, p.215-238

ISO, (2004). 14688-2: 2004: Geotechnical investigation and testing–identification and classification of soil–Part 2: Principles for a classification. European Standard.

Iverson, R. M. (2000). "Landslide triggering by rain infiltration". Water resources research, 36(7), 1897-1910.

Jain, L.C., Patwardhan, N.K. (1960). Physical properties of soils from the Ganges valley. Journal of Scientific and Industrial Research (India), 19A(4): 162-167.

Jacquet, D. (1990). Sensitivity to remoulding of some volcanic ash soils in New Zealand." Engineering Geology 28.1-2: 1-25.

Jarvis A., H.I. Reuter, A. Nelson, E. Guevara, (2008), Hole-filled seamless SRTM data V4, International Centre for Tropical Agriculture (CIAT), available from http://srtm.csi.cgiar.org.

Jefferson, I., Rogers, C. D. F. (1998). Liquid limit and the temperature sensitivity of clays. Engineering geology, 49(2), 95-109.

Jose, B.T., Sridharan,A., Abraham,B.M. (1988). A study of geotechnical properties of Cochin marine clays. Marine Georesourses & Geotechnology, 7(3), 189-209.

Jose, B.T., Sridharan,A., Abraham,B.M. (1999). Variability of properties of marine clays due to sample conditions. Proceedings of the International Conference on Offshore and Nearshore Geotechnical Engineering, December 2-3,1999.

Jotisankasa, A., Mairaing, W. (2009). Suction-monitored direct shear testing of residual soils from landslide-prone areas. Journal of geotechnical and geoenvironmental engineering, 136(3), 533-537.

Kadir, S., Karakaş, Z. (2002). Mineralogy, chemistry and origin of halloysite, kaolinite and smectite from Miocene ignimbrites, Konya, Turkey. Neues Jahrbuch für Mineralogie-Abhandlungen: Journal of Mineralogy and Geochemistry, 177(2), 113-132.

Kanıt, R., Özer, M., Özdemir, Ş. (2006). The effect of sample preparation technique to liquid limit obtained from cone penetration test. Selcuk Techical Journal, 5(3), 89-99. (in Turkish)

Karsli F, Atasoy M, Yalcin A, Reis S, Demir O, Gokceoglu C (2009) Effects of land-use changes on landslides in a landslide-prone area (Ardesen, Rize, NE Turkey). Environ Monit Assess 156:241–255. doi: 10.1007/s10661-008-0481-5

Karube, D., Kato, S., Hamada, K., Honda. M. (1996). The relationship between the mechanical behavior and the state of pore water in soil. Journal of JSCE, 535, 83-92.

Kaya A, Demirbaş C, Dağ S (2018) Gündoğan (Ardeşen-Rize) köyü yerleşim alanındaki yamaç duraysızlığının jeoteknik açıdan incelenmesi. Doğal Afetler ve Çevre Derg 90:221–235. doi: 10.21324/dacd.417920 (in Turkish)

Kenanoğlu, M. B., Ahmadi-Adli, M., Toker, N. K., and Huvaj, N. (2019). Effect of Unsaturated Soil Properties on the Intensity-Duration Threshold for Rainfall Triggered Landslides. Teknik Dergi, 30(2).

Kim, J. B. (1973). A study on the General and One Point Method of Test for Liquid Limit Procedure, Journal of the Korean Society of Agricultural Engineers, Vol. 15(4), pp. 3153-3159.

Lambe, T. W., Whitman, R. V. (1969). Soil mechanics. John Willey & Sons. Inc., New York, 553.

Lu, N. (2019). Revisiting Axis Translation for Unsaturated Soil Testing. Journal of Geotechnical and Geoenvironmental Engineering, 145(7), 02819001.

Lu, N. and Likos, W. J. (2004). Unsaturated soil mechanics. Wiley.

Lu, N., Godt, J. W. (2013). Hillslope hydrology and stability. Cambridge University Press.

Lu, N., Likos, W. J. (2006). Suction stress characteristic curve for unsaturated soil. Journal of geotechnical and geoenvironmental engineering, 132(2), 131-142.

Lumb, P. (1975). Slope failures in Hong Kong. Quarterly Journal of Engineering Geology, 8(1), 31-65.

Maghsoudloo A. (2013) Nonlinearity of the residual shear strength envelope in stiff clays. Master of Science dissertation in civil engineering, Middle East Technical University.

Malkawi, A. I. H., Alawneh, A. S., Abu-Safaqah, O. T., (1999). Effects of organic matter on the physical and the physicochemical properties of an illitic soil. Applied Clay Science, 14(5-6), 257-278.

Mitchell, J. K. (1993). Fundamentals of soil behavior. University of California, Berkeley, USA.

Mohan, D. and Goel, R. K. (1958) Rapid methods of determining liquid limit of soils, Journal of Scientific and Industrial Research (India) A 17, p.498-501

Moore, D.M. and Reynolds, R.C., Jr., (1997). X-ray Diffraction and the identification and analysis of clay minerals. Oxford University Press, New York, 378

Moon, V. (2016). Halloysite behaving badly: geomechanics and slope behaviour of halloysite-rich soils. Clay Minerals, 51(3), 517-528.

Morin, W. J., and P. C. Todor. (1975). Laterite and Lateritic Soils and Other Problem Soils of the Tropics, USAID 3682. Baltimore, MD: Lyon Associates.

Murray, H. H., (1988). Kaolin minerals; their genesis and occurrences. Reviews in Mineralogy and Geochemistry, 19(1), 67-89.

Nagasawa, K., (1978). Weathering of volcanic ash and other pyroclastic materials. In Developments in Sedimentology, 26, 110-12. Elsevier.

Nefeslioglu HA, Gokceoglu C, Sonmez H, Gorum T (2011) Medium-scale hazard mapping for shallow landslide initiation: The Buyukkoy catchment area (Cayeli, Rize, Turkey), Landslides, 8(4), 459-483

Ng, C. W. W. and Zhou, R. Z. B. (2005). Effects of soil suction on dilatancy of an unsaturated soil. In proceedings of the international conference on soil mechanics and geotechnical engineering (vol. 16, no. 2, p. 559)

Norman, L.E. J. (1959) The One-Point Method of Determining the value of the Liquid Limit of a Soil, Geotechnique, v. 9 (1), p.1-8

Oberg, A. L., Sallfors, G. (1995). A rational approach to the determination of the shear strength parameters of unsaturated soils. In proceedings of the first international conference on unsaturated soils/unsat'95/paris/france/6-8 september 1995. Volume 1.

Okalp, K., and Akgün, H. (2016)."National level landslide susceptibility assessment of Turkey utilizing public domain dataset". Environ Earth Sci. 75:847.

O'Kelly, B. C., (2005). Oven-drying characteristics of soils of different origins. Drying Technology, 23(5), 1141-1149.

O'Kelly, B. C., Sivakumar, V., (2014). Water content determinations for peat and other organic soils using the oven-drying method. Drying Technology, 32(6), 631-643.

Olmstead, F. R., Johnston, C. M. (1955). Rapid methods for determining liquid limits of soils. Highway Research Board Bulletin, (95).

O'Rourke, T. D., Crespo, E. (1988). Geotechnical properties of cemented volcanic soil. Journal of Geotechnical Engineering, 114(10), 1126-1147.

Önalp, A. (1980) Doğu Karadeniz heyelanları, tanımlanması, analizi. Ankara: TUBITAK (in Turkish)

Önalp, A. (1991) Doğu Karadeniz Bölgesi heyelanlarının nedenleri, analizi, kontrol olanakları. 1. Ulusal Heyelan Sempozyumu Bildiriler Kitabi, Trabzon, pp 38–63 (in Turkish)

Önalp, A, Tarhan, F, Sevinç, N (1987) Doğu Karadeniz heyelanları: Analiz- dengel, yamaç tasarımı. Ankara: TUBITAK (in Turkish)

Önalp, A., Arel, E., (2013). Determination of Liquid Limit of Clays from European Section of İstanbul (Likit limitin tek nokta yöntemi ile ölçümü ve İstanbul killerinde uygulama)", 5. Geoteknik Sempozyumu, 5-7 Aralık 2013, Çukurova Üniversitesi, Adana (in Turkish).

Önalp, A., Balta, İ. (1987). Formation and properties of Eastern Black Sea clays. Proceedings of the 2nd National Soil Mechanics and Foundation Engineering Conference, İstanbul, 59-68 (in Turkish)

Önalp, A., Kılıç, C. (1994). One-point method for liquid limit of clays of Eastern Black Sea. Proceedings of the 5th National Soil Mechanics and Foundation Engineering Conference, Ankara, 155-160. (in Turkish)

Özer, M., 2008. Effects of sample preparation on the liquid limit determined by cone penetration test. Journal of Faculty of Engineering, Architecture, Gazi University, 23, 3,689-698. (in Turkish)

Özkutlu, F., Akkaya, Ö.H, Özlem, E.T.E, Şahin, Ö., Korkmaz, K. (2015) Rize ilindeki bazı çay bahçelerinin toprak ve yaprak analizi ile besin element düzeylerinin

belirlenmesi. Harran Tarım ve Gıda Bilimleri Dergisi, 19(2), 94-103 (in Turkish).

Özyazıcı, M.A., Dengiz, O., Aydoğan, M. (2013). Çay yetiştirilen tarım topraklarının reaksiyon değişimleri ve alansal dağılımları. Toprak Su Dergisi, 2(1) (in Turkish).

Papke, K.G. (1971). Halloysite deposits in the Terraced Hills Washoe County, Nevada". Clays and Clay Minerals, 19, 71-74.

Picarelli, L., Damiano, E., Greco, R., Minardo, A., Olivares, L., Zeni, L. (2015). Performance of slope behavior indicators in unsaturated pyroclastic soils, Journal of Mountain Science, 12: 1434.

Rahardjo, H., Leong, E. C., Choa, V. (1997). Characterization of residual soil properties for analyses of rainfall-induced slope instability. In proceedings of the international conference on soil mechanics and foundation engineering-international society for soil mechanics and foundation engineering (Vol. 1, pp. 577-580).

Rahardjo, H., Aung, K. K., Leong, E. C., Rezaur, R. B. (2004). Characteristics of residual soils in Singapore as formed by weathering. Engineering Geology, 73(1-2), 157-169.

Rao, S. M., Revanasiddappa, K. (2002). Collapse behaviour of a residual soil. Géotechnique, 52(4), 259-268.

Reddy,K.(2015).http://cemmlab.webhost.uic.edu/Experiment%202Organic%20Cont ent.pdf (retrieved on Janurary 28, 2018)

Reis, S., Bayrak, T., Yalçın, A., Atasoy, M., Nişancı, R., Ekercin, S. (2008). Rize Bölgesinde Yağış Heyelan İlişkisi. HKMO Jeodezi, Jeoinformasyon ve Arazi Yönetimi Dergisi, 99, 5-9 (in Turkish)

Reis, S., Bayrak, T., Yalçın, A., Sancar, C., Erduran, M., Atasoy, M., Nişancı, R., Ekercin, S. (2009). Rize iline ait heyelan risk bölgeleri ve uygun yerleşim alanlarının cağrafi bilgi teknolojileri ile belirlenmesi. Ankara: TUBITAK (in Turkish)

Reis, S., and Yomralıoğlu, T. (2005). Provincal disaster risk management using GIS". Turkish chamber of survey and cadastre engineers, 10th Scientific and technical meeting on Turkish mapping, 28 March-1 April 2005, Ankara

Roje-Bonacci, T. (2004) Liquid limit determination of the high plastic clays by one-point method, 4th Slovenian Geotechnical Congress and 5th Sukljetovi days, p. 199-204

Rouse, W. C., Reading, A. J., & Walsh, R. P. D. (1986). Volcanic soil properties in Dominica, West Indies. Engineering Geology, 23(1), 1-28.

Sattari, A. S., Toker, N. K. (2016). Obtaining soil–water characteristic curves by numerical modeling of drainage in particulate media. Computers and Geotechnics, 74, 196-210.

Schuster, R.L. (1996). "Socioeconomic significance of landslides," Landslides: Investigation and Mitigation, Special Report 247, 12-35. Washington: Transportation Research Board.

Sen, P., Sarin, M., Dixit, M., (2016). Properties of fine grained soil blended with organic matter, Proc. Indian Geotechnical Conference IGC2016 15-17 December 2016, IIT Madras, Chennai, India, 1-4

Sidle, R.C. and Ochiai, H. (2006). Landslides: Process, Prediction and Land use, Water Resources Monograph 18, American Geophysical Union, Washington D.C.

Skempton, A. W., Petley, D. J. (1970). Ignition loss and other properties of peats and clays from Avonmouth, King's Lynn and Cranberry Moss. Geotechnique, 20(4), 343-356.

Stanchi, S., Catoni, M., D'Amico, M. E., Falsone, G., Bonifacio, E. (2017). Liquid and plastic limits of clayey, organic C-rich mountain soils: Role of organic matter and mineralogy. Catena, 151, 238-246.

Stanchi, S., D'Amico, M., Zanini, E., Freppaz, M. (2015). Liquid and plastic limits of mountain soils as a function of the soil and horizon type. Catena, 135, 114-121.

Sunil, B. M., Krishnappa, H. (2012). Effect of drying on the index properties of lateritic soils. Geotechnical and Geological Engineering, 30(4), 869-879.

Tarbuck, E.J., Lutgens, F.K., Tasa, D.G. (2012). Earth Science. Upper Saddle River, NJ: Pearson.

Tarhan, F. (1991) Dogu Karadeniz heyelanlarina genel bir bakis. 1. Ulusal Heyelan Sempozyumu Bildiriler Kitabi, Trabzon, pp 38–63 (in Turkish)

Terzaghi, K. (1936). The shearing resistance of saturated soils, in Proceedings of the First International Conference on Soil Mechanics, Vol. 1, 54–56.

Terzaghi, K. (1950). Mechanism of landslides, in Application of Geology to Engineering Practice, ed. S. Paige, Geological Society of America, New York, p.83-123.

Terzaghi, K., Peck, R. B., Mesri, G. (1996). Soil Mechanics in Engineering Practice. John Wiley & Sons.

Thu, T. M., Rahardjo, H., Leong, E. C. (2006). Shear strength and pore-water pressure characteristics during constant water content triaxial tests. Journal of Geotechnical and Geoenvironmental Engineering, 132(3), 411-419.

Townsend, F. C. (1985). Geotechnical characteristics of residual soils. Journal of Geotechnical Engineering, 111(1), 77-94.

TSMS (2019), Turkish State Meteorological Service of Ministry of Agriculture and Forestry https://www.mgm.gov.tr/veridegerlendirme/il-ve-ilceler istatistik.aspx?m=RIZE

Tüysüz, O., Genc, S.C., Tarı, U., Erturac, M. K. (2008). Geological, geographical and man-made factors controlling landslide potential of Rize province, Northern Turkey, the 33rd Geological Congress, Oslo, Norway, 6-14 August 2008.

US Waterways (1949) Simplification of the Liquid Limit Test Procedure, U.S. Army Corps of Engineers Waterways Experiment Station, Technical Memorandum No. 3-286, 64 p.

Uyeturk, E., Huvaj, N. (2018). Power coefficient in one point liquid limit test for soils of northern Turkey at various temperatures. Selçuk Üniversitesi Mühendislik, Bilim ve Teknoloji Dergisi, 6(4), 643-653.

Uyeturk, E., Huvaj, N. (2019). Drying Changes Consistency Limits. In Geo-Congress 2019: Geotechnical Materials, Modeling, and Testing (pp. 532-540). Reston, VA: American Society of Civil Engineers.

Uysal, A. (2004). Adapazarı ve Civarında Likit Limit Deneyinde Kullanılacak β Katsayısının Bulunması, Yüksek Lisans Tezi, Sakarya Üniversitesi.

Varnes, D. J. (1958). Landslide types and processes. Landslides and engineering practice, 24, 20-47.

Vaughan, P. R. (1985). Mechanical and hydraulic properties of in situ residual soils. Proceedings, First International Conference on Geomechanics in Tropical, Lateritic, and Saprolitic Soils, Brazil, 1–33,

Wesley, L. D. (1990). Influence of structure and composition on residual soils. Journal of geotechnical engineering, 116(4), 589-603.

Wesley, L. D. (2010). Geotechnical engineering in residual soils. John Wiley & Sons.

Wesley, L.D. (1973). Some basic engineering propertıes of halloysite and allophane clays in Java, Indonesia, Geot., 23, 4, 471-494

Wilson, S.D. (1970). Suggested method of test for moisture-density relations of soils using Harvard compaction apparatus." Special Procedures for Testing Soil and Rock for Engineering Purposes: Fifth Edition. ASTM International

Yalcin, A. (2008). GIS-based landslide susceptibility mapping using analytical hierarchy process and bivariate statistics in Ardesen (Turkey): Comparisons of results and confirmations. Catena 72:1–12. doi: 10.1016/j.catena.2007.01.003

Yalcin, A., Bulut F. (2007) Landslide susceptibility mapping using GIS and digital photogrammetric techniques: A case study from Ardesen (NE-Turkey). Nat Hazards 41:201–226. doi: 10.1007/s11069-006-9030-0

Yalcin, A. (2005). An investigation on Ardesen (Rize) region on the basis of landslide susceptibility, Doctoral dissertation, Ph. D. Dissertation. Karadeniz Technical University, Trabzon, Turkey (in Turkish).

Yılmaz S (2010) Rize bölgesel heyelan ve sel afeti müdahale ve iyileştirme çalışmaları. Unpublished presentation. Rize, Turkey (in Turkish)

Yuksek T, Yuksek F (2009) Effects of clear-cutting alder coppice on surface soil properties and aboveground herbaceous plant biomass. Communications in Soil Science and Plant Analysis, 40(15-16), 2562-2578.

Zolfaghari, Z., Mosaddeghi, M. R., Ayoubi, S., Kelishadi, H. (2015). Soil atterberg limits and consistency indices as influenced by land use and slope position in Western Iran. Journal of Mountain Science, 12(6), 1471-1483.

APPENDICES

A. Direct shear test results for tube samples

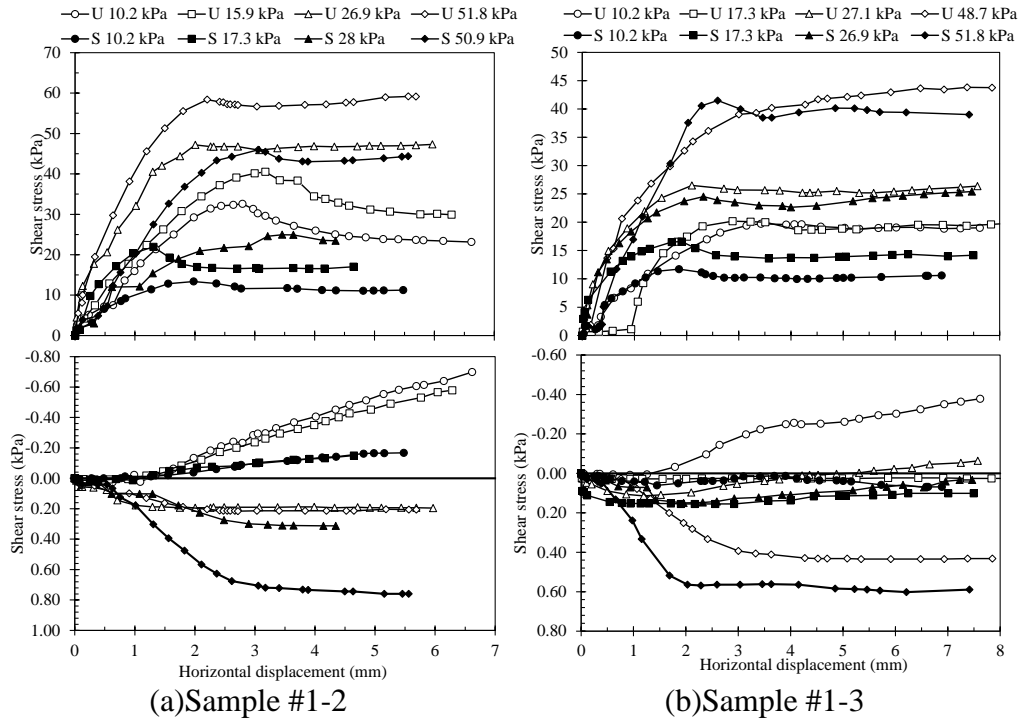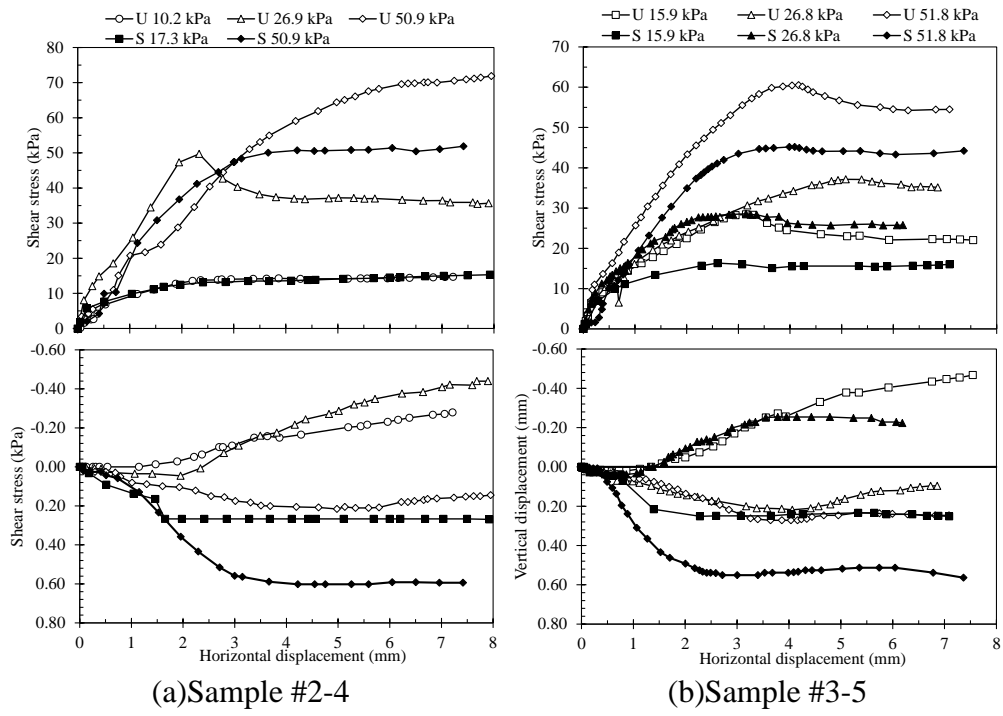*Figure A.1.* Direct shear test results for (a) sample#1-2, (b) sample#1-3

Figure A.2. Direct shear test results for (a) sample#2-4, (b) sample#3-5
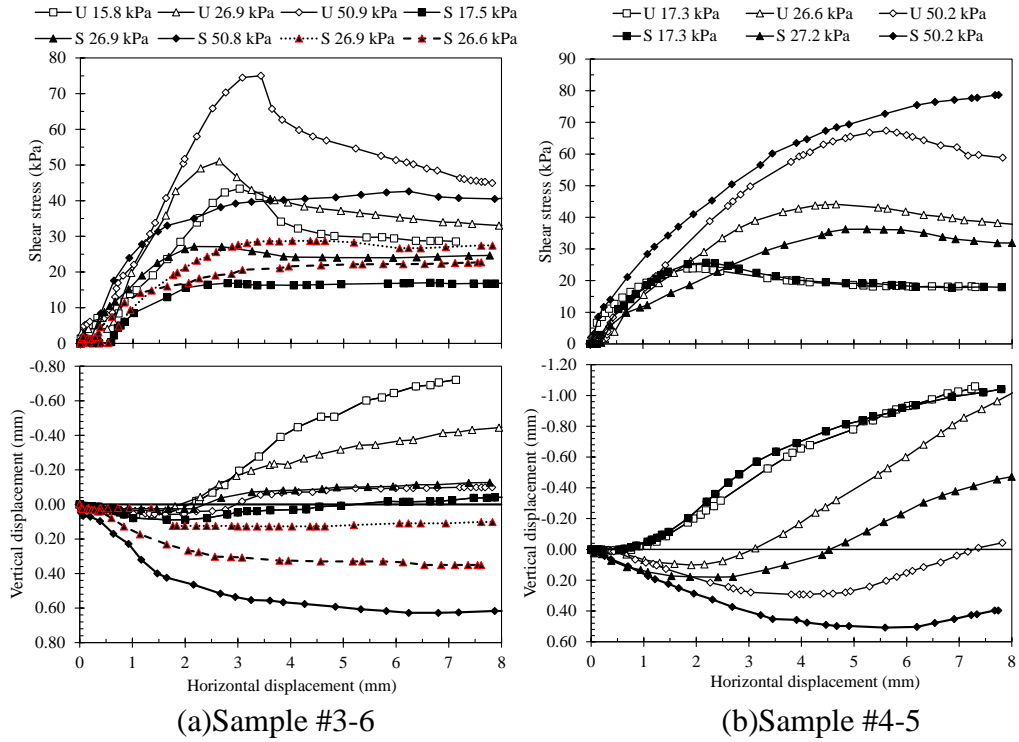
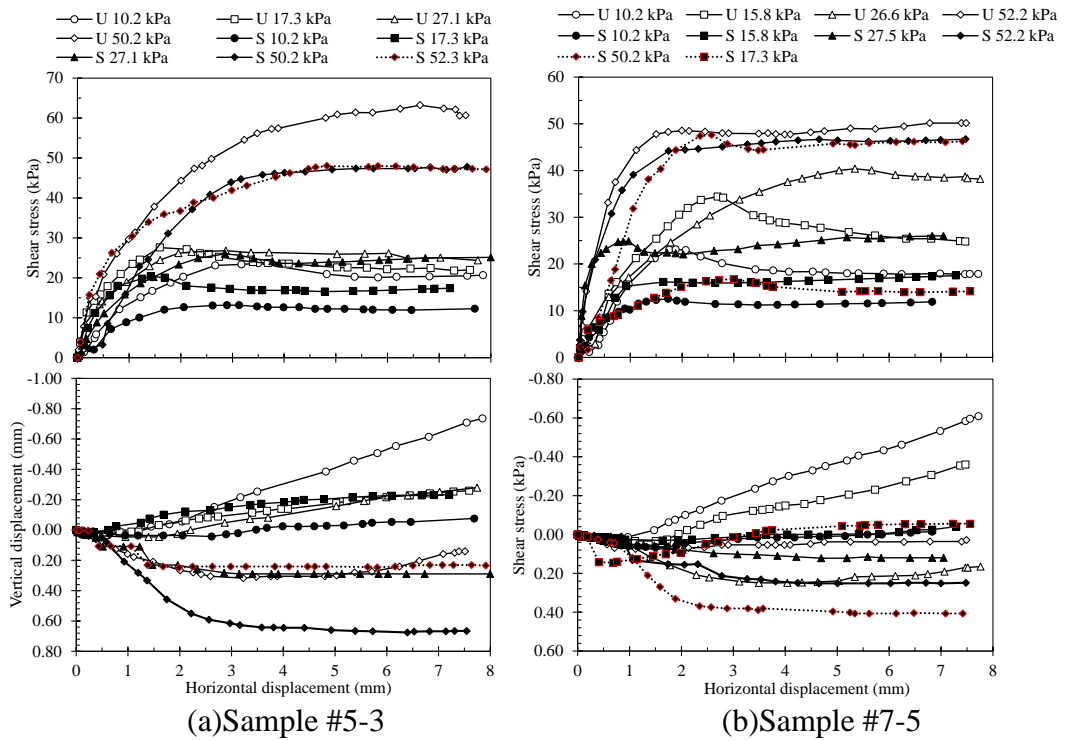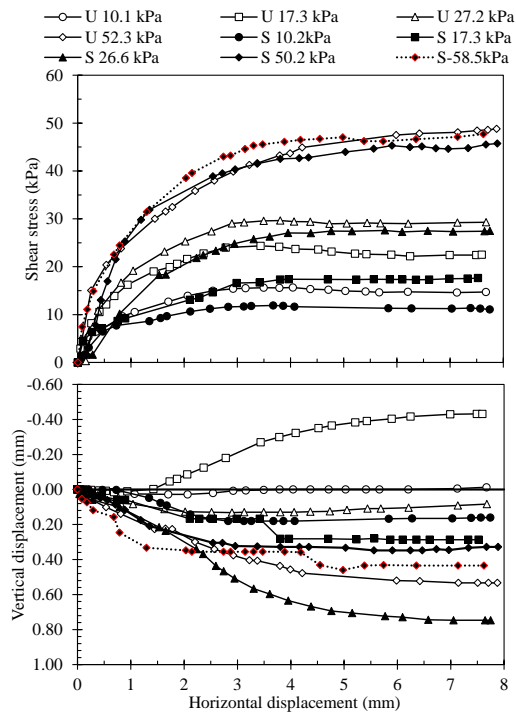*Figure A.3.* Direct shear test results for (a) sample#3-6, (b) sample#4-5

Figure A.4. Direct shear test results for (a) sample#5-3, (b) sample#7-5

Sample #7-6

Figure A.5. Direct shear test results for sample #7-6

B. Direct shear test results for reconstituted samples

Table B.1. *Reconstituted specimen direct shear test results for sample 10-1*

Test ID	Dry density (g/cm3)	Initial water content (%)	Final water content (upper part) (%)	Final water content (lower part) (%)	Normal stress at the start (kPa)	Normal stress at failure (kPa)	Shear stress at failure (kPa)	Displacement at failure (mm)	Void ratio (e)	Initial Sr (%)
U60 16kPa	1.35	22.2	21.3	21.6	16.4	17.1	57.7	2.24	1.009	59.7
U60 28.9kPa	1.36	21.7	21.2	21.3	27.7	28.9	73.0	2.67	0.994	59.4
U60 28.8kPa	1.33	21.6	21.4	21.5	27.6	28.8	70.5	2.37	1.053	55.9
U60 45.1kPa	1.36	22.0	21.9	22.3	42.5	45.1	86.2	2.83	1.002	59.8
U60 64.7kPa	1.37	22.1	21.4	21.6	19.8	64.7	91.4	2.34	0.991	60.7
U80 16kPa	1.36	29.2	31.0	29.7	16.1	18.7	16.4	6.99	1.002	79.2
U80 35.8kPa	1.36	29.2	30.5	29.5	31.6	35.8	25.5	6.89	1.002	79.2
U80 47.1kPa	-	29.5	29.0		41.6	47.1	32.4	7.09	-	-
U80 61.1kPa	1.37	29.2	28.4		52.3	61.1	39.1	7.20	0.991	80.1
S 18.6 kPa	1.38	38.5	34.2		16.1	18.6	12.3	6.86	0.972	100
S 34 kPa	1.35	39.6	33.6		29.1	34.0	24.5	7.13	1.008	100
S 46.2 kPa	1.35	38.3	32.7		41.8	41.8	46.2	5.79	1.021	100
S 67.4 kPa	1.35	38.3	31.3		59.3	67.4	26.2	7.23	1.012	100

Table B.2. *Reconstituted specimen direct shear test results for sample 10-2*

Test ID	Dry density (g/cm3)	Initial water content (%)	Final water content (upper part) (%)	Final water content (lower part) (%)	Normal stress at the start (kPa)	Normal stress at failure (kPa)	Shear stress at failure (kPa)	Displacement at failure (mm)	Void ratio (e)	Initial Sr (%)
U60 16kPa	1.23	28.0	26.6	26.7	15.6	16.0	24.7	1.35	1.288	61.1
U60 28.7 kPa	1.23	27.1	27.2	27.1	27.6	28.7	36.3	1.81	1.288	59.1
U60 45.2 kPa	1.23	27.2	26.9	27.2	41.8	45.2	47.0	4.47	1.286	59.5
U60 72.3 kPa	1.23	26.9	26.5	27.0	62.0	72.3	62.5	7.09	1.286	58.8
U80 16.7 kPa	1.22	36.9	35.8	35.3	15.9	16.7	20.2	2.98	1.297	79.9
U80 29.7 kPa	1.22	36.9	36.2	35.6	27.3	29.7	32.6	3.93	1.303	79.6
U80 47.5 kPa	1.22	37.1	35.4	35.1	41.6	47.5	43.6	7.48	1.301	80.0
U80 72.1 kPa	1.22	37.2	35.3	35.9	62.0	72.1	55.7	6.98	1.297	80.6
S 17.4 kPa	1.22	40.8	43.5		15.3	17.4	12.0	7.19	1.299	100
S 32.1 kPa	1.22	41.2	43.7		27.6	32.1	22.7	7.10	1.301	100
S 46.8 kPa	1.23	40.6	42.3		41.2	46.8	32.0	7.12	1.293	100
S73.2 kPa	1.23	40.4	41.8		62.9	73.2	50.3	7.01	1.286	100

Table B.3. *Reconstituted specimen direct shear test results for sample 11*

| Test ID	Dry density (g/cm3)	Initial water content (%)	Final water content (upper part) (%)	Final water content (lower part) (%)	Normal stress at the start (kPa)	Normal stress at failure (kPa)	Shear stress at failure (kPa)	Displacement at failure (mm)	Void ratio (e)	Initial Sr (%)
U60 16.6 kPa	1.266	25.1	24.01	25.09	16.4	16.6	41.7	0.86	1.164	59.1
U60 16.4 kPa	1.251	26.71	25.68	25.59	16.2	16.4	37.7	0.76	1.191	61.5
U60 32.7 kPa	1.265	25.31	25.79	26	31.9	32.7	53.0	1.49	1.166	59.5
U60 65.6 kPa	1.270	26.45	25.6	26.85	59.9	65.6	74.4	4.36	1.157	62.6
U80 16.1 kPa	1.260	34.40	33.7	33.87	15.7	16.1	29.6	1.52	1.175	80.2
U80 33.3 kPa	1.264	33.82	33.9	33.76	31.9	33.3	43.0	2.41	1.168	79.4
U80 62.8 kPa	1.259	34.05	34.1	34.54	53.7	62.8	57.6	7.24	1.176	79.3
U80 69.9 kPa	1.255	34.55	34.2	34.28	59.9	69.9	64.9	7.15	1.184	80.0
S 16.1 kPa	1.259	40.73	47.8		15.7	16.1	14.7	1.52	1.176	100
S 34.2 kPa	1.259	41.13	44.4		31.9	34.2	24.9	4.03	1.176	100
S 62.5 kPa	1.254	41.41	47.1		53.7	62.5	43.4	7.04	1.185	100
S 70.3 kPa	1.254	37.0	47.4		59.9	70.3	47.3	7.37	1.185	100

Table B.4. *Reconstituted specimen direct shear test results for sample 12 (1.427 g/cm³)*

| Test ID	Dry density (g/cm3)	Initial water content (%)	Final water content (upper part) (%)	Final water content (lower part) (%)	Normal stress at the start (kPa)	Normal stress at failure (kPa)	Shear stress at failure (kPa)	Displacement at failure (mm)	Void ratio (e)	Initial Sr (%)
U60 16.5 kPa	1.43	20.65	20.41	19.51	16.1	16.5	41.2	1.20	0.940	60.9
U60 27.5 kPa	1.42	21.75	20.67	21.42	26.8	27.5	45.8	1.37	0.956	63.0
U60 43.9 kPa	1.42	21.65	21.51	21.38	42.6	43.9	55.1	1.45	0.955	62.8
U60 64.7 kPa	1.42	21.07	19.86	19.39	62	64.7	65.9	2.50	0.954	61.2
U80 17.6 kPa	1.41	28.71	27.53	27.24	16.1	17.6	23.0	4.48	0.966	82.3
U80 30.2 kPa	1.42	28.14	27.18	26.63	25.9	30.2	31.0	7.04	0.956	81.5
U80 47.8 kPa	1.42	28.07	26.84	27.18	42.1	47.8	43.3	7.09	0.955	81.4
U80 70.6 kPa	1.42	27.97	27.46	27.88	62	70.6	57.3	7.24	0.949	81.6
S 17.3 kPa	1.43	32.4	31.1		16.1	17.3	15.7	3.67	0.944	100
S 29.6 kPa	1.43	32.3	30.3		27.5	29.6	22.0	4.29	0.941	100
S 46.7 kPa	1.43	32.1	29.8		42.6	46.7	38.5	4.34	0.933	100
S 73.5 kPa	1.42	32.5	29.5		66.1	73.5	54.4	6.02	0.948	100

Table *B.5. Reconstituted specimen direct shear test results for sample 12 (1.58 g/cm³)*

| Test ID	Dry density (g/cm3)	Initial water content (%)	Final water content (upper part) (%)	Final water content (lower part) (%)	Normal stress at the start (kPa)	Normal stress at failure (kPa)	Shear stress at failure (kPa)	Displacement at failure (mm)	Void ratio (e)	Initial Sr (%)
U60 16.3 kPa	1.58	16.5	16.0	15.3	16.1	16.3	62.8	0.64	0.755	60.4
U60 28.1 kPa	1.58	16.7	16.2	15.4	27.6	28.1	72.7	0.89	0.757	61.1
U60 27.5 kPa	1.58	16.4	15.7	15.5	27.0	27.5	79.9	0.89	0.753	60.2
U60 42.8 kPa	1.58	16.2	15.7	15.5	42.0	42.8	106.4	1.13	0.752	59.8
U60 42.1 kPa	1.57	16.6	15.2	15.5	41.0	42.1	105.9	1.22	0.762	60.4
U60 62.3 kPa	1.57	17.4	16.8	17.1	60.6	62.3	125.9	1.60	0.766	63.0
U60 64.5 kPa	1.56	17.2	15.6	15.7	62.8	64.5	116.5	1.28	0.770	61.7
U80 15.8 kPa	1.59	21.4	21.1	21.1	15.6	15.8	42.7	0.74	0.745	79.4
U80 16.4 kPa	1.58	22.6	22.2	21.4	16.1	16.4	41.9	1.03	0.757	82.6
U80 28.3 kPa	1.57	22.4	21.1	20.8	27.6	28.3	57.0	1.22	0.761	81.5
U80 43 kPa	1.58	22.0	21.4	21.1	42.0	43.0	76.2	1.42	0.757	80.7
U80 42.6 kPa	1.59	21.3	21.2	20.9	41.7	42.6	77.2	1.23	0.743	79.4
U80 64.8 kPa	1.58	21.9	21.2	21.4	62.8	64.8	86.2	1.52	0.753	80.6
S 15.8 kPa	1.59	25.1	32.0		15.6	15.8	22.9	0.64	0.745	93.4
S 28 kPa	1.59	25.3	34.0		27.7	28.0	34.3	0.81	0.745	94.2
S 28.2 kPa	1.58	25.4	29.8		27.6	28.2	33.9	1.06	0.752	93.4
S 42.1 kPa	1.59	25.0	32.5		41.1	42.1	46.3	1.40	0.737	93.9
S 64.9 kPa	1.59	25.6	28.9		62.9	64.9	60.2	1.55	0.744	95.3
S 64.9 kPa	1.57	26.1	29.0		62.9	64.9	55.5	1.52	0.765	94.5

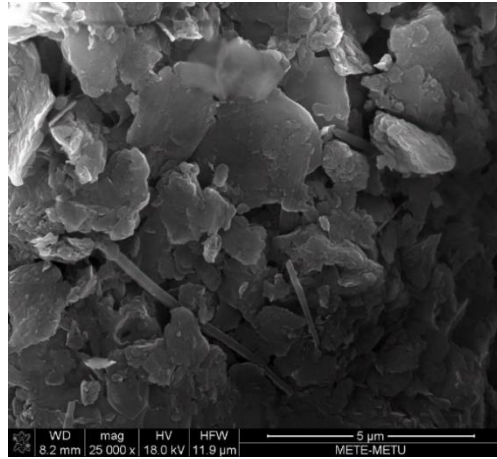## C. SEM pictures of some of the samples
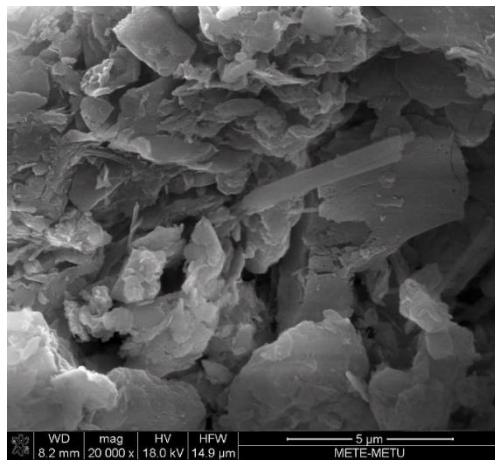
(a)
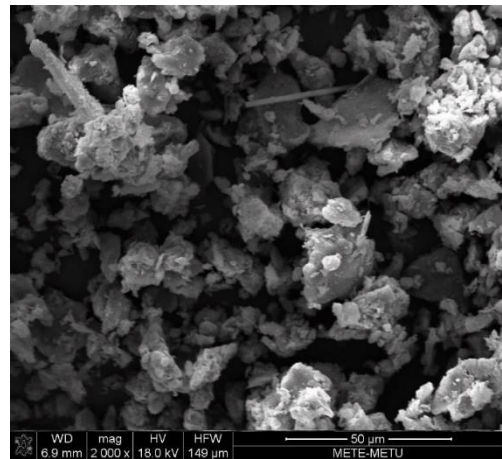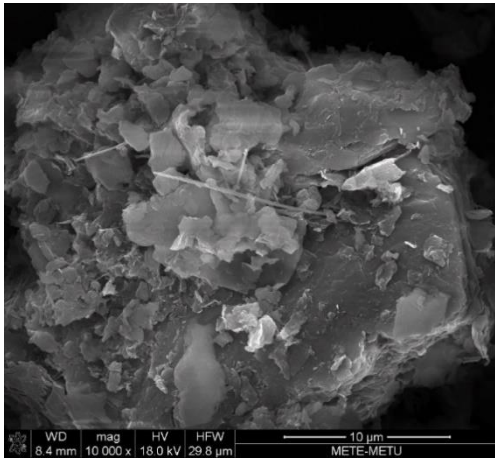

(b)
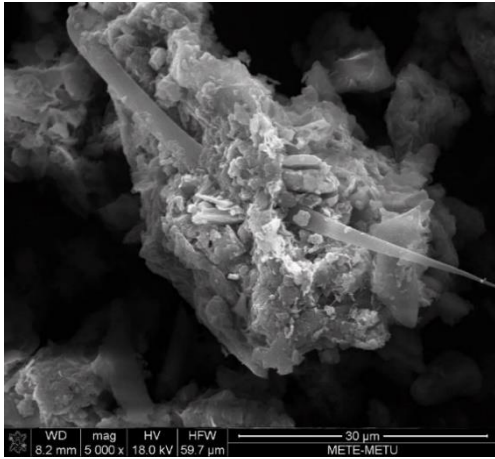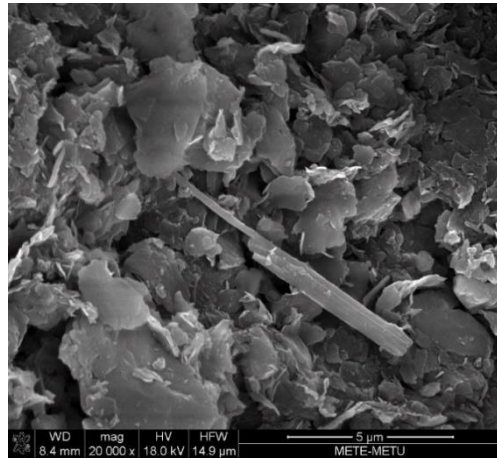
(c)

(d)

(e)

(f)

Figure C.6. SEM photos of samples from site #3 ((a), (b), (c), (d) air-dried and, (e)-(f) 110°C dried samples

CURRICULUM VITAE

PERSONAL INFORMATION

Surname, Name	: Üyetürk, Celal Emre
Nationality	: Turkish (TC)
Date and Place of Birth	: 22 December 1994, Ankara
E-mail	: emreuyeturk@gmail.com

EDUCATION

Degree	Institution	Year of Graduation
MS	METU Civil Engineering	2019
BS	METU Civil Engineering	2017
High School	Ayrancı Anadolu Lisesi, Ankara	2012

WORK EXPERIENCE

Year	Place	Enrollment
2018-2019	METU	Research Assistant
2016 August	KASKTAŞ	Intern Engineering Student
2015 August	LIMAK CONSTRUCTION	Intern Engineering Student

FOREIGN LANGUAGES

Advanced English

PUBLICATIONS

1. Huvaj, N., Uyeturk, E., (2018). Effects of drying on Atterberg limits of pyroclastic soils of Northern Turkey, Applied Clay Science, Volume 162, pp. 46-56, https://doi.org/10.1016/j.clay.2018.05.020.

2. Uyeturk, E., Huvaj, N. (2018). "Power coefficient in one point liquid limit test for soils of Northern Turkey at various temperatures", Selcuk University Journal of Engineering, Science and Technology, 6 (4), 643-653.

3. Oguz, E. A., Huvaj, N. Uyeturk, C.E. (2018). "Variability in offshore soils and effects on probabilistic bearing capacity", 9th European Conference on Numerical Methods in Geotechnical Engineering, June 25-27 2018, Porto, Portugal

4. Uyeturk, E., Huvaj, N. (2019). "Drying changes Consistency Limits", ASCE Geo-Congress 2019

5. Uyeturk, E., Bayraktaroglu, H., Huvaj, N., Huseyinpasaoglu, M. (2018) "Material Properties of Soils in Rainfall-Triggered Landslides in Rize Province" 2. National Landslides Symposium, October 11-12, Ankara, Turkey

6. Uyeturk, C.E., Huvaj, N. (2018). "Atterberg Limits Determined at Different Drying Temperatures", 17. National Soil Mechanics and Geotechnical Engineering Conference, 26-28 September 2018, Istanbul